12-16-2021 10:00 AM

Biomechanical Analysis of Ligament Modelling Techniques and Femoral Component Malrotation Following TKA

Liam A. Montgomery, *The University of Western Ontario*

Supervisor: Willing, Ryan, *The University of Western Ontario*
Co-Supervisor: Brent Lanting, *London Health Sciences Center*
A thesis submitted in partial fulfillment of the requirements for the Master of Engineering Science degree in Biomedical Engineering

Abstract

Previous studies have demonstrated that satisfaction and revision rates following total knee arthroplasty (TKA) are lower than those of comparable surgeries such as total hip replacements. A leading cause for these revisions is joint instability which may be due to improper ligament balancing or poorly aligned surgical implants. One of the methods used to investigate biomechanical forces and kinematics is computational modelling of the post-operative TKA knee.

A unique knee model was used to investigate the biomechanical and kinematic effects of ligament model complexity, as well as the effects of simulating ligament wrapping versus ignoring ligament wrapping. We then used these ligament models to investigate the biomechanical effects of femoral implant malalignment. Our results show no discernable differences in kinematics due to ligament complexity or ligament wrapping except during specific loading scenarios. We also observed that an externally rotated femoral implant results in a more varus knee with lower medial collateral ligament tension compared to the TKA knee with a neutrally aligned femoral implant.

Keywords

Total Knee Arthroplasty, Ligaments, Knee Modelling, Kinematics, Force Contribution

Summary for Lay Audience

Total knee replacement (TKR) surgery is a fairly common surgery in Canada, being performed over 70 000 times each year. TKR surgery is used as an end-stage treatment option for knee osteoarthritis which causes extreme joint pain and makes normal functional tasks such as walking and stair climbing a difficult ordeal for patients. Though it is typically successful at providing the patient with a pain-free knee, TKR satisfaction and revision rates remain lower than those of comparable surgeries such as total hip replacement surgery.

One of the leading causes for revision is joint instability following the initial TKR surgery. Instability may be caused by improperly balanced ligaments which leads to an imbalanced force distribution across the knee joint. Another cause of instability is poorly aligned implants. The femoral and tibial implants must be properly aligned to both each other, and their respective bones. A better understanding of both the biomechanical and the kinematic effects of malalignment could be key to improving patient outcomes.

We used a simulation software package for a novel application: constructing a virtual knee model that could conduct independent biomechanical analysis on knee motion without a physical joint motion simulator. This model was used to investigate the effects of femoral component malalignment on kinematics and ligament tensions during a variety of motions. We also looked at the effects of ligament model complexity and ligament model wrapping on the kinematics and ligament tensions of our TKR knee model.

Ligament model complexity had no discernible effect on kinematics of the TKR knee, however simulating ligament wrapping ensured that no unnatural motions occurred. This indicates that using simple ligament models may be a viable option during the computational modelling of the TKR knee. Analysis of femoral component malrotation demonstrated that a poorly aligned component can lead to a poorly aligned knee and results is different ligament tensions compared to a correctly aligned component.

Co-Authorship Statement

Chapters 1 and 6 were written solely by Liam Montgomery.

Chapters 2, 3, 4, and 5 were drafted by Liam Montgomery and revised by Drs. Willing and Lanting.

Acknowledgments

I would first like to thank my two supervisors Drs. Willing and Lanting. Dr. Willing introduced me to both the worlds of academia and engineering in 2019. I was lucky to have someone as experienced and knowledgeable as him to help me navigate through the complex world of research. Under his guidance I have learned a great deal about the research world and have acquired many skills that I will be able to translate into many facets of my life. Dr. Lanting provided integral clinical understanding throughout my project and made himself available as often as possible to answer questions I had related to my own work as well as clinical practice itself.

I would also like to thank the members of the Biomedical Engineering Research Lab who were always available to help with any problems I may have had with my research. In particular, I want to thank Samira Vakili and Alexandre Galley whom I saw as my student mentors throughout my time with this lab.

Finally, I want to thank my parents Chris and Darlene Montgomery. Having both written and submitted theses themselves, they were able to be a strong source of support at the end of my research as I began writing.

Table of Contents

List of Tables

List of Figures

Chapter 1

1 Introduction

1.1 Motivation

Total knee arthroplasty (TKA) is a surgical procedure used as an end stage treatment for knee osteoarthritis. In Canada, over 10% of people age 15 and up suffer from osteoarthritis and over 58% of these patients suffer in their knee [1]. With so many patients across the country TKA surgeries are performed over 70 000 times annually [2]. Unfortunately, as few as 58% of patients are satisfied with the functional outcomes of the surgery indicating aspects of TKA can be improved. Furthermore, satisfaction rates following TKA (84%) remain lower than those for total hip replacements (96%) and revision rates remain relatively high [3], [4]. One of the three leading causes of revision surgery is joint instability. Instability following surgery may arise due to improper intraoperative ligament balancing or malalignment of TKA components with respect to bony anatomy [2]. This joint instability is responsible for an uneven distribution of force which can cause further discomfort for the patient.

There is a need to improve TKA outcomes, and a better understanding of the ligament loads crossing the post-operative knee joint may be key to improving knee stability following TKA. There have been a number of case series studies investigating the effect femoral implant malalignment has on the TKA knee, with some being able to link malalignment to a high risk of revision surgery and many others determined that malalignment posed a low risk for revision.

This thesis aims to conduct biomechanical analysis of a TKA knee with a femoral implant malalignment using a virtual knee model. Biomechanical analysis will include descriptions of kinematics and ligament tensions throughout various motions tested by surgeons following TKA surgery. Many virtual knee models exist in the literature, almost all of them take a different approach to the design of their virtual ligament model. Therefore, our study also investigates the difference in resulting biomechanics as they are affected by different ligament models. These include comparisons between ligaments that

wrap around bony geometry, and ligaments that ignore bony anatomy and travel directly from tibia to femur. We will also examine the effect ligament model complexity has on TKA knee kinematics. The effects of femoral component malalignment, ligament wrapping, and ligament model complexity will be investigated during simulated neutral flexion, as well as posterior, varus/valgus, and internal/external laxity tests.

1.2 Objective

This study aims to use a new platform for biomechanical testing of the knee joint in a fully virtual environment. It uses a virtual TKA knee model with virtual ligaments in order to investigate the effects of different virtual ligament complexities and femoral component malalignment. Therefore, the objectives of this study are to:

1. Develop a functional virtual TKA model using the software VIVO Sim and validate it against a comparable experimental cadaver study.

2. Investigate the effect of ligament model complexity as a function of the number of bundles used to model each individual ligament on the resulting TKA biomechanics.

3. Measure the effect that using a wrapped virtual ligament model has on resulting TKA biomechanics versus uses simple point-to-point springs.

4. Investigate the effect of an internally and externally rotated femoral component on the post-TKA kinematics, contact forces, and ligament tensions during neutral flexion and various laxity tests.

1.3 Organization of Thesis

Chapter 2 discusses the anatomy of the intact human knee joint including the anatomy and physiology of several ligaments of interest including the superficial medial collateral ligament (sMCL), the lateral collateral ligament (LCL), and the posterior cruciate ligament (PCL). This is followed by a description of TKA surgery, components used, and alignment types. A review of previous computational models used to study TKA

biomechanics has also been added. Chapter 2 also contains a review of the literature available on the effects of component malalignment during TKA surgery.

Chapter 3 describes how we developed a computational model using the software VIVO Sim. After developing this model, we validated it by comparing resulting kinematics and ligament tensions for a number of motions to a similar study that was carried out experimentally using a physical joint motion simulator. We then compare the results and discuss the validity of VIVO Sim and the virtual knee model.

Chapter 4, comprised of the first manuscript from this study, studies how variance in computational modelling of the knee ligament complexity affect resulting kinematics, ligament tensions, and contact forces following TKA. This chapter also investigates the effect modelling ligament wrapping has on TKA kinematics and ligament tensions during a variety of motions. This chapter begins with an exploration into the computational TKA knee models available in the literature as well as the inconsistency in how virtual ligaments are represented. A brief overview of methods used, including the experimental setup is then described along with the results and a discussion.

Chapter 5, comprised of the second manuscript from this study, investigates the effect of femoral component malalignment on the kinematics, ligament tensions, and contact forces experienced by the TKA knee during a variety of motions. This chapter starts with discussing TKA surgical malalignments and the lack of in vitro studies investigating the kinematics following TKA. This chapter continues with an outline of the experimental setup used in the first part of the study including the development of the virtual model. It then goes into a description of the results, and a discussion.

A summary discussion including conclusions is presented at the beginning of Chapter 6. Limitations and strengths are then presented. Finally, this thesis discusses the significance of its findings including potential clinical and pre-clinical relevance.

Chapter 2

2 Background

This chapter begins with a brief review of knee anatomy to familiarize the reader with the anatomical and physiological concepts that are discussed in later chapters of this text. The chapter then moves to discuss the procedure of TKA including implants used, and possible alignment types. It also includes a review of computational models of both the intact knee, and the TKA, knee available in the literature. This chapter then discusses previously published computational ligament modelling techniques. In the last part of this chapter, results gleaned from investigations surrounding the effect of TKA implant malalignment on TKA patients are examined.

2.1 Knee Joint Anatomy

Before introducing the anatomy of the knee, it would be prudent to review common anatomical planes, axes, and terminologies that are integral to understanding both TKA surgical procedure and knee motions. The human body can be described by three planes (transverse, coronal, sagittal) shown in Figure 2-1. Directions can then be described with respect to these planes. *Anterior-Posterior (AP)*: anterior being towards the front of the body and posterior being towards the back of the body, these directions are perpendicular to the coronal plane. *Medial-Lateral (ML)*: medial being the direction heading towards the mid-sagittal plane and lateral heading away from the mid-sagittal plane, these directions are perpendicular to the sagittal plane. *Inferior-Superior (IS)*: inferior being in the direction towards the bottom of the body and superior being in the direction towards the top of the body, both are perpendicular to the transverse plane. *Proximal-Distal*: with proximal being closer to the torso and distal being further away from the torso. AP, ML, IS are also used to describe the three translational degrees of freedom (DoF) a human joint may have.

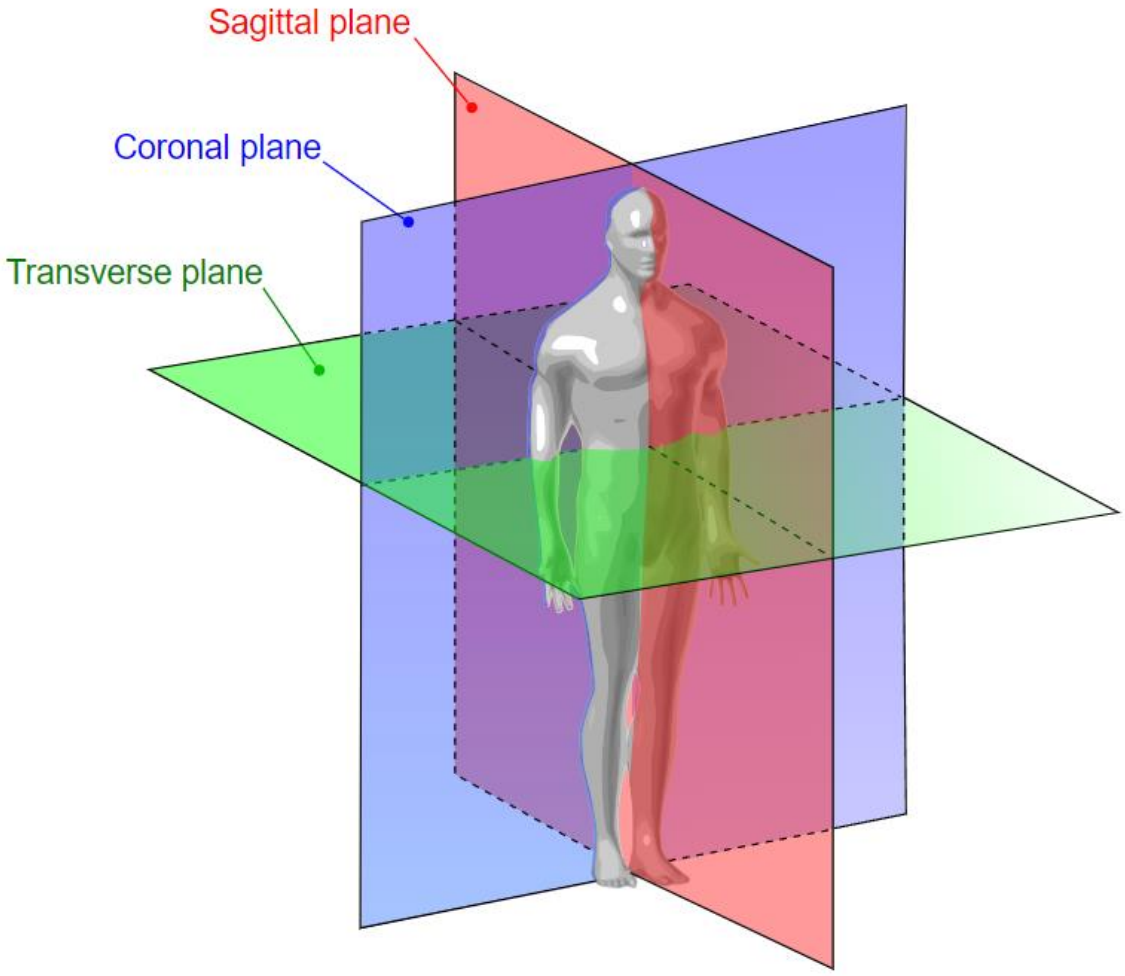

Figure 2-1: Common planes used to describe anatomical motion in the human body. (*image courtesy of LibreTexts powered by MindTouch® through the following creative commons license:* https://creativecommons.org/licenses/by-sa/4.0/*)*

Human joints (i.e., the knee) may have up to six degrees of freedom: three are translational (above), and three are rotational. The three rotational degrees of freedom are described as follows for the knee. *Flexion-Extension (FE)*: bending within the sagittal plane, where the angle between the proximal and distal ends of the knee decreases in flexion and increases in extension. *Abduction/Adduction (AA)*: abduction being a movement in the coronal plane that moves the joint away from the mid-line of the body and adduction being a movement that moves the knee joint towards the midline of the body. When discussing the knee, the terms varus and valgus (VV) refer to the alignment

of the joint. With varus referring to the adduction of the tibia with respect to the femur, and valgus referring to the abduction of the tibia with respect to the femur. *Internal-External rotation (IE)*: internal rotation describes the inward rotation of the tibia with respect to the femur, and external rotation being an outward rotation of the tibia.

The tibia (shinbone) and femur (thighbone) are two of the major bones that make up the knee joint as seen in Figure 2-2. The other two bones visible in Figure 2-2 are the patella and the fibula. Figure 2-3 shows the motions described above as they pertain to the human knee.

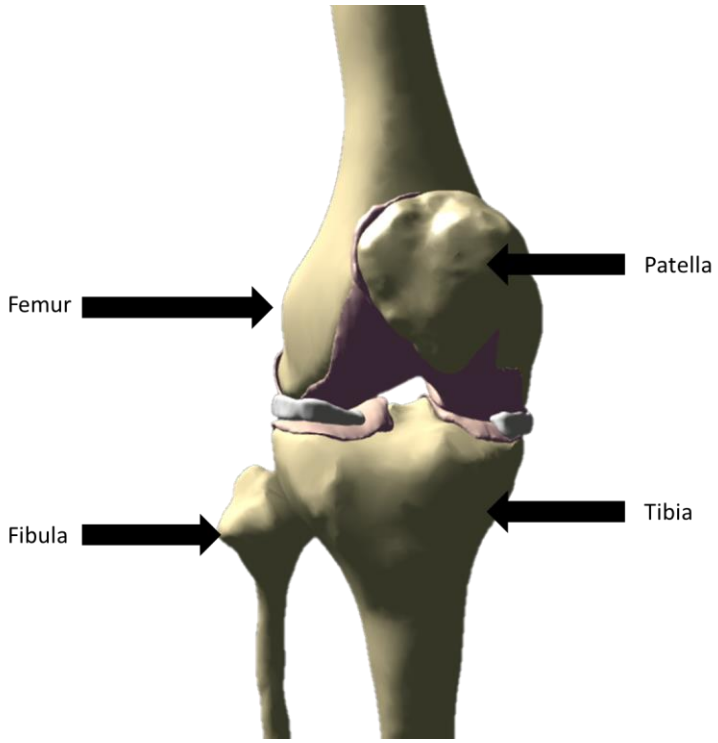

Figure 2-2: Bony anatomy of the knee joint including the femur, tibia, fibula, and patella. These four bones make up the tibiofemoral joint as well as the patellofemoral joint.

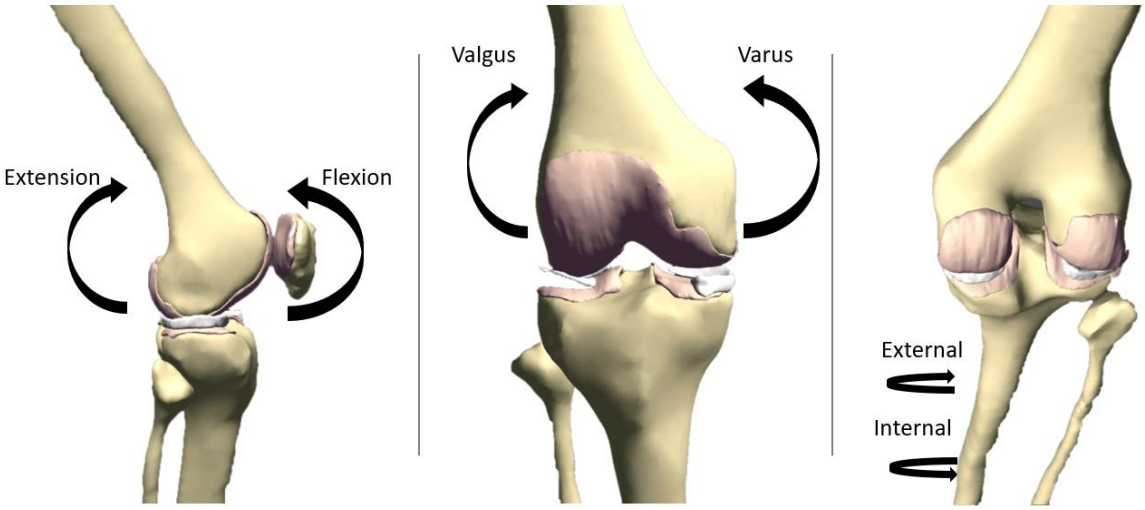

Figure 2-3: Anatomical rotations of the knee. Flexion-extension, and varus valgus rotations are interpreted with respect to the femur. Internal-external rotation are determined with respect to the tibia.

The femur, tibia, fibula, and patella comprise the knee as well as two distinct joints: the patellofemoral joint and the tibiofemoral joint. The content enclosed in this thesis will focus exclusively on the tibiofemoral joint and how it is affected following TKA. In the healthy knee, the femur and tibia are separated by a layer of cartilage on each bone, as well as two separate fibrous menisci on the tibia – the lateral meniscus and the medial meniscus. The menisci distribute load about the tibia and can also act as shock absorbers within the tibiofemoral joint [5]. Though the menisci help with load and some shock absorption, overall knee stability is possible thanks to a strong capsule as well as soft tissue structures such as ligaments and muscles. The studies in later chapters of this thesis focus exclusively on the ligaments in the knee so a review of these structures will be necessary.

Ligaments are critical to knee stability as it is a major joint with no degrees of freedom restricted by bone. Ligaments restrict AP translation, and along with the knees geometry they restrict VV and IE rotation. Our models, shown in Figure 2-4, include the posterior cruciate ligament (PCL), the superficial medial collateral ligament (sMCL), and the lateral collateral ligament (LCL). The anterior cruciate ligament (ACL) and deep MCL were not included in our model as they are routinely released during TKA [6], [7]. The

ACL is responsible for resisting the anterior translation of the tibia with respect to the femur which is explained by its attachments located anteriorly on the tibia and posteriorly on the femur [8]. The PCL is primarily responsible for preventing the posterior translation of the tibia with respect to the femur. It has an attachment site in a large footprint at the posterior edge of the tibia – hence its name [9], [10]. Its attachment footprint on the femur stretches along the inferior-medial inner surface of the femoral notch [9], [10]. The PCL can be classified into two distinct yet inseparable bundles: the anterolateral posterior cruciate ligaments (alPCL) and the posteromedial posterior cruciate ligament (pmPCL). The PCL is split categorically into these two bundles due to their unique behaviour as the knee flexes. The alPCL is slack in full extension and becomes more taught as the knee flexes; however, the pmPCL is slack in deep flexion and becomes taught in extension [6], [11], [12]. The two collateral ligaments synergize to prevent ML translation as well as VV and IE rotations. The sMCL is one of three ligament bundles that make up the medial complex of the knee – along with the deep MCL and the posterior oblique ligament (POL) – and the most important following TKA due to its high force contributions [7], [13], [14]. The sMCL is the largest medial side ligament and has a single femoral insertion around the medial epicondyle of the femur. Its tibial insertion is quite large and situated further distal along the tibia than most other knee ligament insertions [15]. The sMCL is most taught in extension and its length reduces significantly every 15° of flexion until 90° leading to reduced force as the knee is flexed [16], [17]. The posterior portion of the sMCL experiences the most significant length change as the knee is flexed. The LCL attaches on the femur near the lateral epicondyle, its distal insertion is on the fibular head rather than attaching to the tibia [11]. Similar to the sMCL, the LCL is most taught during extension and becomes more lax as the knee is flexed [16].

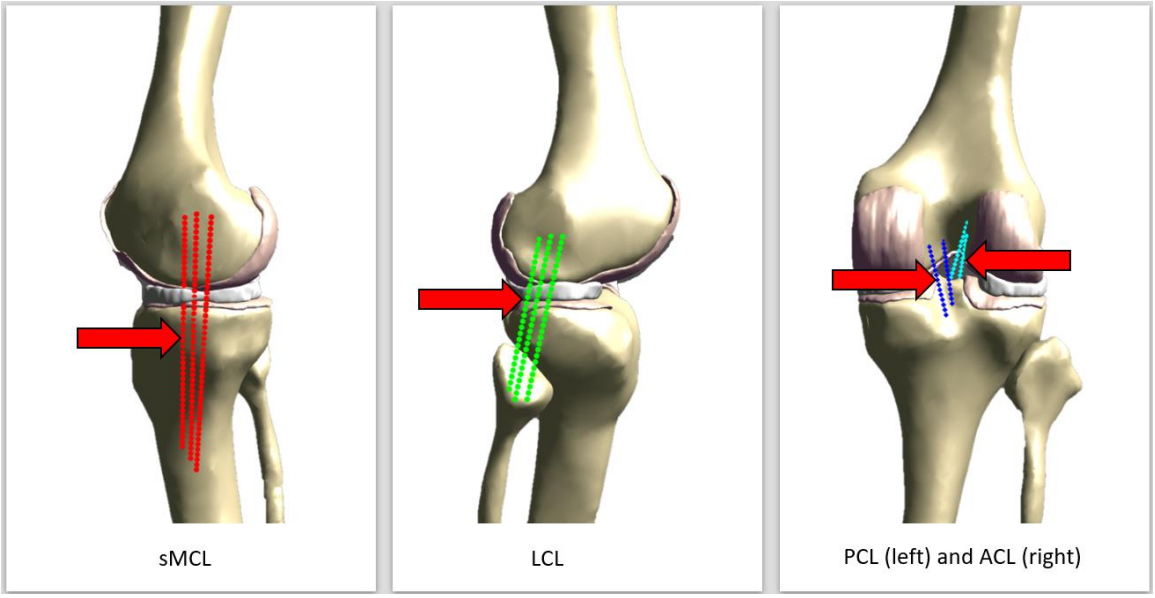

Figure 2-4: Important ligaments in the knee including the sMCL, LCL, ACL, and PCL.

2.2 Total Knee Arthroplasty and Modelling

TKA is a highly invasive surgery that is typically performed as an end stage treatment for knee osteoarthritis, though on rare occasions it is used to treat severe knee trauma [18]–[21]. Osteoarthritis (OA) is the fourth leading non-fatal cause of disability worldwide [22]. The most common form of OA is knee osteoarthritis which affects over 250 million people across the world [23]. In Canada, this high disease prevalence results in over 70 000 TKA surgeries being performed each year [24].

TKA surgery involves a series of cuts made on both the femur and tibia so that the prosthetic components can be attached as seamlessly as possible. The size of the knee varies from person to person and needs to be kept constant despite the addition of three separate prosthetic components, i.e., the correct amount of bone needs to be resected to ensure that prosthetics don't add length to the normal healthy knee. Typically, there are 8 mm to 10 mm cut off the distal end of the femur in accordance with typical femoral component thicknesses [25]. A resection guide is used to make the distal femoral resection. This resection aligns most closely to the transverse (axial) plane. Following this, four resections are made to match the distal femur's shape to that of the femoral

component. The four resections are as follows: anterior cortex, posterior condyles, posterior chamfer, anterior chamfer [25]. They can be made in any order. The measurements taken and the cuts made vary depending on the surgeons' TKA alignment method. TKA alignments such as mechanical and kinematic alignment will be discussed in more depth during section 2.4 of this thesis. Careful cuts and ligament release can properly balance the joint which will have superior outcomes compared to an unbalanced knee [26]. Two common methods of ensuring a balanced joint in TKA include gap balancing and measured resection. The gap balancing technique uses ligament release prior to bone resection which can result in improved stability during flexion [27]. This technique relies heavily on the integrity of the sMCL and the LCL following surgery. In comparison, the measured resection technique requires bone cuts to be made independently of soft tissue tension while using bony landmarks such as the transepicondylar axis to set femoral component rotation. Due to variation in bony anatomy among patients, substantial error in component rotation can occur when using a measured resection technique [27].

The only resection of the tibia aligns most closely to the axial plane, not unlike the first cut of the femur described above. This tibial cut uses another sizing tool to align the resecting plane of interest [28]. Like the first femoral resection, the tibial resection is most closely aligned to the transverse plane and dependent on the desired alignment. An Ultra High Molecular Weight Polyethylene (UHMWPE) insert is a plastic tray that snaps into the top of the tibial component and allows for the smooth flexion of the femoral component upon it which is essential for normal flexion and extension.

TKA research over the past 20 years has included serial case studies based on patient reported outcomes and gait analysis, but that has lacked quantitative data necessary for biomechanical analysis [29], [30]. *In vivo* studies can be done to study gait kinematics and with recent advances instrumented implants can be used to measure joint contact forces as well [31]. In fact, recent technological advances have created instrumented implants that allow joint contact forces to be recorded post-surgery and communicated to a separate device without the need to retrieve the device from the patient [32]. Despite having the most reliable, biologically accurate data, *in vivo* studies are costly, time-

consuming, and must be limited to what the patient can withstand. That is to say that parametric analysis is often not possible, nor is acquiring data that would require invasive procedures (e.g., ligament force data). The drawbacks of *in vivo* studies can be addressed through other study designs that allow parametric analysis and can easily measure joint contact forces including ligament forces. One way to investigate applied forces is through *ex vivo* cadaver studies aided by joint motion simulators. One machine of interest to this thesis is the AMTI VIVO 6 DoF joint motion simulator (Advanced Mechanical Technology, Inc., Watertown, MA, USA), herein referred to as the VIVO. This servohydraulic joint motion simulator is capable of manipulating joints through the relative movement of a femoral and tibial actuator [33], [34]. The upper (femoral) actuator provides flexion-extension movement and varus-valgus rotations while the lower (tibial) actuator initiates medial-lateral, anterior-posterior, and inferior-superior translation as well as internal-external rotation. Forces are recorded using a 6 DoF load cell within the tibial actuator operating with closed loop controls which allow each DoF to be operated independently in either force- or displacement-control mode. The VIVO is also the first joint motion simulator that fully expresses motions in clinically relevant Grood-Suntay (GS) coordinates [35]. The GS coordinate system was designed to easily translate biomechanical information between researchers and clinicians and thus can be used to convert cartesian coordinates and motions into the clinically relevant motions discussed above (e.g., varus-valgus rotation of the femur, internal-external rotation of the tibia).

The VIVO also has a related visualization software that operates simultaneously while the VIVO is being used but can function independently as a virtual joint motion simulator as well. VIVO Sim Visualization software (Advanced Mechanical Technology, Inc., Watertown, MA, USA) emulates the VIVO's functionality in a fully virtual environment. Therefore, it is capable of operating each DoF independently in either force- or displacement-control mode. The virtual simulator also possesses virtual ligament modelling capabilities. Using proximal and distal origins of insertion, stiffness value, and reference strain, the digital simulator determines an exerted ligament force based off 1991 findings published by Blankevoort and Huiskes. [36]. Blankevoort's model was a complex ligament model that required articular surface geometry, origins of insertion,

stiffnesses, and reference strain of the ligaments being modelled. Blankevoort, et al. also demonstrated that knee motion predicted by a model with deformable contact surfaces was not necessarily different from the motion predicted by non-deformable contact surface meaning knee modelling using rigid-body models is a viable option. During this thesis, a unique ligament model for a TKA knee will be created using VIVO Sim.

Many computational knee models in the literature are subject-specific, with geometries based on cadaveric CT or MRI data and ligament origins determined manually by experienced surgeons or from MRI images [36]–[41]. Creating subject-specific models requires defining subject ligament insertions, thus there has been research devoted to automating the definition of ligament insertions based on bony anatomy [40]. Jeong, et. al. used their computational model to identify isometric ligament position by using a model based on 10 patients' CT data [41]. Other groups refined available virtual ligament models using experimentally determined reference strains [37]. Scott Illsley defined an intraoperative method to precisely identify ligament anatomy to be used in a knee model for computer assisted TKA surgery as part of a surgical advisory system [42]. Guess, et. al. used various models to investigate ligament mechanics in the TKA knee, as well as forces experienced by the meniscus in the healthy knee [39], [43]. The abovementioned models all consider ligaments to be either simple one-dimensional point-to-point springs, or one-dimensional springs that also simulate ligament wrapping. Ligament modelling techniques will be covered in more depth in the next section, however, regardless of their representation, simple ligament models determine force based on elongation and ligament stiffness according to Equation 2-1 [36]. None of these models have been used to investigate the effect of ligament complexity, ligament wrapping, or to investigate the biomechanical effects of surgical malalignment following TKA. Thus, using a rigid-body computational model to investigate the biomechanical effects of ligament modelling techniques and TKA malalignment will help inform future researchers on their possible modelling techniques.

Eq. 2-1
$$f = \begin{cases} \frac{k\varepsilon}{4\varepsilon_1} & 0 \le \varepsilon \le 2\varepsilon_1 \\ k(\varepsilon - \varepsilon_1) & \varepsilon > 2\varepsilon_1 \\ 0 & \varepsilon < 0 \end{cases}$$

2.3 Virtual Ligament Modelling

High incidence of knee ligament injuries during activity has led to a surge in effort to quantify knee ligament force-strain behaviour during various motions and activities [44]. The human ligament – insensitive to strain rate over time, and able to reach a preconditioned state after multiple loadings without experiencing hysteresis – has born two approaches to its modelling [45]. These approaches were modeled in a paper by Frisen, et al. in 1969. Frisen looked to provide a mathematical explanation to the tangible one-dimensional model created by Viidik in 1968 that represented ligaments as a series of springs and dashpots [46], [47]. Frisen explains the two approaches where the non-linear elastic behaviour can either be explained by multiple elastic elements engaging at different magnitudes of total ligament strain, or by a single elastic element coiled into a spring shape. Either of these two models explain the toe-region of a ligament's stress-strain behaviour (Figure 2-5). This toe-region is a non-linear stress response to strain, represented as an upward-facing concave region on a graph, where the entire ligament has yet to become taught and thus is not able to exert its full potential stress.

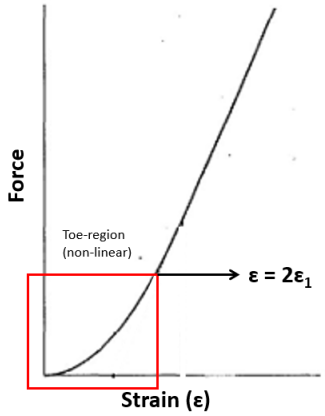

Figure 2-5: The stress-strain relationship of a human ligament. With a strain greater than 2ε1 the relationship is linear. Prior to this, in the toe region, the ligament exhibits non-linear behaviour. Adapted from Blankevoort, et al. [35].

Viscoelastic models have also been developed despite ligaments' insensitivity to strain rate. In unique cases such as high-rate loading, high impact moments, creep, and stress relaxation, viscoelasticity must be considered [48], [49]. A model for ligament viscoelasticity still widely used today is quasi-linear viscoelasticity (QLV) developed by Fung [50]. Though commonly used, this model has met criticism for sometimes representing so-called physically unreasonable behaviour [51]. Frisen and Viidik also did work to implement this model but these were for one-dimensional scenarios as well. This thesis, however, only includes quasi-static loading protocols and thus viscoelasticity – which is affected by strain rate – is not included in analysis [52].

Computational knee models define individual ligament bundles using origins of insertions, stiffnesses, and reference strains. Origins of insertion are typically subject-specific and easily determined using magnetic resonance imaging (MRI) techniques. The relative motion of the proximal (femoral) and distal (tibial/fibular) insertions changes ligament length, thus creating strain which will generate a predictable force via Equation 2-1 where ε_1 is the spring parameter which is assumed to be 0.03 for human ligaments [37]. Reference strain is the strain of the ligament at the reference pose – which is typically the knee in full extensions. Stiffness denotes a ligaments ability to resist strain at any pose. The reference strain is subject specific, and thus varies between computational models. Though ligament stiffness is also subject specific, much more agreement exists in the literature on which values to use while modelling. Bloemker, et al. determined zero-load lengths experimentally through manually flexing cadaver knees and determining the length at which ligaments first go taught [37]. Li, et al. used a minimizing function to determine zero-load lengths based on Equation 2-2, where ε_r is the reference strain, l_r is the length of the ligament at the reference pose, and l_0 is the zero-load length of the ligament [53].

Eq. 2-2 $$\varepsilon_r = \frac{l_r - l_0}{l_0}$$

Ligament model complexity has since been able to increase thanks to technological advances which include three-dimensional ligament models. These models are typically analyzed using finite element modelling (FEM) techniques. Thus, current research aims

to refine modelling techniques related to material properties and three-dimensional deformability, still building on mathematical models established in the past [54], [55]. Other studies, including one by Halloran, et al., compare model complexities based on computational cost and biological accuracy [56]. However, these studies on ligament complexity continue to surround three-dimensional finite element modelling. The same effort has not been put forth to study complexity in one-dimensional ligament modelling, with one study suggesting that modeling ligaments as one-dimensional springs with FEM reduces accuracies in reported kinematics and contact pressures compared to modelling ligaments as a continuum [57]. This group used an optimized spring model where each ligament was represented by two bundles and compared it to a literature-based continuum model, and an optimized continuum model. Kwon, et al. also investigated ligament model complexity using FEM by measuring the effect of reconstructing the ACL with one-dimensional point-to-point bundles of varying diameter. They found that bundle diameter had a minimal effect compared to insertion, although it did provide a slight increase in stability [58].

However, FEM is not the only way to model ligaments so virtual ligaments as a three-dimensional continuum of material is not always a possibility. Thus, simpler rigid-body CAD knee models must rely on one-dimensional non-linear elastic springs for ligament modelling. Guess, et al. has demonstrated their model's ability to effectively simulate a subject-specific *in vivo* experiment, demonstrating simple computational modeling's ability to generate biologically accurate data [39]. They determined that the cruciate ligaments do not engage during passive flexion which compared well with experimental lengthening patterns. Smith et al. used a computational model to predict contact force distribution within the TKA knee and found that an implant's coronal plane alignment affects knee contact loading patterns [28]. For some groups, the creation of a computational knee model is simply a means to efficiently predict *in vivo* knee loads [32]. With most simple computational models being subject specific, a plethora of unique ligament models have been established with no real agreement on how individual ligaments should be represented. Peters, et al. organized the material properties of many knee models in a critical review published in 2018 [38]. Even though many models exist, their subject-specific nature makes them difficult to compare. Thus, there exists a need to

determine the effect different ligament representations in computational models has on the resulting kinematics.

2.4 Surgical Malalignment

A topic of debate in the current literature is the effect of surgical malalignment of implants during surgery. Malalignment is a broad term that can refer to imperfect positioning of the either the tibial or femoral implants with respect to the bone in any degree of freedom. Before discussing malalignment, a review of currently practiced alignment types would be prudent.

Normal knee joint alignment typically has a knee joint angle (HKA) 2°-3° varus compared to the mechanical axis [19], [59]. A normal knee HKA is shown below in Figure 2-6. However, the goal for many TKA techniques is to reduce this difference to 0°. This means that many TKA outcomes have HKA angles of 0°. This is known as neutral alignment. A 2012 study by Bellemans et. al. has shown that 32% of men observed and 17% of women observed have knee joint angles greater than 3° [60]. Fahlman et al recently found that 81.8% of observed subjects had the same alignment in both knees [22]. One of the classical methods of TKA is the mechanical alignment. This method aims to neutrally align the post-TKA knee. The idea behind this method is to resect both the femur and tibia perpendicularly to each of their respective mechanical axes which results in a 0° knee joint alignment. The goal of this alignment is to ensure even stress distribution of force about the knee joint [28], [59], [61]. There will also be a posterior slant to the tibial resection of 3°-5° to reduce ligament stress in flexion. This method is seen as potentially disadvantageous due to the changing of the physiological joint line [62]. This study uses a mechanical alignment in its TKA models, but that isn't the only alignment type practiced in the operating room. Another approach exists that still has some controversy surrounding it in the literature: kinematic alignment. This approach does not focus on achieving a neutral knee alignment, but rather attempting to replicate the healthy knee alignment which is typically 2°-3° varus to neutral knee alignment. This is achieved by making a more valgus resection of the femur, and a more varus resection of the tibia. A comprehensive meta-analysis by Feng, et. al. suggests that outcomes of kinematically aligned knees are at least as favourable or superior to those of mechanically

aligned TKA knees, yet no literature conclusively states that one provides superior outcomes to the other [63].

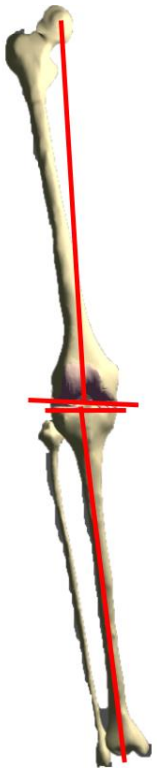

Figure 2-6: HKA of healthy knee, which is a few degrees varus.

Unfortunately, malalignment is possible whether a procedure is using mechanical or kinematic alignment. Malalignment in each DoF has been characterized in the literature. For example, the varus-valgus alignment is considered to be normal if limb alignment is within 0±3° of the mechanical axis [64]. Fang et al. and Ritter et al. suggest varus-valgus malalignment increases component failure rate within 8 years of the primary surgery [30], [65]. However, malalignment has not been linked to revision rates. Of interest to our study is femoral component rotation. Optimal femoral component rotation can be determined by one of four methods: the trans-sulcus axis (TSA, better known as Whiteside's line), the surgical transepicondylar axis (sTEA), the anatomical transepicondylar axis (TEA), and the posterior condyle axis (PCA) [66]. For all landmarks, a high degree of interpatient variability exists meaning the amount of rotation varies from patient to patient [67]. This study used the PCA to determine the femoral rotational alignment. This is achieved with an internal rotation of the femoral component

with respect to the femur by 3.0±1.2° which has been shown to reduce the need for lateral retinacular release [68], [69]. The goal of the femoral component rotation is to achieve a rectangular flexion gap [67]. By rotating the femoral component, the gap between said component and the UHMWPE insert will remain consistent between the medial and lateral sides of the knee. This is due to the asymmetry of the femur's medial and lateral condyles; without the femoral component rotation the flexion gap would become trapezoidal as the knee is flexed. Anything more internally or externally rotated is said to be a malalignment which can affect early patient reported outcomes [70]. Determining component rotation based on the above-mentioned anatomical landmarks can result in error if a patient has irregular bony anatomy. In these cases, using a patient-specific CT-guided approach will result in more accurate component alignment at a higher time and financial cost [71].

2.5 Summary and Motivation

This chapter has illustrated that the knee is a complex joint with six degrees of freedom whose motion is mainly restricted by soft tissue forces. TKA surgery was also discussed, particularly is ubiquity as an end stage treatment for knee osteoarthritis and how that makes it a fairly common surgery here in Canada. Though the surgery is generally successful at providing the patient with a pain-free knee, there are alarming patient satisfaction rates when compared against those of comparable joint arthroplasties (e.g., unicondylar knee arthroplasty, total hip arthroplasty). With TKA being such a common surgery, there is a need to improve negative patient reported outcomes. One of the reasons for these poor outcomes is joint instability, which may be addressed by a better understanding of the loads crossing the knee joint following TKA. Computational models have been and continue to be used to investigate joint biomechanics following TKA, however, a large degree of variation exists between the way published ligament models choose to represent their virtual ligaments. Though it has been examined for finite element models, a gap in the literature exists when it comes to examining the biomechanical effect of different ligament modelling techniques for simple rigid body knee models. Thus Chapter 4 of this thesis quantifies the biomechanical effect of

ligament model complexity as a function of the number of bundles as well as the effect of simulating ligament wrapping.

Section 2.4 of this chapter discussed another cause for overall instability following TKA: femoral component malrotation. We examined the various ways this rotation is determined in the operating room, and how it contributes to the overall balance of the knee through flexion. However, most studies examining femoral component malrotation look at the qualitative outcomes. Though these outcomes are integral for improving patient satisfaction, an understanding of kinematic and mechanical effects of component malrotation would improve our understanding of component malrotation. Thus Chapter 5 of this thesis aims to quantify the kinematic and soft tissue force contribution effects of femoral component malrotation.

Chapter 3

3 Validating a Novel Computational Model Against a Previously Tested Experimental Model

This chapter describes the practical applications of using rigid body static analysis to conduct biomechanical studies in our lab. The motivation is followed by a discussion about a previous experimental setup and series of studies that will be emulated using this software and how the two were compared. Results are then presented, and the chapter concludes with a brief discussion

3.1 Introduction

TKA surgery is an extremely common procedure in Canada with over 70 000 being performed each year [2]. Though the surgery is generally successful at providing patients with a pain-free knee following osteoarthritis, patient satisfaction during functional outcomes remains low [3]. Thus, there is a drive in the academic community to better understand how TKA surgery can be improved. Though *in vivo* studies are useful for collecting biologically accurate data, they are extremely limited in the types of data they can collect. An *in vitro* knee study on the other hand can invasively examine a cadaver knee to obtain a wealth of force and kinematic data. Joint motion simulators are machines used to simulate biologically accurate motion while using cadaver knees. The commercially available AMTI VIVO 6 Degree of Freedom (6DoF) joint motion simulator (AMTI, Watertown, MA, USA) is a piece of equipment capable of simulated knee joint motion with each axis able to operate in either force- or displacement-control mode [33]. Whether in force or displacement control mode, knee kinematics and applied forces are dictated by either the femoral or tibial actuator in each degree of freedom. The tibial actuator controls all translational degrees of freedom (anterior-posterior, medial-lateral, inferior-superior) as well as the internal and external rotation of the tibia. The femoral actuator is responsible for the varus and valgus rotation of the femur, as well as its flexion and extension relative to the tibia. This machine – herein referred to as the VIVO – is considered to be the most realistic knee motion simulator available due to a combination of its force, range, speed, programmability, and virtual ligament modelling

capabilities [72]. The VIVO can operate with cadavers to investigate biomechanics in *in vitro* studies or operate in "knee mode" to test implants restricted solely by virtual ligaments. Our lab has used the VIVO to determine that PCL-deficiency may not be fully compensated by condylar-stabilized (CS) geometry total knee replacement (TKA) implants during a cadaver study [34]. While in knee mode, however, TKA implants are directly affixed to machine actuators as shown in Figure 3-1. As shown, knee-mode uses TKA implants only; no cadaver knee is necessary for these studies. The joint is kept intact through a combination of contact forces (implant geometry), and virtual ligaments. These virtual ligaments are modeled as non-linear elastic, one-dimensional, point-to-point springs – meaning they exert force along a singular linear axis – and each ligament can be modeled with multiple bundles.

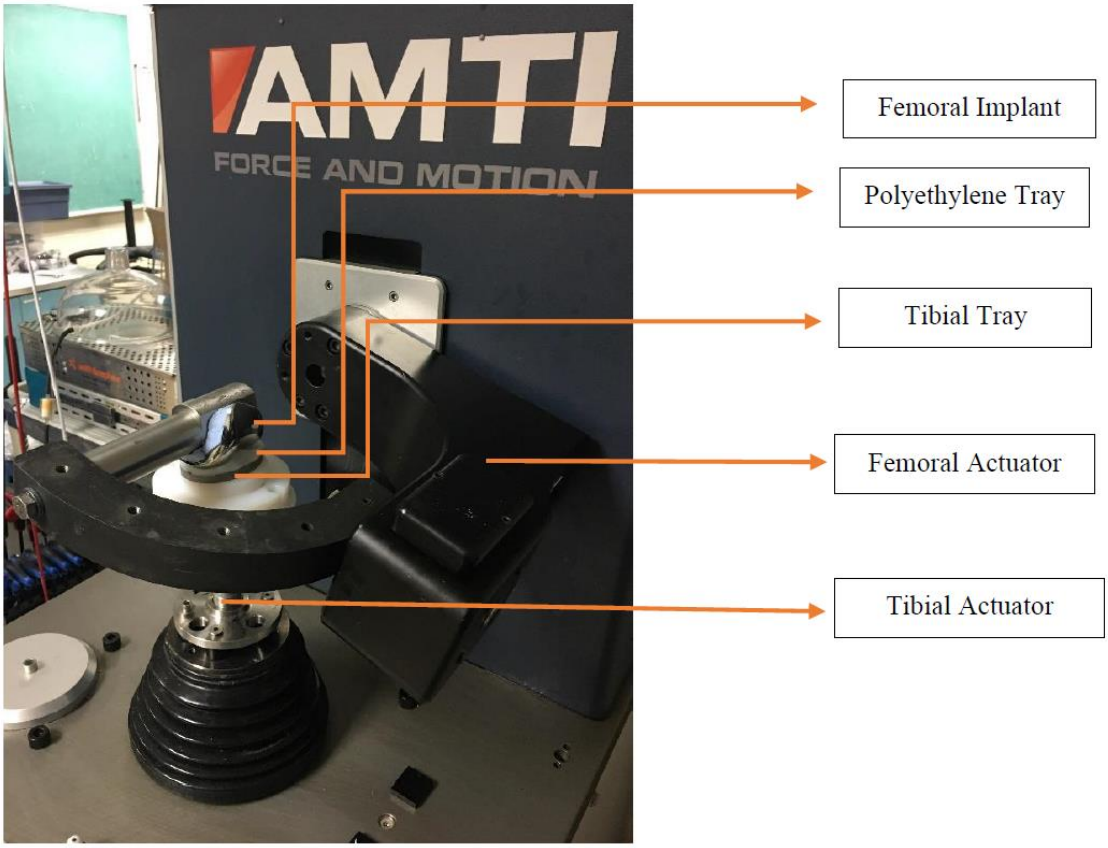

Figure 3-1: AMTI VIVO in knee mode setup with TKA implants cemented to machine actuators.

The VIVO is accompanied by a simulation package meant to aid in the simulation of experiments that include virtual ligaments. VIVO Sim Visualization Software (AMTI, Watertown, MA, USA) simulates the physical VIVO and all its capabilities in a fully virtual environment as a digital twin. VIVO Sim can be synched up to a physical VIVO to show the movement and strain of any virtual ligaments in real time. Though this is an extremely useful visualization tool, our lab wanted to determine if the software could be used to conduct joint motion studies without accompaniment from the physical joint motion simulator. While *in vitro* studies may have improved efficiency over *in vivo studies*¸ the use of computational models are even less costly and provide endless repeatability along with opportunity for parametric analysis at the cost of biological accuracy.

The Biomedical Engineering Research Lab conducts research related to orthopedic biomechanics and thus the physical simulator is always in use. Much of our research surrounds TKA surgery. Since issues still exist within this common procedure there is a drive to optimize every aspect of the surgery. This is something members of our lab work diligently toward, but physical joint motion simulator studies are time consuming and can be expensive when they use cadavers. VIVO Sim – herein referred to as the digital twin – could potentially be used as an independent means of investigating TKA knee biomechanics with high repeatability and efficient parametric analysis. Thus the primary objective of this study was to validate a model operating independently in VIVO Sim against an experimental model tested previously by our lab with the VIVO in knee-mode. We hypothesized that we could closely emulate resulting kinematics and ligament forces in VIVO Sim since both the computational and experimental models would be using the same virtual ligament model.

3.2 Methods

Experimental Model

Figure 3-1 above shows the general experimental set up for the experimental knee model. The TKA components used were for a Triathlon Cruciate Retaining (CR) knee (Stryker Corporation, Kalamazoo, MI, USA) including a size 7 femoral component, size 5 tibial

component, and a 9 mm Ultra High Molecular Weight Polyethylene (UHMWPE) CR insert. This model was based on a cadaver knee used during a previous experiment done in this lab, hence our virtual ligament model was based on the cadaver's CT-scanned knee geometry. Before we could determine ligament parameters, we had to align virtual TKA components to a 3D CAD model of the knee geometry. This will be called our virtual reference model. The TKA components were aligned to bone geometry of our virtual reference model by emulating a mechanically aligned TKA knee. This means that the distal and proximal resections of the femur and tibia, respectively, were made perpendicular to each bone's mechanical axis [19]. We then aligned our reference model in virtual space such that its position in a global coordinate system corresponded to the position our experimental model would be in when placed on the physical joint motion simulator. This would ensure that our ligament insertions were as accurate as possible. To determine the physical model's position within the global coordinate system we took a sphere-fit of the femoral implants when they were affixed the physical simulator and from there determined the experimental model's condylar axis. The condylar axis is the line that passes through the centers of each individual condyle. These centers were determined using the sphere-fits. We then determined the condylar axis of our virtual reference model by sphere-fitting both condyles of our model's femoral implant. The midpoint of these two sphere centers also acted as our origin. We aligned our condylar axis with the axis determined from the experimental model's sphere fit and transformed the rest of the model accordingly. We were then ready to build our virtual ligament model.

The experimental model used a simple virtual ligament model considering the posterior cruciate ligament (PCL), the superficial medial collateral ligament (sMCL) and the lateral collateral ligament (LCL) as single bundles. The deep MCL (dMCL) was not represented as it is routinely released during surgery [73]. Insertions were identified based on information from the literature and were confirmed by a high-volume orthopedic surgeon [9], [10]. Virtual ligaments also require stiffnesses and reference strains to be fully defined by the VIVO, and these values were also obtained from the literature [37], [38]. With the experimental setup in place and the virtual ligament model fully defined, this model could be put through cyclical motions with prescribed kinematics and forces.

This was done with all DoF in force-control mode except for flexion-extension (FE) which was in displacement-control mode. Many motions were tested but for the purposes of our validation study we are only focusing on the following laxity tests: posterior, varus, and valgus. To ensure that the virtual ligament model translated well between the physical simulator and its digital twin, we only looked at laxity tests that demanded high engagement from our three ligaments including posterior laxity, varus laxity, and valgus laxity. All motions were done with 10 N of compression, and with the knee flexed from 0° to 90°. For each laxity test, additional forces or moments were applied at 0°, 15°, 30°, 45°, 60°, and 90°. For posterior laxity, this was a 100 N force acting posteriorly against the tibia. For varus and valgus laxity this was a 10 Nm and a -10 Nm torque, respectively, applied by the femoral actuator. The posterior laxity force was exerted by the tibial actuator. Varus and valgus torques were exerted by the femoral actuator and applied to the femoral component. The compressive force was applied superiorly along the mechanical axis of the tibia. The VIVO automatically records kinematic and force data which we used to compare against results obtained using our computational model.

VIVO Sim Model

Both the VIVO and VIVO Sim calculate kinematics with respect to a reference pose defined by the operator. Thus, if we wanted to accurately compare kinematic data, we would need to ensure that the experimental and virtual models had the same reference pose. This reference pose was taken with the knee in extension, the same pose the CT-based CAD model was in when we determined ligament insertions (from above). Therefore, we simply had to ensure that our VIVO Sim model was positioned in virtual space identically to our virtual reference model. We had already determined the condylar axis of the reference model so we simply had to determine the condylar axis of the VIVO Sim model and transform it to the former's axis placement. This is illustrated in below in Figure 3-2.

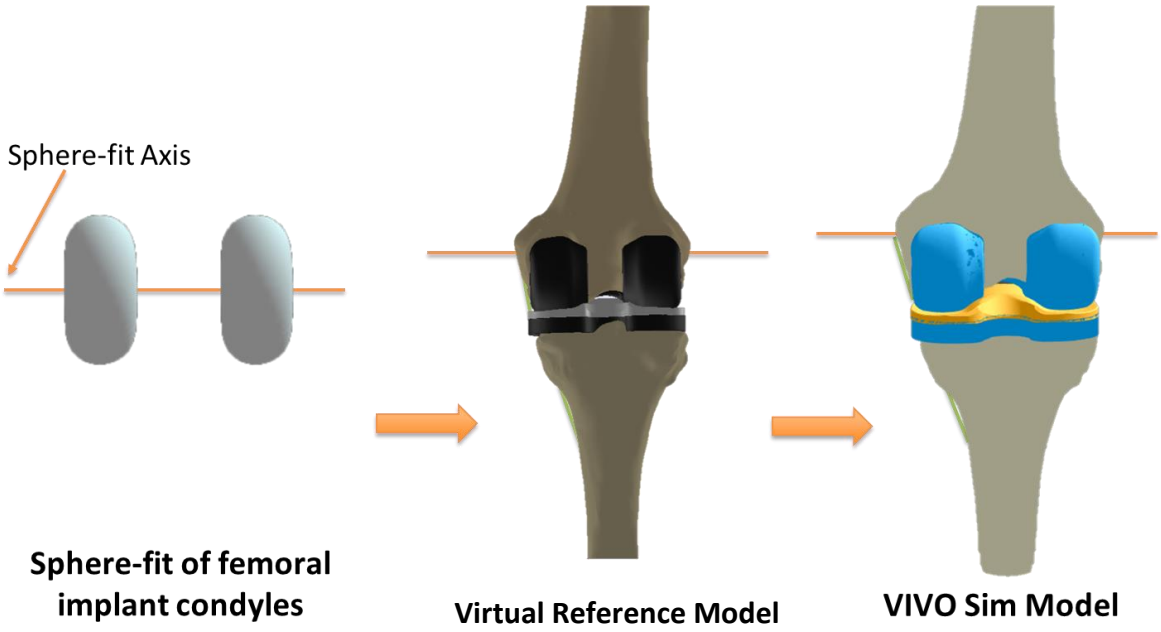

Figure 3-2: A sphere fit of the femoral implant condyles from the experimental model is used to determine its condylar axis. The condylar axis of our reference model is then determined. Our VIVO Sim model must perfectly emulate the reference model's reference pose and is thus aligned to the same axis.

Once positioned in the correct reference pose, we could then apply the exact same virtual ligament model used by the experimental model. Both bone and implant geometries were assumed to be rigid bodies. Coefficient of friction used was $\mu = 0.04$ which is defined in the literature as the coefficient of friction between polyethylene and chromium-cobalt, which are the two contact surfaces in our experimental TKA knee [54], [74]. Within the digital twin the exact same virtual ligament model was used as the experimental study. Though this may suggest that kinematics are guaranteed to be similar, the physical and digital joint motion simulators have different ways of calculating contact force which can affect overall kinematics. Contact on the physical joint motion simulator is determined by the physical contact between components while its digital twin uses an optimization function that minimizes overlap between two predefined contact surfaces, e.g., between the femoral component and UHMWPE insert. VIVO Sim also easily allowed us to apply the same loads as those used in the experimental laxity tests. However, VIVO Sim can only model discrete motion and the experimental motions were continuous. For each test

the VIVO Sim model was simply flexed from the reference pose at 0°, with a 10 N compressive force applied, stopping at each 15° interval for the system to solve, until 90° of flexion. Each laxity test also had the relevant forces or torques (described above) applied throughout the motion. The digital twin has identical machine kinematics to the physical simulator and thus the tibial actuator was responsible for the compressive and posterior forces and the varus and valgus torques were exerted by the femoral actuators in the same fashion as the physical simulator. VIVO Sim has an automatic data acquisition tool called ligament verification. Unfortunately, this tool only collects data at particular points of flexion and is unable to simulate compression, so the data for this study had to be collected manually from VIVO Sim's display.

The physical simulator and its digital twin collect force data in terms of the Grood-Suntay (GS) coordinate system [75]. This coordinate system – represented by three axes – is defined by the relative position of the tibia to the femur. Two axes are embedded in the femur and tibia and align with their respective mechanical axes. The third axis is a common perpendicular to both fixed axes and moves in relation to those two. Thus it is a floating axis. This allows joint-relative forces to be recorded along clinically relevant lines of action for the knee. Unfortunately, the digital twin does not record kinematics in GS coordinates. Thus, in order to compare our VIVO Sim kinematics to the experimental model results we had to process the kinematic data from VIVO Sim. As described in Grood and Suntay's 1983 paper, we converted VIVO Sim kinematics from being in the machine actuators' coordinate system, to the joint's Grood-Suntay coordinate system [35].

3.3 Results

The average anterior-posterior (AP) position of the experimental model during the posterior laxity test with a 100 N posterior force was -5.60±2.55 mm. This was compared its virtual counterpart whose average position was -4.87±2.38 mm (R = 0.92). The average absolute difference between the two was 0.73 mm. A negative value denotes a position where the tibia is posterior relative to reference pose where the knee is in full extension. Ligament tension is measured in VIVO Sim as the total tension acting along the axis of a specific DoF. For posterior laxity we examined the ligament tensions in the

AP direction. The average AP ligament tension of the experimental model during posterior laxity was 64.62±18.66 N. The average virtual ligament tension in the AP direction was 61.81±23.86 N for the virtual model (R = 0.85). The average absolute difference between the two sets of tensions was 6.60 N. Both kinematics and ligament tensions were very similar between the experimental and virtual models, as shown in Figure 3-3 below.

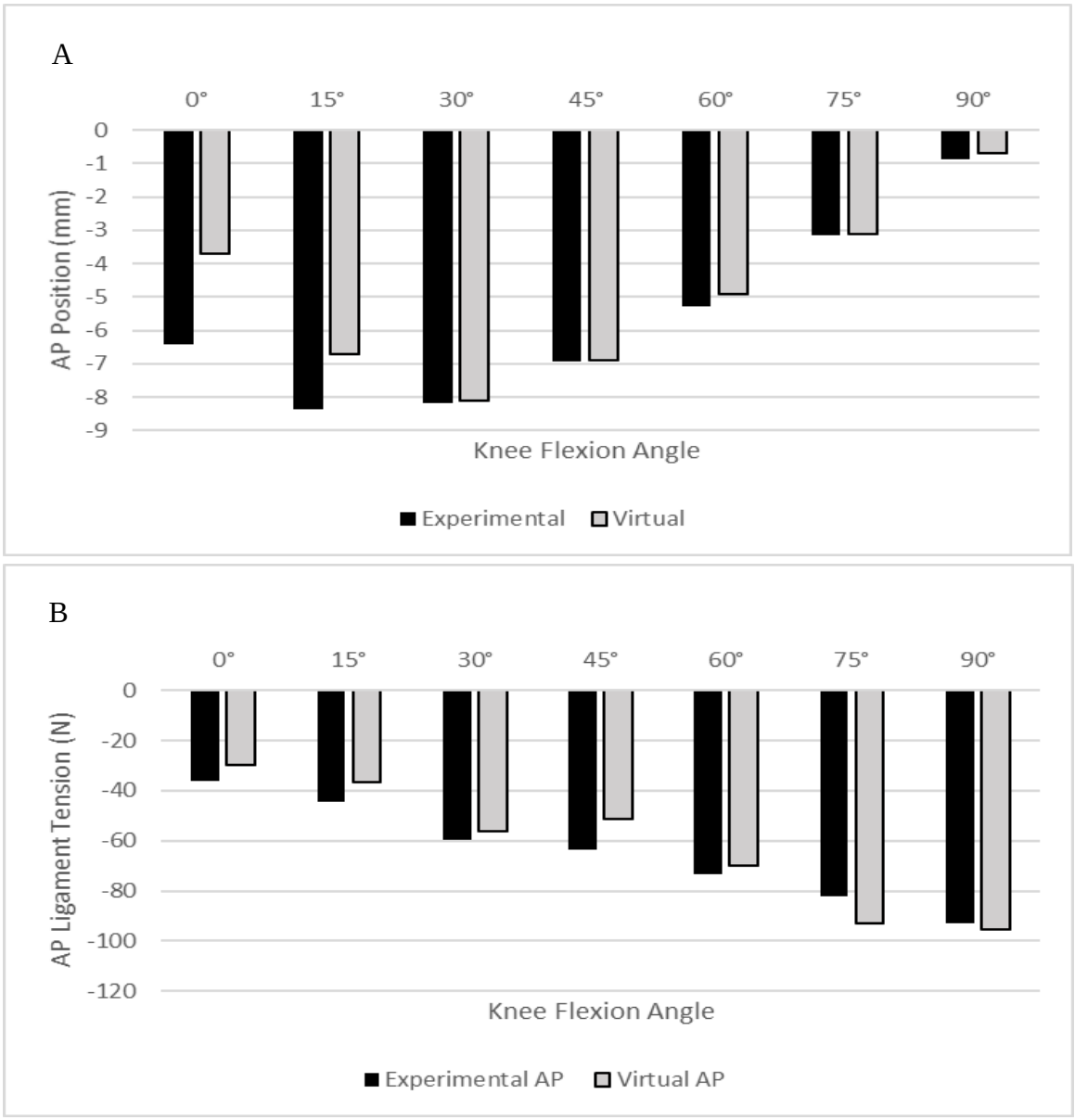

Figure 3-3: Figure 3 3: A comparison of an experimental and virtual knee model's kinematics (A) and ligament tensions (B) in the AP direction during a posterior

laxity test that involved a 10 N compressive force and a 100 N posterior force applied to the tibia. Negative values denote a negative position of the tibia with respect to the reference pose, or a ligament force pulling the tibia anteriorly.

During varus laxity, the average varus-valgus (VV) position for the experimental model through flexion was 2.2±2.1°. The average VV position for the virtual model during the same test was 2.1±2.1° (R = 0.99), with an average absolute difference from the experimental model of 0.3°. Figure 3-4A shows that not only were the average values similar, but the motion paths between the experimental and virtual models were nearly identical as well. The average ligament tensions exerted in the VV degree of freedom by the experimental and virtual models were -5.67±0.22 Nm and -5.25±0.52 Nm, respectively (R = 0.67). The average absolute difference between the two was 0.49 Nm. Valgus laxity also had very similar kinematics between the virtual and experimental models, however, there were some discrepancies in ligament tensions as shown in Figure 3-5B. Average VV kinematics for the experimental and virtual models were -4.0±0.6° and -3.9±0.8°, respectively (R = 0.86). The average absolute difference between the two was 0.4°. Average ligament tensions in the VV direction were still similar at 1.19±1.93 Nm and 2.62±1.81 Nm for the experimental and virtual models, respectively (R = 0.99). The average difference in ligament tension between the two models was 1.42 Nm. However, after 60° of flexion, ligament tension in the VV direction acted in the direction of the applied force as opposed to resisting it (shown by negative values in Figure 3-5B).

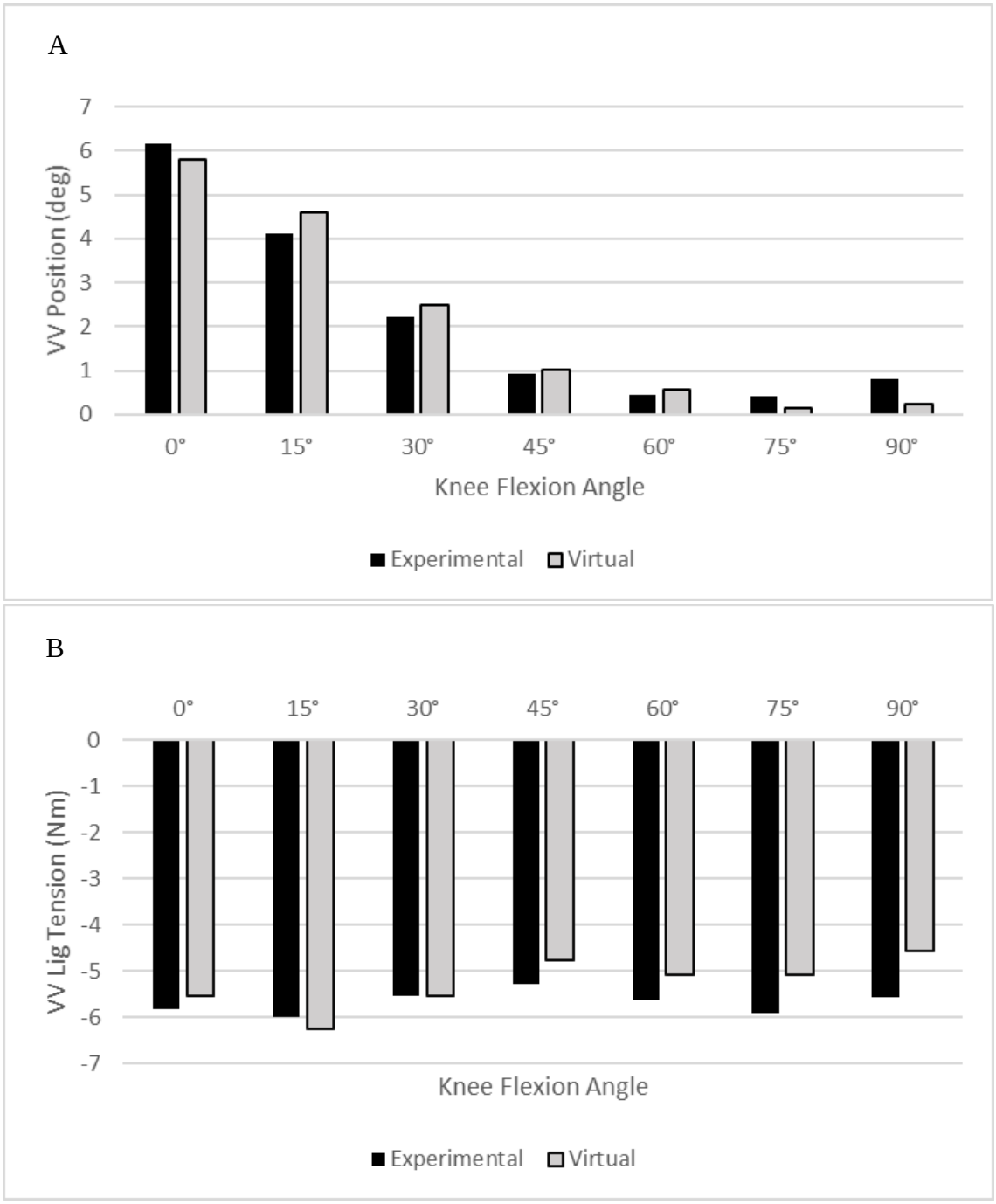

Figure 3-4: A comparison of an experimental and virtual knee model's kinematics (A) and ligament tensions (B) in the VV direction during a varus laxity test that involved a 10 N compressive force and a 10 Nm varus torque applied to the femur. Negative values denote a valgus position of the femur with respect to the reference pose, or a ligament torque pulling valgus.

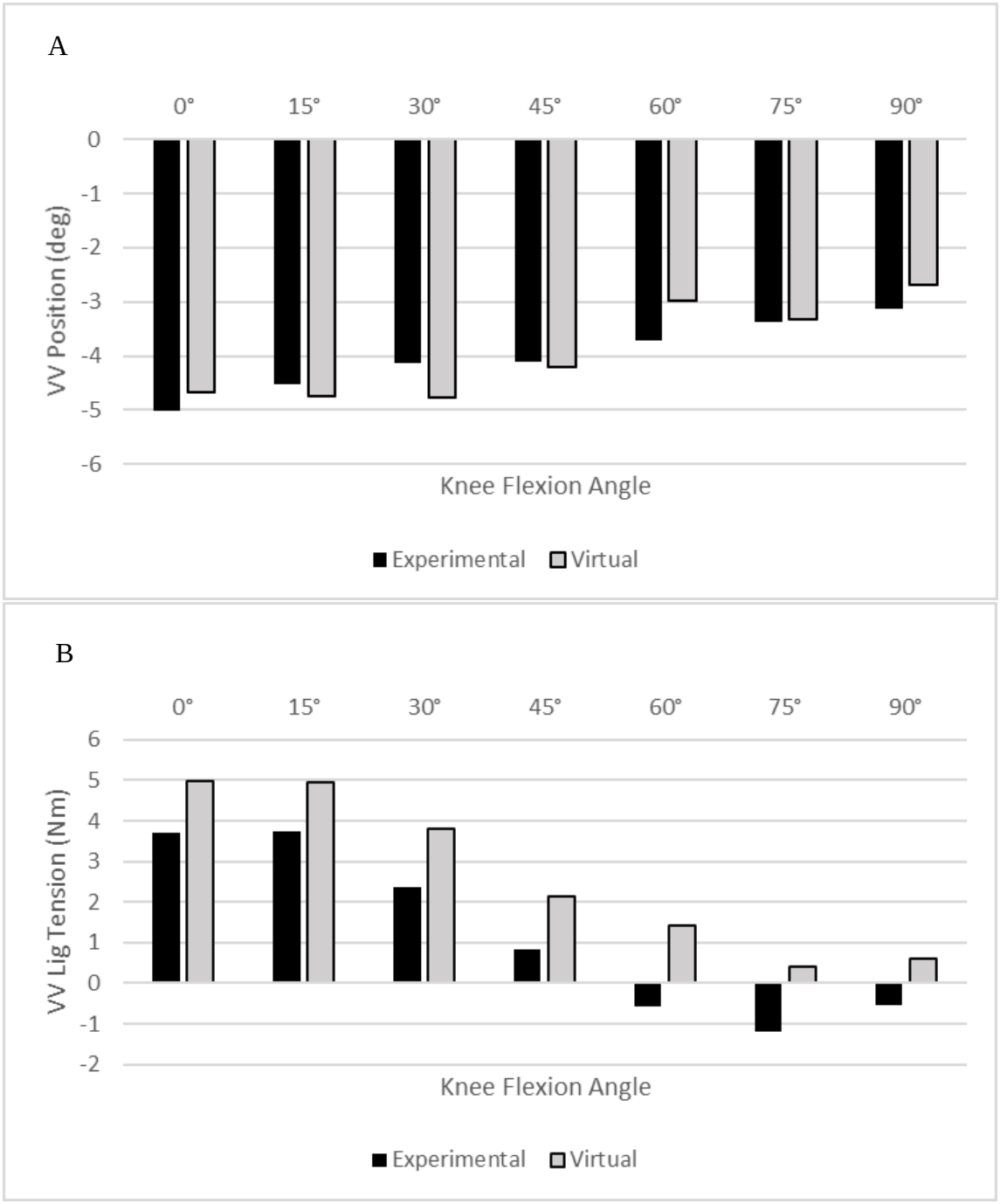

Figure 3-5: A comparison of an experimental and virtual knee model's kinematics (A) and ligament tensions (B) in the VV direction during a valgus laxity test that involved a 10 N compressive force and a 10 Nm varus torque applied to the femur. Negative values denote a valgus position of the femur with respect to the reference pose, or a ligament torque pulling valgus.

3.4 Discussion

The objective of this study was to assess the software VIVO Sim's ability to replicate the kinematics and the ligament forces of a physical joint motion simulator by validating a virtual model against a previous experimental model tested on the physical VIVO joint motion simulator. We compared kinematics and ligament tensions during three loading scenarios: posterior laxity, varus laxity, and valgus laxity. These motions were selected to engage all ligaments of interest: the PCL bundle will be most engaged during posterior laxity, the LCL will engage most during varus laxity, and sMCL is the main ligament contributor during valgus laxity. For all motions studied, the virtual model was able to replicate the experimental model's kinematics within an average of 1 mm (posterior laxity) or 0.1° (varus and valgus laxities). Furthermore, the virtual model's average ligament tensions that were examined fell within one standard deviation of the experimental model's ligament tensions. The only comparison that had noticeable discrepancies was ligament tensions during valgus laxity. During this motion we saw that the experimental model had a lower average ligament tension in the VV direction, particularly in late flexion when the overall ligament tension was acting with the applied valgus moment as opposed to resisting it. This indicates that the lateral side of the joint was tighter while a valgus moment was being applied. This is unlikely to be the case for two reasons. Firstly, a valgus moment will rotate the femur about the AP axis such that separation appears on the medial side of the joint. This means the insertions of the sMCL will move further apart and the insertions of the LCL will move closer together. This results in the sMCL having a higher strain and thus exerting more force so there is no reason for the LCL to be exerting a higher force as the experimental valgus results suggest. Secondly, the medial side of the healthy knee joint is tighter through flexion and a balanced TKA should replicate this [26]. Based on these two observations, we are comfortable with the behaviour exhibited by the virtual model, which exemplifies a tighter medial side throughout the entire motion. Furthermore, strong correlation between tension values during valgus laxity ($R = 0.99$) show that ligaments exert tension in the same pattern for both models. Based on these findings we can conclude that VIVO Sim can emulate the testing environment of a physical joint motion simulator.

This study had a few limitations. Firstly, we only compared kinematics and tensions during laxity tests which only allows us to compare models under high stress. We also only tested one model. Testing multiple models with either different geometries or different implant alignments would have strengthened the conclusions made during this study.

In summary, this study looked to assess a visualization and simulation tool's useability as an independent virtual biomechanical joint motion simulator so that it could be used as a tool to improve knee-related research efficiency in our biomedical engineering research lab. We compared kinematics and ligament tensions during three laxity testing motions between a previously used physical experimental model and a comparable virtual model within the software VIVO Sim. We found that the virtual model emulated the experimental kinematics and ligament tensions very well, so we concluded that VIVO Sim was capable of simulating knee motion tests independent of the physical joint motion simulator. Future work will use VIVO Sim to conduct biomechanical analysis on fully computational knee models to assess the kinematic results of different ligament modelling techniques. We will also use a VIVO Sim knee model to investigate a variety of clinically relevant scenarios.

Chapter 4

4 Using a Virtual Knee Model to Investigate the Importance of Simulated Ligament Wrapping in a Virtual Ligament Model

The purpose of this chapter is to compare the kinematic effect of different ligament modelling techniques used in the literature. This chapter begins with a review of the importance of TKA surgery and how computational models have been used to investigate TKA biomechanics in the past. It then moves on to discuss the computational model used in this study to compare ligament model complexity as well as ligament wrapping vs non-ligament wrapping techniques. Results are then shared, and this chapter concludes with a discussion.

4.1 Introduction

Total knee arthroplasty (TKA) is a common end-stage surgical treatment to knee osteoarthritis performed over 70 000 times per year in Canada [2]. This highly invasive surgery is generally successful and providing the patient with a pain-free knee, but one study reports nearly 50% of patients studied still remain unsatisfied with the functional outcomes of TKA, e.g., stair-climbing [3]. TKA surgery can also have lower satisfaction rates compared to other joint replacement surgeries such as hip replacement and has been shown to have increased stiffness and wound complication rate compared to unicondylar knee arthroplasty [4], [76], [77]. The key to improving patient outcomes may be linked to a better understanding of the loads crossing the knee joint. The total joint contact force is a result of forces applied to the knee, internal contact forces, and soft tissue forces which can all be studied through a variety of different biomechanical testing methods. Thus, there remains a need to investigate each part of the total joint contact force in the TKA knee.

One way to study and conduct parametric analysis on multiple facets of TKA is computational modelling. Though computational models may lack the biological accuracy of *in vivo* studies and cadaver studies, their comparative cost, and ability to

perform repeatable parametric analysis make them useful tools in the study of TKA knees. Previously published models include a variety of subject-specific ligament models based on geometries from *in vivo* and cadaver studies [37], [78]. Ligaments used in these computational knee models use one-dimensional spring-damper elements that exhibit a non-linear stress-strain relationship as described by Blankevoort, *et al.* [36]. In most cases, the posterior cruciate ligament (PCL) is modeled as two distinct bundles while the medial collateral ligament (MCL) and the lateral collateral ligament (LCL) are modeled with three bundles [8], [79]. The MCL can be further broken down into the superficial MCL (sMCL) and the deep MCL (dMCL), however, the dMCL is often released during TKA surgery as its distal insertion lies too close to the tibial plateau [7], [80]. For the purposes of a TKA knee model, other soft tissue structures such as the anterior cruciate ligament (ACL) and anterolateral ligament (ALL) are ignored as they are also routinely released during surgery [81].

Collateral ligaments are often modelled with three bundles and cruciate ligaments are represented by two. This is due to the way ligaments are represented in literature – with the PCL being represented by an anterior PCL bundle and the posterior PCL bundle for example – but little work has been done to investigate the effect of ligament model complexity on a TKA knee model when modelling ligaments point-to-point springs [82]. Certainly, ligament model complexity has been investigated for the intact knee, particularly when using finite element models. Kiapour, et al. demonstrated that modelling ligaments with 3D geometry along with anisotropic hyperelastic material resulted in a more physiological representation of human knee motion than a uniaxial elastic representation [55]. Kwon et al. measure the effect of ligament bundle diameter on post-TKA knee kinematics and found that diameter had little influence over resulting kinematics but did provide additional stability in some cases [58]. Unfortunately, this work and other studies investigating knee ligament model complexity are dedicated to finite element models (FEMs) [83], [84]. These studies investigate parameters whose importance does not translate well to other computational ligament models such as material parameters and continuum mechanics. Evidently, there is a need to investigate the effects of ligament complexity for other computational modelling strategies such as rigid body models.

To increase their biological accuracy, many computational models use subject-specific bone geometries and ligament insertions [37], [78]. Though the insertions are subject-specific, in simple computational knee models the ligaments themselves are modeled as non-linear elastic, one- or two-dimensional springs that exhibit a stress-strain relationship as described by Blankevoort et al. (Figure 2-5) [36]. Many studies that use 1D ligaments model the posterior cruciate ligament (PCL) as two bundles: the anterolateral PCL (aPCL) and the posteromedial PCL (pPCL) [8], [37], [39], [78]. Other soft tissue structures are also excluded from TKA knee models for the same reason including the anterolateral ligament (ALL), the posterior oblique ligament (POL), and the anterior cruciate ligament (ACL) [81].

Three-dimensional ligament modelling can be advantageous as it allows ligaments to be modeled in a continuum which is more biologically accurate, but this comes with a high computational cost [55], [56]. To circumvent the need to create costly finite element models (FEMs), point-to-point ligament models are used in conjunction with rigid body representations of bony anatomy and implant geometry. Researchers may also choose to simulate the wrapping of the MCL about the medial side of the tibia, as opposed to representing the ligament as point-to-point and having it pass through the tibia's geometry. Bloemker et al. created and validated a computational knee model and chose to represent the medial side ligaments as one-dimensional point-to-point springs that passed through tibial geometry, whereas Guess et al. developed a model that simulated the wrapping of medial side ligaments with midpoint attachments near the tibial meniscus [37], [39]. Though functional models have been developed with both representations of medial side ligaments, to our knowledge, there has been little investigation to determine the biomechanical effects of simulated ligament wrapping.

With these considerations in mind, the primary objective of this study is to determine the effect ligament complexity has on TKA knee kinematics during neutral flexion and laxity testing. Here, ligament complexity will be defined by the number of bundles used to model each ligament. Prior to this, a computational knee model was constructed for the simulation package VIVO Sim Visualization Software (Advanced Mechanical Technology, Inc., Watertown, MA, USA) which emulates the behaviour of the

commercially available 6 degree of freedom (DoF) AMTI VIVO joint motion simulator (Ibid). These equipment will herein be referred to as the physical simulator and its digital twin. Another group used AMTI VIVO technology to model a virtual PCL, but that study did not use the digital twin alone [85]. Thus, this will be the first time the joint motion simulator's digital twin will be used to conduct an independent study. This computational model will use geometries established by Guess et al., with ligament models adapted from their findings [39], [43]. The adapted Guess ligament model will use the common three bundles for the collateral ligaments and two bundles for the PCL. A multi-bundle model will use five for collaterals and three for the PCL, which simply inserts another bundle between those present in the Guess model. The single-bundle model will use a single bundle to model each ligament. A higher number of bundles increases the model complexity, while the single-bundle model will represent each ligament as the bare minimum so that we can gauge how important complexity is while modelling virtual ligaments. As these ligament models will all be designed to exert a similar force, any differences in kinematics will likely be due to force distributions. A secondary objective will be to assess the functionality of the physical simulator's digital twin for modelling TKA knee motion independently.

Healthy human knee ligaments are made up of many bundles and fibers thus it would be logical to assume a more complex model will provide unique results compared to a simple single-bundle model. However, previous finite element modelling studies found that changes in virtual ligament diameter had little influence on knee kinematics but did provide some increased stability [58]. When ligaments are modelled as a continuum of material, a larger diameter is comparable to increasing the number of bundles used as a larger number of bundles will cover a larger area of the bone. Since the ligament will still exhibit a similar force, we assume that the difference in kinematics between the various ligament model complexities will be negligible. However, in some instances the higher complexity may provide increased stability.

The second objective of this study is to determine the effect ligament wrapping has on the kinematics of a TKA knee model. Wrapping of the sMCL will be simulated about the tibia as one of three conditions: unwrapped, simple wrapping, and wrapping with

compensation. Compensation of the reference strain is likely necessary to account for the fact that a wrapped ligament will be longer at a reference pose with the knee in extension. Medial-side ligament wrapping better emulates the healthy knee so we would expect the resulting kinematics to be more indicative of healthy knee motion, particularly with less medial-lateral (ML) movement.

4.2 Methods

Computational Knee Model

Knee modelling will be done using the simulation package VIVO Sim Visualization Software (Advanced Mechanical Technology, Inc., Watertown, MA, USA) which is the digital twin to a commercially available 6 degree of freedom (DoF) joint motion simulator. The computational TKA knee model used in this study was adapted from a validated and peer-reviewed healthy knee model developed by Guess et al [39], [43]. We used the same bone geometries which were obtained from magnetic resonance imaging of a 29-year-old female (height = 170cm, weight = 70kg) free of any lower extremity issues. Though this model was easily adaptable to VIVO Sim's environment, it required a simulated virtual TKA surgery. The geometries used were for a Triathlon Cruciate Retaining (CR) implant (Stryker Corporation, Kalamazoo, MI, USA). This included a size 3 CR femoral implant, an 11mm CR Ultra High Molecular Weight Polyethylene (UHMWPE) insert, and a size 3 tibial tray. These implant components were affixed to bony geometries in an emulation of a mechanically aligned total knee replacement surgery. The mechanical alignment aims to create a 0° joint line between the tibia and femur which requires that resections on both bones be made perpendicular to their respective mechanical axes [19]. The mechanical axis of the femur runs from the center of the femoral head to the intercondylar notch of the distal femur while the tibia's mechanical axis runs from the center of the proximal tibia to the center of the ankle – defined by the midpoint between the medial and lateral malleoli (Figure 4-2) [59]. Furthermore, the tibial resection is made with a 5° posterior slope which aids with ligament balancing, and the femoral implant is externally rotated with respect to the bone [21]. The femoral rotation was evaluated with the condylar axis of the femoral implant being rotated internally by 3° with respect to the condylar axis of the femur [64].

Implant placement and sizing were verified by a high-volume orthopedic surgeon. These geometries were modelled as rigid bodies and the coefficient of friction used was $\mu = 0.04$. This value is defined in the literature as the coefficient of friction between polyethylene and cobalt-chrome, which are the two contact surfaces in a TKA knee [54], [74].

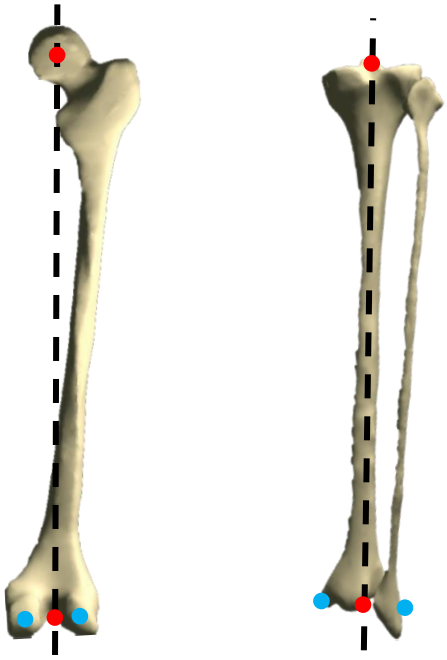

Figure 4-1: Mechanical axes of both the femur (left) and the tibia (right) shown as dashed lines with reference points being red dots. Condyle centers (left) and malleolus points (right) are shown with blue.

Ligament Model

VIVO Sim represents each ligament bundle as a one-dimensional point-to-point spring that exhibits non-linear elastic behaviour as described by Blankevoort, et al. [36]. This non-linear behaviour is not changeable, thus the only two variables that can be changed to affect ligament force contribution are the stiffness and the strain of the ligament at the reference pose, i.e., the reference strain. Within VIVO Sim, multi-fiber ligament models calculate forces that are collinear with the ligament fibers, which are resolved to equivalent forces and moments acting through an origin chosen to lie approximately collinear with the resultant of contact forces [75]. This study used ligament models

adapted from one developed by Guess et al. for a healthy knee [39], [43]. Their model provided origins of insertion, stiffnesses, and zero-load lengths for fourteen bundles that represent seven distinct ligaments. The zero-load length is defined as the length at which the ligament first becomes taught, i.e., the length at which the ligament strain is exactly zero [37]. Our TKA ligament models did not include the ACL, ALL, POL, or dMCL as these ligaments are routinely released as a part of ligament balancing during TKA surgery [73], [81]. What remained were three bundles representing the LCL, three bundles representing the sMCL, and two bundles representing the PCL. This initial model had to be further edited to reduce the initial strain on the sMCL in order to balance the joint in extension such that the joint was reduced without the need to involve compressive forces. The slight release of the sMCL was simulated by reducing the reference strain of one of its bundles. Effectively, the release of taught fibers in extension reduces the strain felt by the whole ligament at this reference pose, thus reducing the reference strain. Reference strains (ε_r) were calculated from the zero load lengths (l_0) given by Guess, et al. and the ligament lengths at the reference pose (l_r) using Equation 4-1. The mid-sMCL (msMCL) bundle's reference strain was reduced from 9.5% to 4.5%. Ligament parameters used for the adapted Guess, et al. model – herein referred to as the "Guess" model – are shown in Table 4-1. Each of the collateral ligaments is represented by three bundles (anterior, mid, and posterior) and the PCL is represented by an anterior and a posterior bundle. Note that a negative reference strain does not mean a ligament bundle is compressed. It is simply a way to illustrate how slack the ligament bundle is so that the system knows at which change in length (strain) that ligament will become engaged.

Eq. 4-1 $$\varepsilon_r = \frac{l_r - l_0}{l_0} \times 100\%$$

Table 4-1: Ligament parameters used for the Guess ligament model.

Ligament	Stiffness (N)	Reference Strain (%)
aLCL	2000	-2.66
mLCL	2000	4.02
pLCL	2000	1.29
asMCL	2500	-4.30
msMCL	2600	4.50
psMCL	2700	4.44
aPCL	12500	-28.6
pPCL	1500	-26.3

The Guess model was used as a baseline model from which two additional models were derived, one that was more complex, and a simpler model. The only parameters that can be varied during virtual ligament modelling are the location of tibial and femoral insertions, ligament bundle stiffnesses, and ligament bundle reference strains. Thus, ligament complexity must be measured as a function of the number of bundles modelled. The more complex model would represent the sMCL and LCL with five bundles each, and the PCL would be represented by three bundles. The extra insertions for this model, herein referred to as “Multi”, were determined by averaging the origins of insertion of the

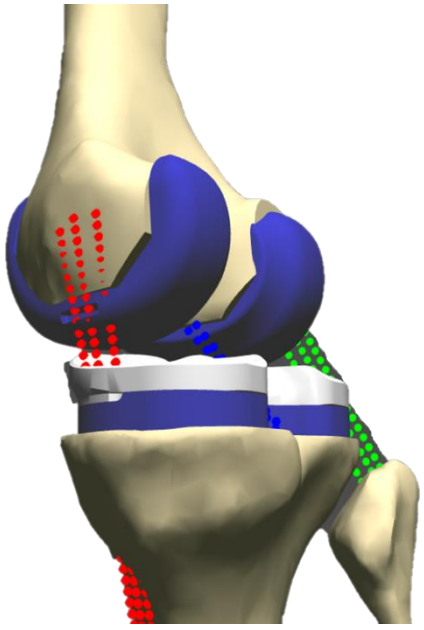

Figure 4-2: Tibia pulled 8 mm inferiorly and 10 mm posteriorly to create tension in all ligaments. These tension values will be used to determine stiffnesses in the new models.

adjacent bundles. For example, the anterior-middle sMCL's (amsMCL) insertion was the average of the asMCL insertion and the msMCL insertion. The reference strains of the new bundles were also determined as the average of the two adjacent bundles' reference strains. The tibia was pulled posteriorly by 10 mm and inferiorly by 8 mm to create tension in all ligaments (Figure 4-3). We measured the forces of all ligament bundles from the Guess model at this reference pose.

From this new reference pose strains of each ligament in the Multi model and the Guess model were calculated. Total forces were calculated for each ligament at this new reference pose using the Guess model, as well as the forces exerted by each individual bundle. These forces were used to create five equations – shown below in Equations 2 through 6 – to determine the forces that would be exerted by the five new bundles of the collateral ligaments.

Eq. 4-2 $$f_T{}' = f_T$$

Eq. 4-3 $$\frac{f_{asMCL}{}'}{f_{msMCL}{}'} = \frac{f_{asMCL}}{f_{msMCL}}$$

Eq. 4-4 $$\frac{f_{msMCL}{}'}{f_{psMCL}{}'} = \frac{f_{msMCL}}{f_{psMCL}}$$

Eq. 4-5 $$f_1 = \frac{f_{asMCL}+f_{msMCL}}{2}$$

Eq. 4-6 $$f_2 = \frac{f_{msMCL}+f_{psMCL}}{2}$$

The first equation assumed that the sum of the forces exerted by all five new bundles ($f_T{}'$) would equal the sum total of the forces exerted by the three bundles of the Guess model at the strained reference pose (f_T). The next two equations assumed that the ratio of the forces exerted by anterior (f_{asMCL}) and middle (f_{asMCL}) bundles, and the middle and posterior (f_{psMCL}) bundles respectively, would be the same between the Multi and Guess models. The final two equations assume that the two added bundles in the multi model would exert a force ($f_1$and f_2) that is the average of the forces exerted by its two adjacent bundles. Once the five forces (f) for the five new bundles are evaluated,

stiffnesses (k) can be calculated with the previously determined strains (ε) using Equation 4-7, where ε_1 is the spring parameter assumed to be 0.03 for knee ligaments [37]. The three PCL bundle stiffnesses were calculated in a similar manner but with two fewer equations since only one extra bundle was being added.

Eq. 4-7
$$f = \begin{cases} \frac{k\varepsilon}{4\varepsilon_1} & 0 \le \varepsilon \le 2\varepsilon_1 \\ k(\varepsilon - \varepsilon_1) & \varepsilon > 2\varepsilon_1 \\ 0 & \varepsilon < 0 \end{cases}$$

The insertions and reference strains for the single-bundle model ("Single") were calculated as follows: the collateral ligaments simply used the insertions and reference strains recorded by Guess, et al. for the msMCL and the mLCL. The single insertion and reference strain of the PCL was determined as the average insertion of the aPCL and pPCL, and the average of their reference strains, respectively. Since we only needed to determine forces for one bundle, only one equation was needed: the force exerted by the single bundle would be equal to the force exerted by the entire ligament in the Guess model. Once the force was determined, Equation 2 was used to calculate the stiffness for each bundle. Ligament parameters used for Single and Multi models are shown in Tables 4-2 and 4-3, respectively. The new models were validated by comparing their total ligament forces exerted at the new reference pose with the total ligament forces exerted by the Guess model. Both the Single and Multi models were within a margin of error of 9% for the PCL, 0.5% for the sMCL, and 0.4% for the LCL when compared to the recorded Guess model forces. A visual of all three model complexities is shown in Figure 4-3.

Table 4-2:Ligament parameters used for the Single ligament model.

Ligament	Stiffness (N)	Reference Strain (%)
LCL	5014	4.02
MCL	5250	4.50
PCL	7663	-27.4

Table 4-3: Ligament parameters used for the Multi ligament model.

Ligament	Stiffness (N)	Reference Strain (%)
aLCL	1157	-2.66
amLCL	1171	0.68
mLCL	1175	4.02
mpLCL	1172	2.66
pLCL	1182	1.29
asMCL	1469	-4.30
amsMCL	1603	0.10
msMCL	1481	4.50
mpsMCL	1509	4.47
psMCL	1105	4.44
aPCL	7841	-28.6
mPCL	2554	-27.44
pPCL	1026	-26.3

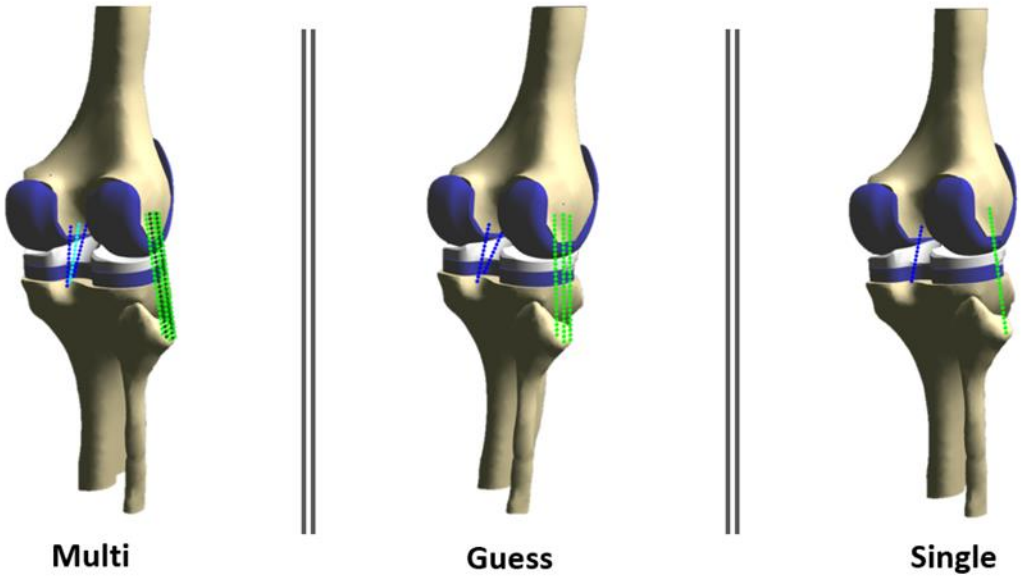

Figure 4-3: The three levels of ligament model complexity tested during this study.

The virtual joint motion simulator allows the user to take advantage of the simulated ligament wrapping capabilities over any of the defined meshes in the model. Wrapping

can only be simulated around one surface at a time, e.g. a ligament can't be wrapped around both the tibia and the tibial tray. The wrapping is simulated by establishing a midpoint attachment site on the wrapping surface that prevents the most penetration by the ligament bundle. In this study, there were three ligament wrapping conditions: one with the normal ligament model, a second that simulates the wrapping of the sMCL bundles around the tibia without compensating the reference strain, and a third with wrapping and compensation. Compensation is done because a wrapped ligament will have a longer length at the reference pose. Ideally, the wrapped ligament will to exert the same strain as the baseline unwrapped models. The compensated reference strain for the wrapped model is calculated using Equation 4-8 and Equation 4-9. First, the zero-load length for the wrapped ligament bundle (l_0^w) is determined using the reference length of the wrapped ligament bundle (l_r^w) and the reference strain of the baseline ligament bundle (ε_r^b). The reference strain of the wrapped ligament bundle (ε_r^w) can then be calculated using the wrapped bundle zero-load length and the baseline bundle's reference length (l_r^b). A wrapped and unwrapped model are also shown below (Figure 4-5).

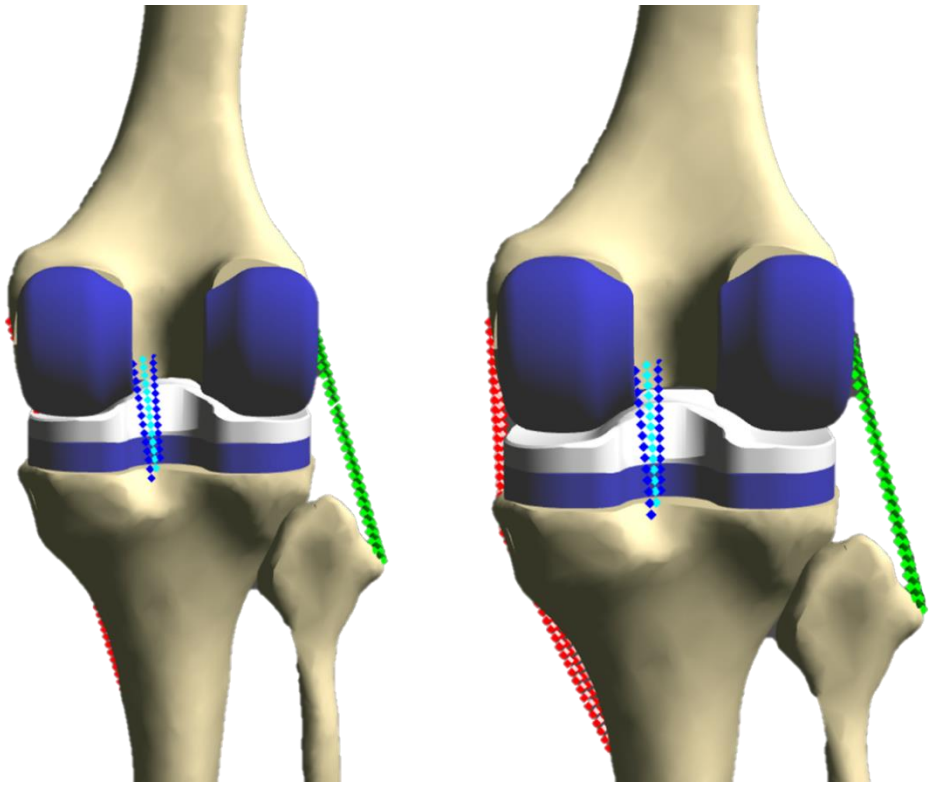

Figure 4-4: Comparison of virtual ligaments without simulating the wrapping of the sMCL about the tibia (left), and a virtual ligament model that simulates ligament wrapping (right).

Eq. 4-8 $$l_0^w = \frac{l_r^w}{\varepsilon_r^b}$$

Eq. 4-9 $$\varepsilon_r^w = \frac{l_r^b - l_0^w}{l_0^w} \times 100\%$$

Testing a Computational Knee Model in a Virtual Joint Motion Simulator

Testing was performed for three levels of model complexity as well as three levels of ligament wrapping. This means each loading scenario was performed for the Single, Guess, and Multi levels of complexity without simulated wrapping first. Then the loading scenarios were repeated for each level of complexity with simple wrapping, and then wrapping with compensation. The gimbals to which the femur is attached control flexion-extension (FE) as well as varus-valgus (VV) rotation, whereas the platen controls all degrees of translation and internal-external (IE) rotation by manipulating the tibia. For all tests, all DoF except for FE were set to force control mode. Neutral flexion had no forces applied and the models were simply flexed from 0° to 90° with data being recorded at 0°, 15°, 30°, 60°, and 90°. Data was recorded at these same intervals during laxity tests as well. Posterior laxity was simulated with a 100 N force applied against the tibia. VV laxity was simulated with an 8 Nm torque applied for varus laxity and a -8 Nm torque applied for valgus laxity. Internal laxity was tested with a 4 Nm torque applied to the tibia, and external laxity used a -4 Nm torque. Loads were selected based on values used in the literature for similar laxity testing [85]. Loading is shown in Figure 4-6 below. Note that the loads used are not indicative of normal joint contact forces experienced during daily motions such as normal gait. In these scenarios total joint contact forces can be upwards of 1500 N. However, as demonstrated by this group in a 2021 abstract, ligaments only make up as little as 11% of this joint contact force during the stance phase of gait [86]. This can increase up to 68% of the total joint contact force during swing phase. Since ligaments make up such a small percentage of the joint contact force during normal daily motions, our laxity tests use much smaller loads so that ligament contributions become more important, and we can draw conclusions that are specific to ligament laxity. Testing was done using VIVO Sim's "Ligament Verification" tool which automatically records data including kinematics, contact forces, and ligament forces at

each of the aforementioned flexion angles. However, VIVO Sim's outputted kinematics are in terms of the machine parts' reference frame and in cartesian coordinates. For ease of understanding, knee joint kinematics are typically reported in terms of clinically relevant rotations using the Grood-Suntay (GS) coordinate system [35]. The GS coordinate system is made up of three sets of axes: two fixed to solid bodies and one floating axis. The fixed axes are the mechanical axes of both the femur and the tibia. The floating axis is a common perpendicular to both fixed axes and moves in relation to both. Rotational kinematics were converted from cartesian to (GS) coordinates using the method described in their 1983 paper using the MATLAB (MathWorks, Natick, MA, USA) script found in Appendix A. For the purposes of this study, we focused solely on the resulting kinematics for each of the three models as well as total ligament forces in each degree of freedom.

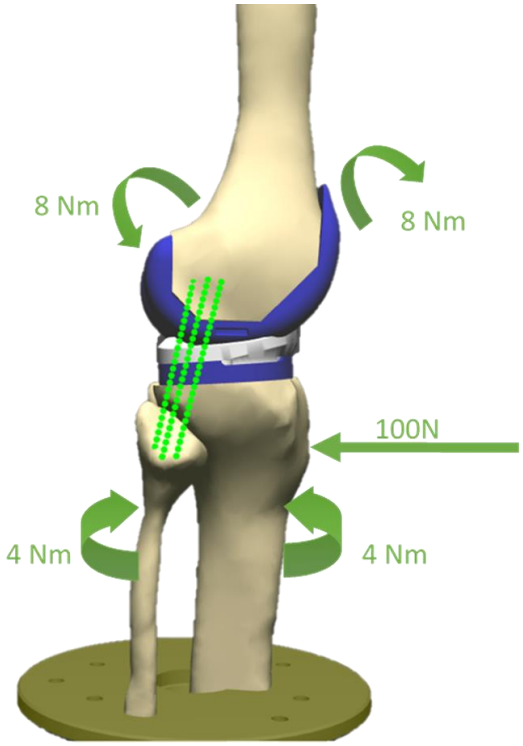

Figure 4-5: Loading scenarios used for testing including a 100 N posterior force acting on the tibia to simulate posterior laxity, 8 Nm torques to simulate varus and valgus laxity, and 4 Nm torques for internal and external laxity.

4.3 Results

Ligament Model Complexity

For the sake of brevity and ease of analysis that may help clarify kinematic effects of ligament complexity, ligament model complexity data is averaged over all simulated ligament wrapping conditions. For detailed results based solely on either ligament model complexity data or simulated ligament wrapping data, refer to Appendix B. During this section, laxity was calculated as the absolute difference between kinematics during a laxity test, and kinematics during neutral flexion. The figures below compare kinematics during each motion for all ligament model complexities. The values in the figures were obtained by averaging kinematics of each motion for each ligament model wrapping condition, i.e. the data for the Multi model is the average of the kinematic data collected with Unwrapped Multi model, the Wrapped Multi model, and the Wrapped & Compensated Multi model. From Figure 4-7, we see that posterior motion limits are similar between all levels of ligament model complexity. Posterior laxity averaged over all points of flexion for the Multi, Guess, and Single models was 4.7±1.5 mm, 5.7±1.4 mm, and 5.7±1.4 mm, respectively. During mid-flexion we see that increased model complexity results in a slight increase in laxity. Neutral flexion kinematics abide by similar behaviour to posterior motion limits. In Figure 4-8 it is demonstrated that neutral VV kinematics remain relatively constant between levels of ligament model complexity. Varus laxities averaged over all points of flexion were 4.1±0.8°, 3.5±0.8°, and 3.0±0.5° for the Multi, Guess, and Single models, respectively. The valgus laxities for the same were 3.3±0.9°, 3.5±1.2°, and 2.63±0.6°. Overall varus and valgus laxity increases with increased ligament model complexity during mid-flexion, though valgus laxity was very similar between Multi and Guess models. Figure 4-9 shows that the overall internal laxity increases with increased model complexity. Inversely, the external laxity decreased with the highest model complexity. Internal laxities averaged over flexion were 30.0±7.7°, 25.3±7.0°, and 23.7±4.9° for the Multi, Guess, and Single models, respectively. The external laxities for the same were 14.9±2.1°, 19.2±3.9°, and 18.1±3.4°. Note that the internal and external motion limits remain similar between

models but the IE position during neutral flexion varies by being more internally rotated with reduced model complexity.

Forces were also measured during neutral flexion and posterior laxity. Average difference in AP ligament force during extension and early flexion (0° and 15° flexion) between posterior laxity and neutral flexion motions for the Single, Guess, and Multi models were 24.62±5.45 N, 12.58±12.29 N, 13.35±6.45 N, respectively. For mid- to late-flexion (30°, 60°, 90°) these values were far greater at 58.21±17.56 N, 64.76±22.62 N, and 62.16±21.63 N, respectively. Also of note is the fact that the Single and Guess models had ML positions of -23.0 mm and -15.6 mm (tibia is medial relative to femur), respectively, at 0° flexion which indicates improper contact between the UHMWPE insert and the femoral implant. This is compared to an ML position of -4.09 mm for the Multi model. To explain these differences, we will need to consider the difference in inferior-superior (IS) ligament forces between neutral flexion and posterior laxity for the Single, Guess, and Multi models. These values were 380.71 N, 290.85 N, and 124.34 N, respectively.

Average difference in VV torque exerted by all ligaments between varus laxity and neutral flexion was 4.07±0.56 Nm, 4.57±0.79 Nm, and 4.53±0.56 Nm for Single, Guess, and Multi models respectively. The differences in VV ligament torques during valgus laxity and neutral flexion were 3.66±0.76 Nm, 3.93±1.18 Nm, 3.64±0.73 Nm. During neutral flexion, all models exhibited an overall valgus average VV ligament torque. These results also affirm that our three ligament models are exerting similar forces and torques during varus and valgus laxities. The large standard deviation in the results involving valgus laxity for the Guess model are due to a large torque experienced at 30° of flexion.

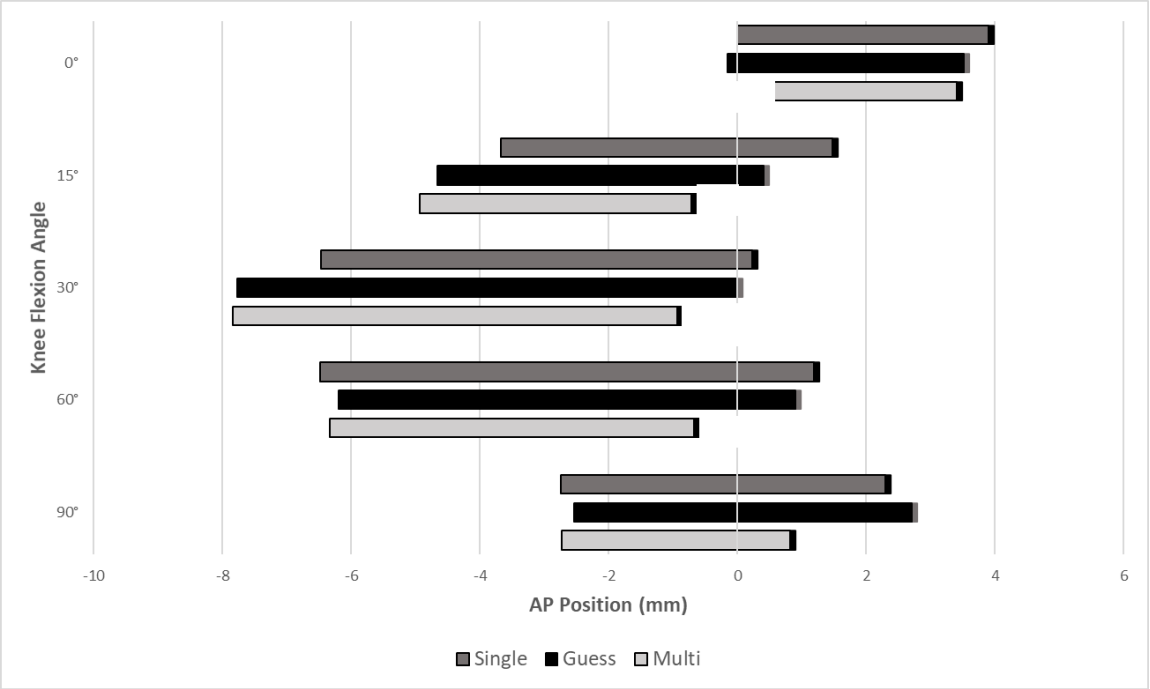

Figure 4-6: Comparison of AP kinematics during posterior laxity between ligament complexity models with data averaged over ligament wrapping models. Averaged AP positions during neutral flexion are shown as solid vertical bars.

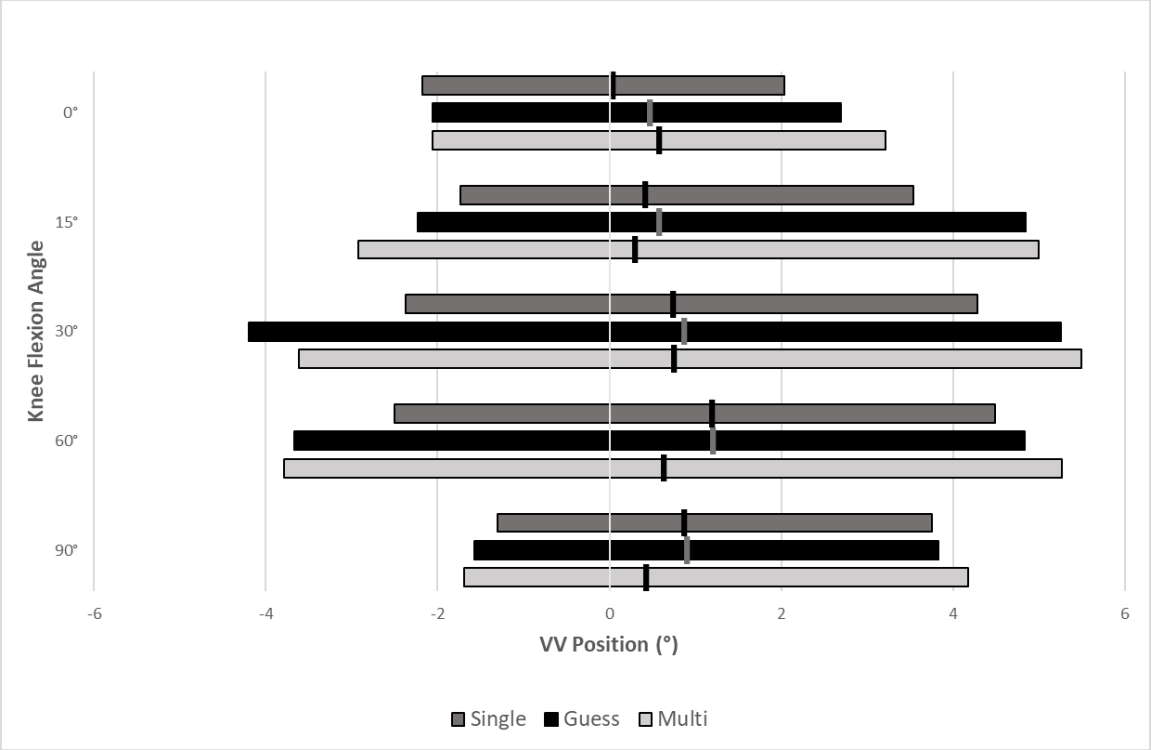

Figure 4-7: Comparison of VV kinematics during varus/valgus laxity between ligament complexity models with data averaged over ligament wrapping models. Averaged VV positions during neutral flexion are shown as solid vertical bars.

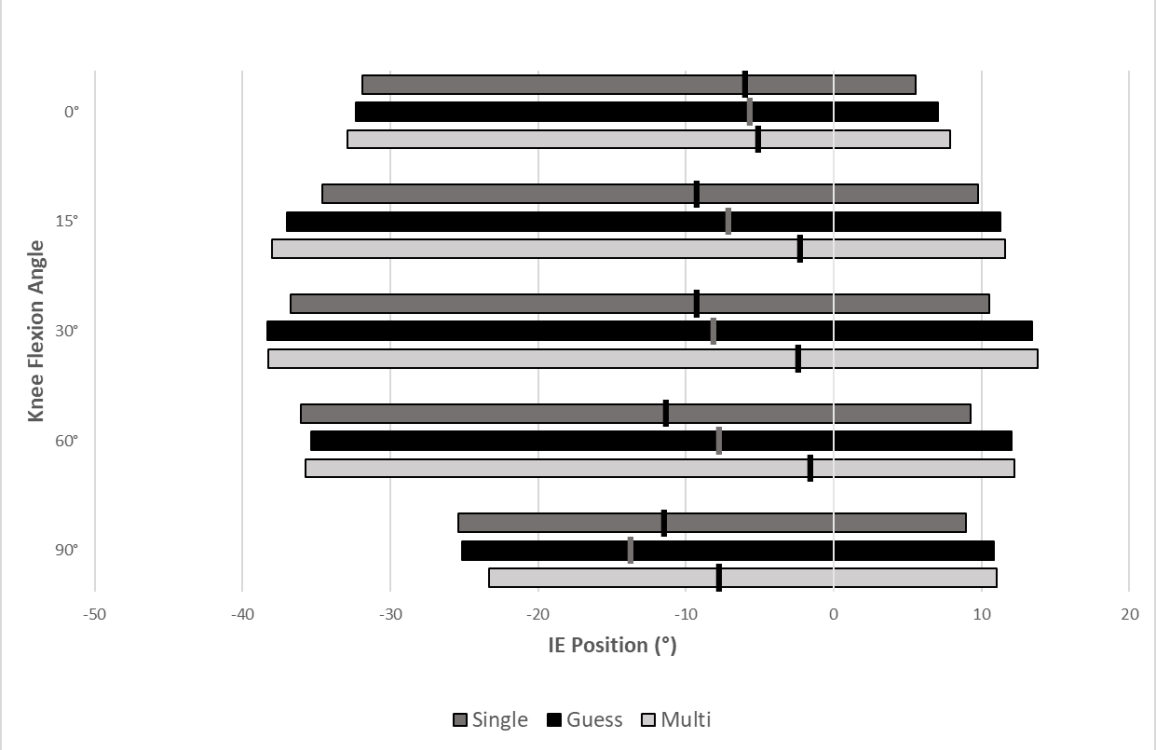

Figure 4-8: Comparison of IE kinematics during IE laxity between ligament complexity models with data averaged over ligament wrapping models. Averaged IE positions during neutral flexion are shown as solid vertical bars.

Simulated Ligament Wrapping

Figures 4-10 through 4-12 show kinematics during each motion and how they vary between levels of simulated ligament wrapping. Data in these figures is averaged between all levels of complexity. This means that the data for the Unwrapped model is the average of the kinematic data gathered with the Multi model, the Guess model, and the Single models. AP laxity averaged through flexion for the unwrapped, wrapped, and wrapped & compensated models was 5.5±0.8 mm, 5.1±1.8 mm, and 5.5±2.0 mm. AP position during both neutral flexion and posterior laxity show no clear pattern in relation to levels of simulated ligament wrapping. Varus laxities averaged over all five flexion angles were 4.0±0.8°, 3.1±0.7°, and 3.5±0.6° for the unwrapped, wrapped, and wrapped & compensated models, respectively. The valgus laxities for the same were 3.5±1.2°, 2.4±0.8°, and 3.5±0.9°. At all points of flexion the simple ligament wrapping without

compensation proved to have the lowest varus and valgus laxities compared to the unwrapped, and the wrapped & compensated models. Though laxities differed, the varus motion limit was similar between all models. Varus and valgus laxities were similar between the unwrapped and wrapped & compensated model but the wrapped and compensated model had a greater valgus motion limit at all points of flexion except 15°. For the unwrapped, wrapped, and wrapped & compensated models the internal laxity averaged over all measured points of flexion was 28.0±9.9°, 23.5±6.5°, and 27.4±5.3°. The averaged external laxities for the same were 19.1±3.6°, 16.8±4.0°, 16.3±1.8°. In general, the simple wrapped model without compensation had the lowest internal and motion limits. Neutral IE position was similar between all models except for at 90° of flexion. The unwrapped model had the greatest external laxity though all three models shared similar external motion limits.

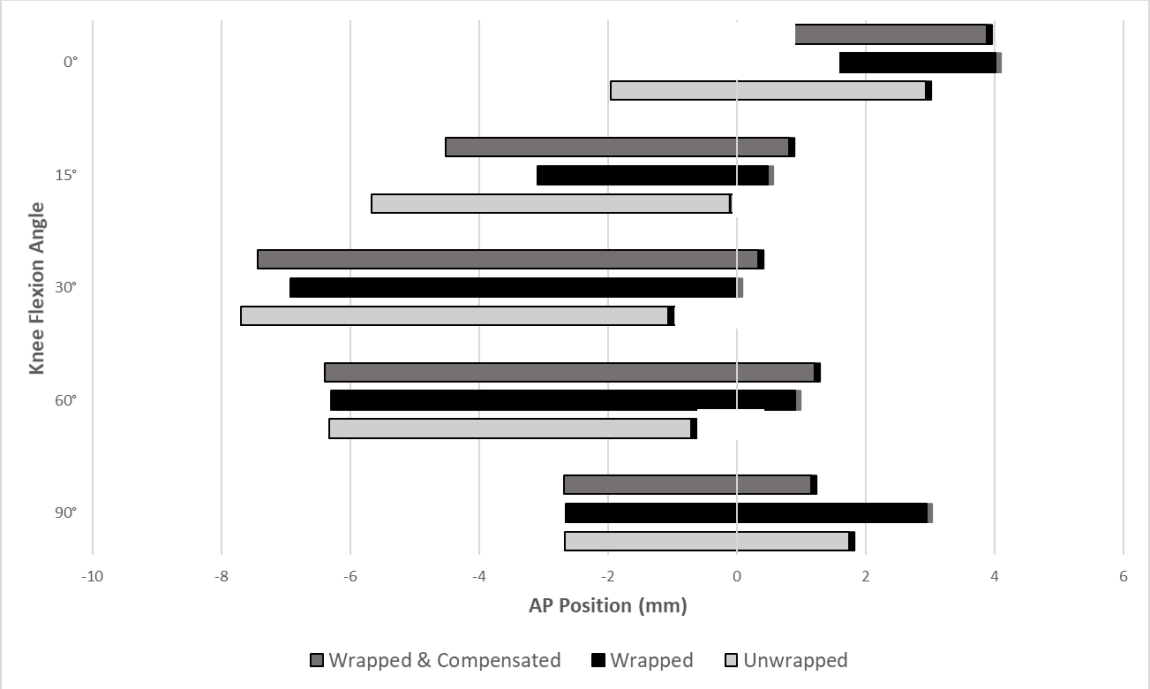

Figure 4-9: Comparison of AP kinematics during posterior laxity between ligament complexity models with data averaged over ligament wrapping models. Averaged AP positions during neutral flexion are shown as solid vertical bars.

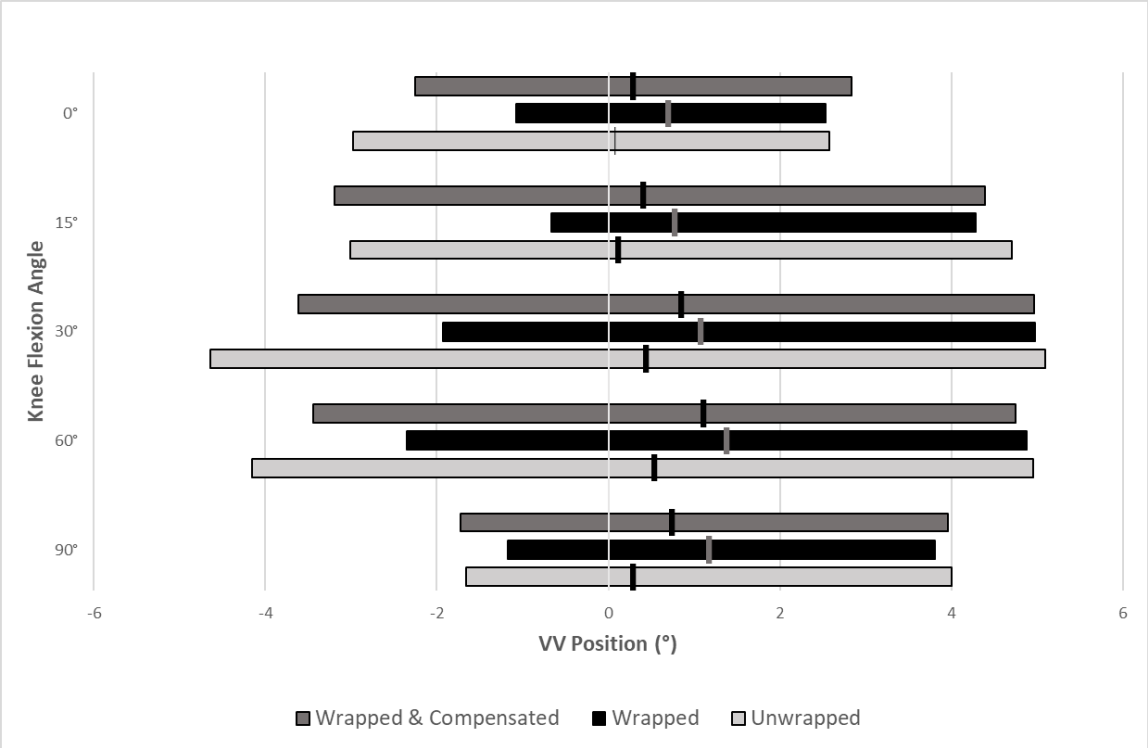

Figure 4-10: Comparison of VV kinematics during varus/valgus laxity between ligament complexity models with data averaged over ligament wrapping models. Averaged VV positions during neutral flexion are shown as solid vertical bars.

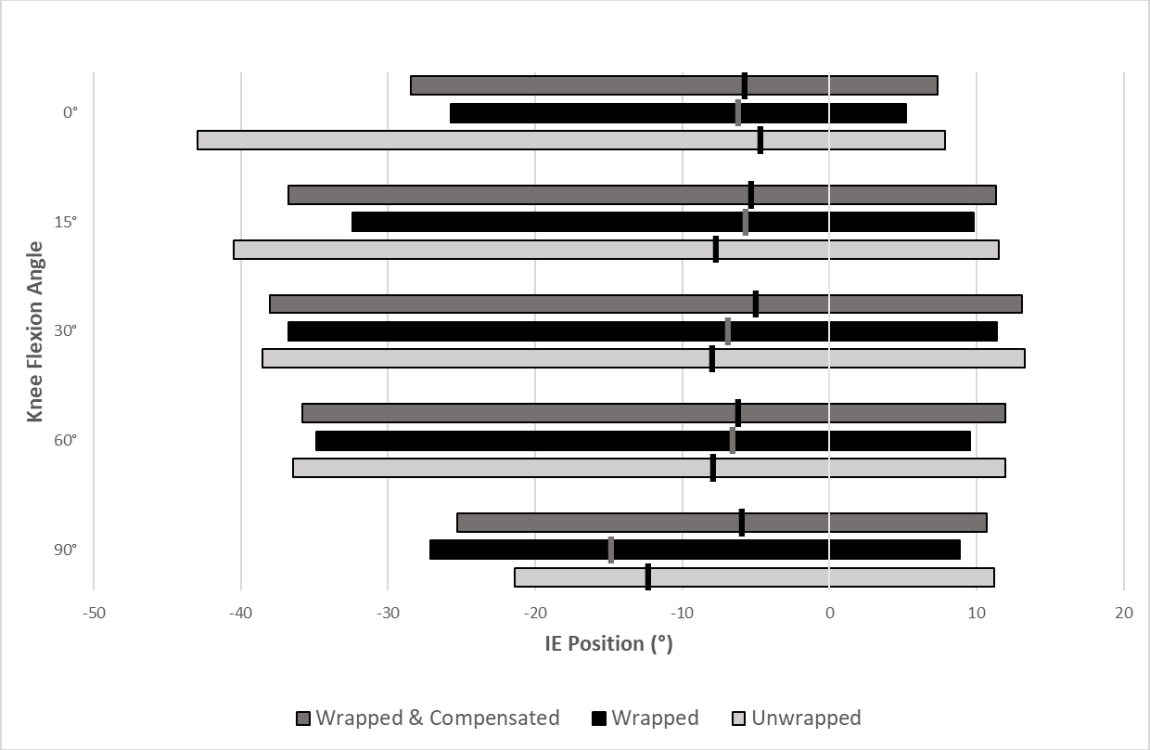

Figure 4-11: Comparison of IE kinematics during IE laxity between ligament complexity models with data averaged over ligament wrapping models. Averaged IE positions during neutral flexion are shown as solid vertical bars.

4.4 Discussion

The main objective of this study was to compare the resulting kinematics of a computational TKA knee model during laxity tests using three different representations of ligament model complexity. With the ligament models having been confirmed to generate similar forces, particularly the sMCL and the LCL, differences in kinematics were likely due to differences in geometry affecting contact force, and the force distribution within the ligaments. Though geometries are identical between the three ligament conditions, differences in ML and AP position can affect the direction and magnitude of contact forces. Furthermore, varied number of bundles to represent ligaments can result in changes in force distribution caused by differing origins of insertion. Ligament engagement patterns are dependent on their position relative to the

femur's flexion axis [86]. For example, ligaments whose insertions are anterior and inferior to the flexion axis will exert a higher force once the knee is flexed. As the knee is flexed, these ligaments will be extended which means they will be exerting a greater force. Average laxities of the three ligament models fell within one standard deviation of each other during all motions. Thus, we cannot conclude that differing the number of bundles in a ligament model results in noticeable differences in laxity test kinematics. A FEM study by Kwon et al stated that bundle footprint size will not influence TKA knee kinematics [58]. Kwon's model was a finite element model which meant it was capable of modelling ligaments as a three-dimensional continuum of material which is analogous to an infinite number of one-dimensional bundles.

Though no clear difference was observed between models, all three knee models simulated neutral motions and laxity tests with predictable kinematics and forces. For example, we saw an increase in ligament forces during flexion compared to extension during posterior laxity. Harfe, et al. identified that collateral ligaments are typically not engaged during late flexion, so the ligament forces beyond this point were likely all due to the PCL bundles [87]. This is logical as the PCL is responsible for resisting posterior translation of the tibia, and thus its contributions will be exaggerated during a posterior laxity test [34]. Furthermore, during neutral flexion with all models we witnessed a gradual internal rotation of the tibia with respect to the femur. This behaviour can be described as the "screw-home mechanism", which describes how the knee joint tightens as the knee is extended which is critical for the knee's stability in extension. Hallén and Lindhal described the mechanism as being influenced by both condyle geometry, and cruciate ligament attachment to the medial side of the knee [88]. With all three models using identically symmetric condyle geometry, it's plausible that the difference in rotations is due to the varied bundle setup of the PCL. In the healthy knee, the PCL is generally represented by two bundles: the anterolateral PCL (aPCL) and the posteromedial PCL (pPCL). During neutral motion, it has been suggested that he aPCL acts primarily during flexion while the pPCL is more active in extension, however recent studies show that the two bundles may work synergistically [82]. In the case of the Single model, there is only one bundle whose position is anterior and lateral with respect to the pPCL insertion of the Guess model. Thus, the Single model is missing a key stabilizer

during flexion of the knee resulting in a more internally rotated knee. Ultimately, the presence of these expected knee motions, and no failures during any of the laxity tests demonstrate VIVO Sim's ability to model and simulate TKA knee motions.

Varus-valgus laxity tests demonstrated the similarity in kinematics between the three ligament models. Neutral VV kinematics are heavily dependent on condyle geometry and contact forces so observing similar VV positions through neutral flexion is expected [73]. When a varus stress is applied, the LCL is engaged to resist the rotation, while the sMCL resists any applied valgus torques. With the sMCL being tighter than the LCL in the healthy knee, the fact that average varus laxity was greater than average valgus laxity comes as no surprise. It was also clearly demonstrated that more bundles resulted in a greater varus motion limit, but during valgus laxity testing the Guess model had the greatest valgus motion limits. The Guess model's outlying positions occurred in early flexion which is when posterior bundles of the sMCL will be the most engaged, with little engagement from the anterior bundles. Since the Single model represents ligaments with a single bundle: there is no force distribution. Since the one bundle is positioned anterior to the flexion axis it will exert a high force throughout flexion leading to reduced valgus motion limit as the knee is flexed. During early flexion, the asMCL bundle of the Guess model will likely not be engaged since its strain in extension is well below 0, thus allowing for greater valgus motion. One reason we don't see the same thing in the Multi model is the presence of a bundle between the asMCL and the msMCL whose reference strain in extension is far greater than that of the asMCL. This bundle, the amsMCL, will therefore engage before the asMCL of the Guess model and resist valgus motion earlier on during flexion.

Posterior laxity tests saw similar behaviour between all models in the AP direction, which was also true during neutral flexion. However, the tibia in the Guess and Single models were positioned extremely laterally compared to the femoral component in full extension (i.e., flexion angle = 0°). This resulted in the lateral femoral condyle not being in contact with the poly. Since the ligaments in these models were modeled as point-to-point springs, the sMCL passes through the tibia, the tibial tray, and the poly meaning the sMCL can do little to resist the lateral movement of the femur with respect to the tibia.

The ligament tensions in the inferior-superior direction were highest in extension for the Single model and lowest for the multi model. Knowing that the sMCL is the tightest ligament during extension, we can assume that the sMCL was the largest force contributor for all models [87]. With a higher IS force from the sMCL, the femoral and tibial attachments are going to try to align coincidentally. Since the geometry prevents excessive IS movement, and the applied posterior force prevents AP motion, the only way for the tibial and femoral insertions to approach one another is in the ML direction. The tibial and femoral insertions of the sMCL are approximately 26 mm apart in the ML direction which explains the 22 mm and 15 mm shift under high tensions. The Single and Guess models are creating a higher force during the posterior laxity test since they don't have additional bundles with lower reference strains to offset the extension that occurs during laxity testing. This motion would be prevented by simulating the sMCL wrapping around the tibia, thus preventing the excessive lateral motion of the femur.

We also used the computational knee model to successfully simulate ligament wrapping with the simulation package VIVO Sim. Ligament wrapping of the sMCL about the tibia was simulated using a midpoint on the proximal and medial edge of the tibia as defined by the virtual joint motion simulator. In the unwrapped model the sMCL simply passes directly through bone, UHMWPE insert, and tibial tray geometry between femoral and tibial insertions which allowed for excessive lateral movement of the tibia with respect to the femur. This limitation of unwrapped models can be clearly seen with the knee in extension during posterior laxity. At the worst, the tibia was 22.95 mm medial to its reference pose in extension (this was using the Single complexity model). With the wrapped model and wrapped & compensated model, this was reduced to below 2 mm. Without wrapping, the sMCL ligament tension primarily acts in the medial-lateral direction due to a diagonal line of action (Figure 5-11A with the Multi model). Furthermore, without wrapping, the only physical boundaries that exist for preventing ML movement rely on the surgical implant geometries; the ligaments generate no contact restraint against the bone. This demonstrates that simulating wrapping is essential for preventing unnatural ML movements from occurring. We also note that the LCL insertions also favour pulling the tibia medially with respect to the femur which evidences that without wrapping that motion is unopposed. From Figure 5-11B we see

that by simulating wrapping, the superior portion of the sMCL acts mainly in the inferior-superior direction to prevent pulling the tibia medially. The tension that acts on the femur (F_1) is primarily pulling the femur directly towards the tibia, there is no ML pull. F_2 may be oriented diagonally with respect to the knee joint but since it is only acting on the tibia it will only serve to increase overall tension. There is also a physical constraint: the tibia cannot move medially with respect to the femur by a large amount as the sMCL can no longer pass through the tibia and implant geometry.

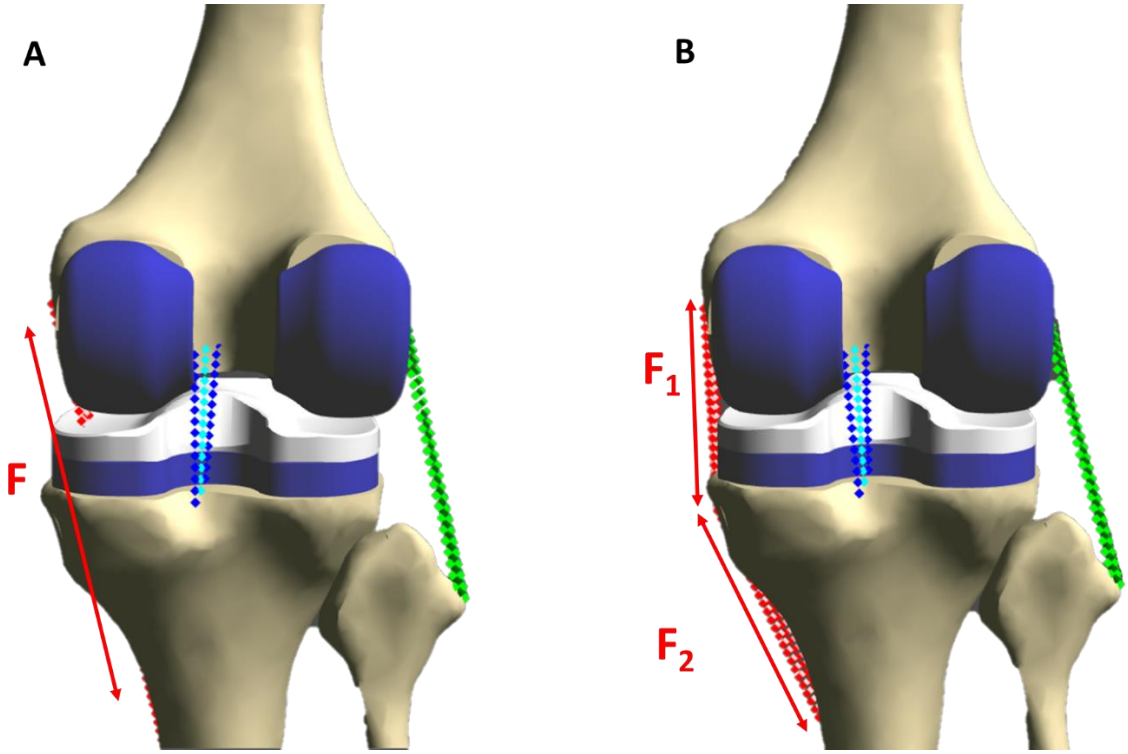

Figure 4-12: Comparison of the line of action through which the sMCL exerts a force in the Multi model without wrapping (A) and while simulating wrapping with compensation (B).

An important consideration when simulating ligament wrapping for a computational model is to change the reference strain accordingly. The wrapped ligament will be longer in extension compared to the unwrapped ligament since it is not traveling a straight path from femoral to tibial insertion. However, we must also assume that the sMCL has a different zero-load length when it is wrapped otherwise the result will be an extremely tight ligament. This was made most clear during valgus laxity tests since the sMCL

mainly resists valgus motion of the joint. For all levels of ligament model complexity, the wrapped ligament model without compensation allowed for far less valgus motion than either the unwrapped or wrapped & compensated ligament models. With an uncompensated reference strain, the elongation due to wrapping will cause the sMCL to exert a much higher force during all motions. Though it is most obvious during valgus laxity when the sMCL is called up the most, we can also see that the VV position during neutral flexion is more varus than models with the other two wrapping conditions. This indicates a tighter medial side of the joint. However, when compensating for wrapping by reducing the reference strain, resulting kinematics rarely varied between unwrapped and wrapped & compensated ligament conditions. The exception was neutral flexion kinematics of the Guess model, and IE kinematics for the Single model. For the Guess model, neutral flexion had a more anterior, valgus, and internally rotated knee with the wrapped and compensated model compared to the unwrapped model. With the Single model, the wrapped & compensated ligament condition was far more externally rotated during neutral flexion. The wrapped & compensated model may offer more laxity during neutral flexion due to reduced compression. The wrapped & compensated model is designed to undergo the same strain as the unwrapped model, but the force this strain creates will be in a slightly different direction. In the unwrapped model the sMCL goes directly from the femoral insertion to the tibial, and thus the force it exerts manifests primarily as compression. The wrapping makes the ligaments less one-dimensional; now some of the exerted force will be in the ML direction as well. A reduction in compression may lead to the joint being more lax in all directions. Further work can be done by testing motions with compression to reduce the dependency on the sMCL.

Wrapping without compensation also influenced the posterior motion limit during posterior laxity. For all levels of ligament model complexity, the wrapped ligament condition without compensation resulted in a more anteriorly positioned posterior motion limit for the Single, Guess, and Multi models. The increased force exerted by the uncompensated wrapped model prevents excessive motion of the femur with respect to the tibia by keeping their origins of insertion in as close proximity as possible. This does not affect the IE laxity tests as much since the sMCL insertions are not being pulled apart like they are during posterior and valgus laxity tests.

A limitation of this study was that results were only obtained from one model. Testing a variety of models – differing either in their bone geometry, implant geometry, or surgical alignment – would allow for quantitative statistical analysis to be performed and thus allow for stronger conclusions to be made. A limitation also exists in the way VIVO Sim models ligament wrapping: wrapping can only be made about a single surface. Our model had the sMCL wrapping around the tibia which didn't present any problems during motions except for internal laxity. During internal laxity, the tibia would rotate so much that the ligament would then pass through the UHMWPE insert and the tibial tray. Furthermore, VIVO Sim also only records data at the five points of flexion shown above meaning it cannot be used to study continuous motions or flexion up to 120° which can be an important clinical marker and is often reported in the literature [16]. Furthermore, the loads we used were not indicative of loads experienced by the knee joint during daily activities such as gait. Though this step in the study of the knee using the digital twin focuses on ligament contributions during joint laxity thus requiring these smaller loads, future work should include physiologically relevant loading.

In summary, we performed simple biomechanical tests on a computational knee model with three virtual ligament models of varying complexity. These tests included posterior laxity testing, varus-valgus laxity testing, and internal-external laxity testing. Though patterns could sometimes be observed between joint laxity and ligament complexity, ultimately there was no discernable difference between motion limits during laxity tests or neutral motion. However, in specific scenarios such as when the knee is extended during posterior laxity tests, the Guess and Single models failed to emulate normal knee motion. Thus, we can conclude that all levels of ligament model complexity in this study may be used to investigate computational biomechanics, but in certain instances a more complex model may provide more accurate knee kinematics. To this author's knowledge, our application of VIVO Sim to analyze multiple virtual ligament models is a novel use. We also compared the effect different ligament wrapping techniques had on the kinematics during simulated neutral motion and laxity tests within VIVO Sim. We showed that if wrapping is simulated without compensating the reference strain, kinematics during posterior laxity tests, valgus laxity tests, and neutral flexion are affected. This condition makes the knee joint tighter and restricts movement during the

aforementioned tests. Simulating wrapping with compensated reference strains gives very similar kinematics as when using unwrapped ligaments. However, during certain instances such as posterior laxity tests with the knee in extension, a wrapped sMCL prevents unnatural motion in the ML direction. We successfully simulated ligament wrapping for three levels of ligament model complexity in VIVO Sim for one knee and implant geometry. Further testing with different knee and implant geometries or varied surgical alignments would be needed to suitably test the significance of these conclusions.

Chapter 5

5 Using a Computational Knee Model to Examine the Biomechanical Effects of Femoral Component Malrotation During TKA

The purpose of Chapter 5 is to use a computational TKA knee model to determine the biomechanical effects of malrotation of the femoral component during surgery. This chapter begins with a summary of measurements taken and cuts made during a total knee arthroplasty (TKA) surgical procedure, as well as the different types of implant malalignment that can occur. We then proceed to describe a computational model used to carry out biomechanical analysis of the effects femoral implant malrotation can have on a TKA knee. The results of this study are shared and then we move into a discussion of said results. This chapter concludes with some limitations and next steps to be addressed.

5.1 Introduction

TKA surgery is an end stage treatment for those suffering from osteoarthritis in the knee. It is an extremely common procedure with over 70 000 being performed each year in Canada [2]. An aggressive, invasive surgery, yet precision is key to providing the patient with a lasting pain-free knee. Unfortunately, satisfaction rates for TKA surgery (81.4%) remain lower than those of comparable surgeries such as total hip replacement surgeries 90% [4]. Furthermore, patient satisfaction rates remain low during functional motions with one study reporting up to 52% of patients being unsatisfied [3]. Dissatisfaction, continued pain, or implant wear can all contribute to revision surgery. These surgeries are more costly to the healthcare system and pose a greater risk to the patient, yet revision rates climb in the years following TKA surgery [2]. One possible cause of these poor outcomes is poor alignment of implants during TKA surgery [28]. Malalignment can occur in any degree of freedom, but to fully understand how an implant can become poorly aligned we must first discuss what a properly aligned implant looks like.

The alignment type used in this study is the classical mechanical alignment, which achieves a balanced force distribution by achieving a 0° hip-knee-ankle (HKA) angle [19], [59]. Figure 5-1 shows a femur and tibia following resections for mechanical alignment.

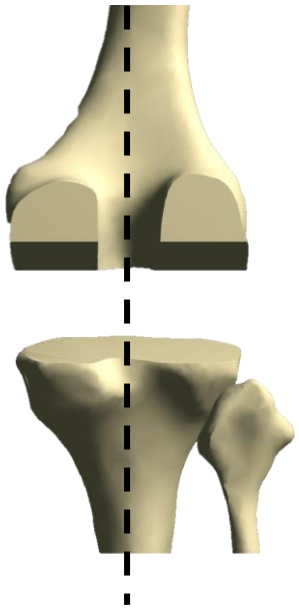

Figure 5-1: A resected femur and tibia prepared for mechanical alignment. Cuts made perpendicular to the bones' mechanical axes result in a hip-knee-angle (HKA) of 0°. The HKA is shown as a black dashed line.

This also ensures that implant wear is evenly distributed which minimizes asymmetrical implant wear [19]. However, the natural HKA angle is not necessarily 0°; it's closer to 2°-3°. In fact, a 2012 study by Bellemans et al has shown that 32% of men and 17% of women observed have knee joint angles greater than 3° [60]. Fahlman et al recently found that 81.8% of observed subjects had the same alignment in both knees [22].

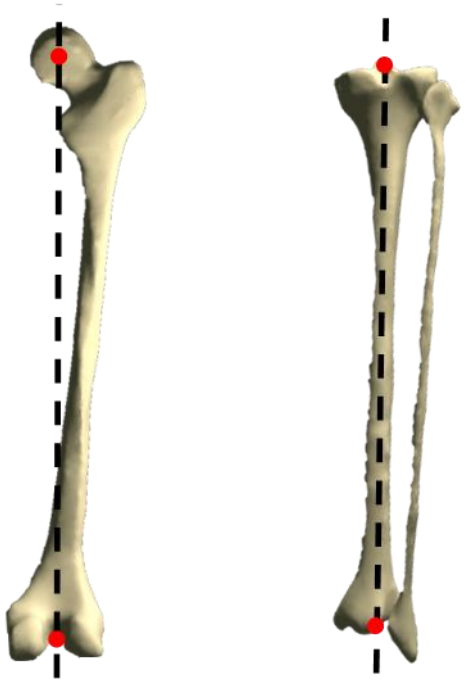

Figure 5-2: Mechanical axes of both the femur (left) and the tibia (right) shown as dashed lines with reference points being red dots.

Achieving neutral knee alignment is done by making resections perpendicular to the mechanical axes of both the femur and the tibia [19]. The mechanical axis of the femur is defined as the line that passes from the center of the femoral head through the intercondylar notch of the distal femur (Figure 5-2). The tibia's mechanical axis passes from the center of the ankle through the center of the proximal tibia [59].

Additionally, there is a femoral component rotation which is done with respect to one of four reference lines: the trans-sulcus axis (TSA, better known as Whiteside's line), the surgical transepicondylar axis (sTEA), the anatomical transepicondylar axis (TEA), and the posterior condyle axis (PCA) [66]. For this study we reference the PCA to determine the rotation as it is the easiest to determine without the help of radiographic images. The

femur will be rotated externally by 3.0±1.2° with respect to the femoral component which has been shown to reduce the need for lateral retinacular release [68], [69]. Anything more internally or externally rotated is said to be a malalignment which can affect early patient reported outcomes [70]. The tibial resection is also made with a 5° posterior slope to reduce collateral ligament strain as the knee is flexed and to keep the joint balanced [89].

Unfortunately, errors in any of these measurements can lead to malignment. Additionally, subject-specific component alignment has been found to achieve joint-contact forces that better replicate those of the healthy knee, but subject-specific is not always possible in practice [28]. Ritter, et al. also found that failure was likely for alignments that caused an extremely valgus (≥8°) knee joint angle (HKA) [65]. Though varus-valgus (VV) alignment is important, the rotational alignment of the femoral is said to be one of the most important factors in TKA due to the negative consequences associated with its malalignment including lateral tilting, and the subluxation and dislocation of the patella with internally rotated femoral component malalignment. An implant that is rotated too far externally can lead to an increased medial flexion gap resulting in instability during flexion [90]. The objective of this study is to assess the kinematics of the TKA knee with over- and under-rotated femoral components and compare that to a baseline TKA knee model with a femoral component internally rotated by 3°. Literature seems to agree that an over-internally rotated femoral component lends the knee to poor outcomes [64]. We anticipate that this study will show that these outcomes are due to an imbalance in ligament forces during late flexion, with medial soft tissues under-contributing. Therefore, we expect to see a larger difference in kinematics the more the knee is flexed. Externally rotating the femoral component will tighten the medial side of the joint during late flexion which may lead to a more varus knee. Under-rotating the femoral component will likely lead to a more lax joint in late flexion, resulting in a laterally tilted knee joint. However, a biomechanical analysis has yet to be performed to investigate what role ligament forces play in the consequences of malalignment.

5.2 Methods

The computational knee model used for this study was adapted from one developed by Guess et al. and modified as described previously to investigate knee ligament mechanics and meniscal loading following ACL release [39], [43]. Bony geometry and ligament insertion data were acquired from the magnetic resonance imaging of a 29-year-old female's healthy right knee (height = 170 cm, weight 70 kg). We subjected the virtual, healthy knee to a simulated TKA surgery using mechanically aligned implants. Mechanical alignment requires cuts to be made perpendicular to both the tibia and femur's mechanical axes within the coronal plane. The femur's mechanical axis was identified by sphere-fitting both condyles as well as the femoral head. The axis was the line that passed through the center of the sphere-fit of the femoral head, and the midpoint of the centers of the sphere-fits of the two condyles. The tibial mechanical axis was the one that passed through the midpoint of the two malleoli extremities, and the center of the tibial plateau. We also angled the tibial cut by 5° posteriorly in the transverse plane. Following the resections, implant geometries were affixed to our femur and tibia. Implant geometries were for a Triathlon Cruciate Retaining (CR) implant (Stryker Corporation, Kalamazoo, MI, USA) which includes a size 3 femoral component, size 3 tibial insert, and an 11 mm CR Ultra High Molecular Weight Polyethylene (UHMWPE) insert. This was the only TKA component geometry used in this study. The CR femoral implant geometry uses a single radius implant design; a multi radius implant design could have different kinematic outcomes due to decreased varus-valgus stability [91]. Other implants Femoral component rotation was done by comparing the posterior condyle axes (PCAs) of both the femur and the femoral condyles (Figure 5-3). These axes were determined as the lines that connected the posterior-most points on each of the femur's/femoral implant's condyles. The femoral implant was then rotated externally by 3° with respect to the femurs PCA [90]. We also designed two more models with identical bony and implant geometry whose femoral implants were rotated externally by 1.5° and 4.5° for our internal, and external model, respectively (Figure 5-4). Implant placement and sizing were verified by a high-volume orthopedic surgeon.

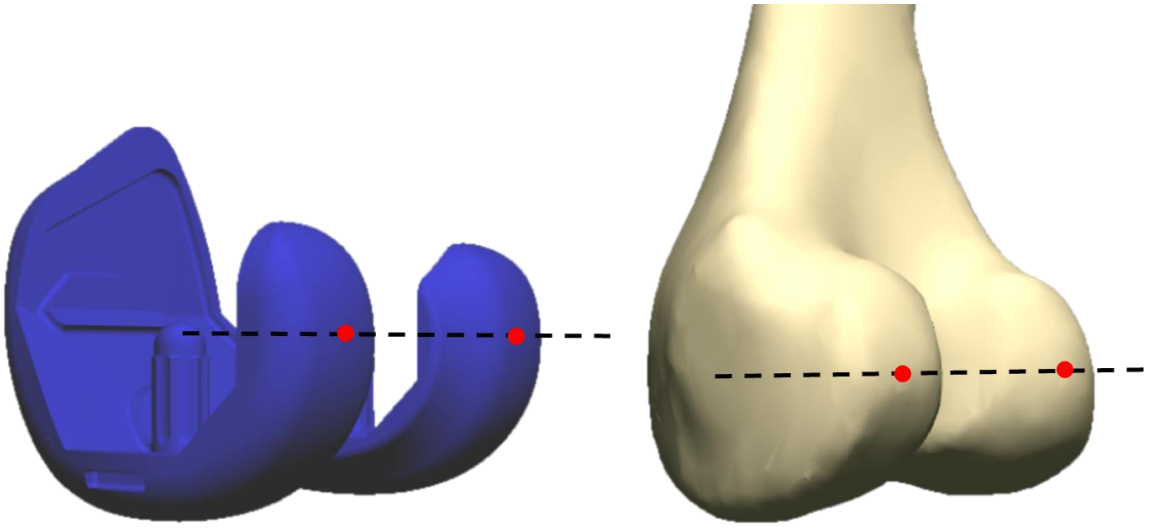

Figure 5-3: Posterior condyle axes of the femoral implant (left) and the femur (right).

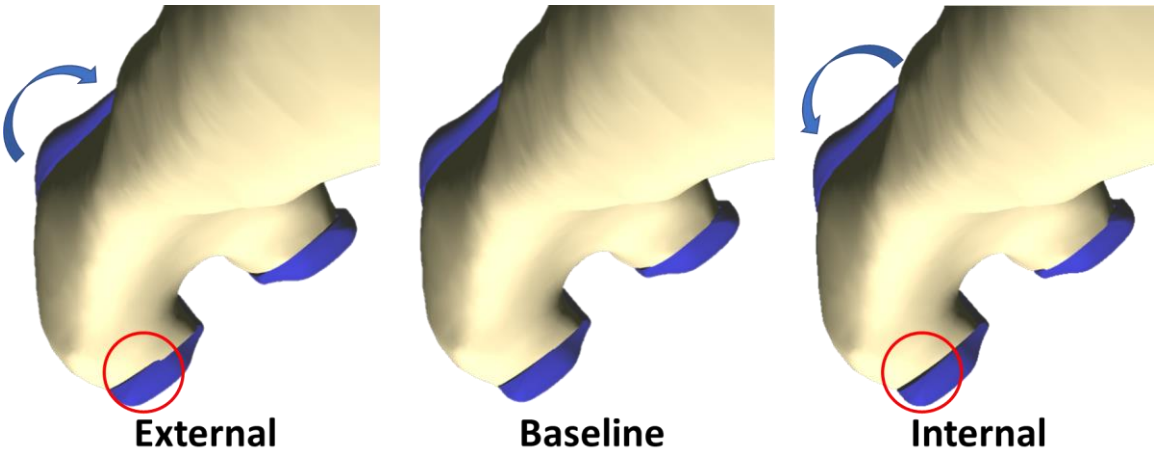

Figure 5-4: Femoral component rotations with a 1.5° internal rotation (left), 3° internal rotation (middle), and 4.5° internal rotation (right). The 4.5° internal rotation is over-rotated, and the 1.5° is externally rotated with respect to the baseline. The differences are slight but overlapping or gapping is identified with a red circle. This did not affect contact forces.

This computational model was loaded into the software package VIVO Sim Visualization Software (Advanced Mechanical Technology, Inc., Watertown, MA, USA) – herein referred to as VIVO Sim – in order to apply a virtual ligament model and simulate various motion

tests. VIVO Sim operates similarly to the AMTI VIVO 6 Degree of Freedom (DoF) Joint Motion Simulator (Ibid), in that motion in each DoF can be operated independently and in either force- or displacement-control mode. Contact was defined between the UHMWPE insert and the femoral component, and though material properties cannot be defined in VIVO Sim, coefficient of friction used was $\mu = 0.04$. This value is defined in the literature as the coefficient of friction between polyethylene and cobalt-chrome, which are the two contact surfaces in a TKA knee [54].

The virtual ligament model used was also adapted from Guess et al. who included parameters for fourteen bundles in order to define seven ligaments. Parameters included tibial and femoral insertions, zero-load lengths, and stiffnesses. VIVO Sim defines ligaments based on insertions, stiffnesses, and reference strains. The latter of which can be calculated from the zero-load length. Our virtual ligament model only retained the superficial medial collateral ligament (sMCL), lateral collateral ligament (LCL), and posterior cruciate ligament (PCL). Other ligaments such as the anterior cruciate ligament, the posterior oblique ligament, and the deep MCL were not included in our model as they are routinely released during TKA surgery [73], [92]. The original Guess model contained three bundles to represent the sMCL, three bundles to represent the LCL, and two bundles to represent the PCL. We adapted this by adding two additional bundles to the collateral ligaments and added one bundle to the PCL. Additional bundles better represent natural ligaments that are made up of many individual fibers. In fact, Kiapour et al. that a uniaxial elastic representation of a ligament models knee ligaments poorly compared to other techniques [55]. Thus, our model will also include ligament wrapping. Ligament wrapping will only need to be simulated for the sMCL whose point-to-point path from femoral to tibial insertion passes directly through the tibia, the tibial tray, and the UHMWPE insert. This ligament wrapping was simulated about the tibia. The original Guess model was expanded to include five bundles for the sMCL and the LCL, as well as using three bundles to represent the PCL. Stiffness and reference strain values are shown below in Table 5-1. Note that a negative reference strain does not mean a ligament bundle is compressed. It is simply a way to illustrate how slack the ligament bundle is so that the system knows at which change in length (strain) that ligament will become engaged.

Table 5-1: Ligament parameters for virtual ligament model.

Ligament	Stiffness (N)	Reference Strain (%)
aLCL	1157	-2.66
amLCL	1171	0.68
mLCL	1175	4.02
mpLCL	1172	2.66
pLCL	1182	1.29
asMCL	1469	-4.30
amsMCL	1603	0.10
msMCL	1481	4.50
mpsMCL	1509	4.47
psMCL	1105	4.44
aPCL	7841	-28.60
mPCL	2554	-27.44
pPCL	1026	-26.30

Our knee models with all three femoral implant rotation conditions were then subjected to six motions via automated testing within VIVO Sim: neutral flexion, posterior laxity, varus and valgus (VV) laxity, and internal and external (IE) laxity. Neutral laxity was simple flexion of between 0° and 90° without any applied forces acting on the knee. Laxity tests were done discretely at flexion angles of 0°, 15°, 30°, 60°, and 90° with an applied force that differed between each test. Posterior laxity testing includes a 100 N force acting posteriorly against the tibia. Varus and valgus laxity tests were simulated by applying a ±8 Nm torque to the femur. Internal and external laxity were simulated with ±4 Nm torques. Kinematic and force data in all degrees of freedom is automatically recorded by VIVO Sim.

5.3 Results

Posterior Laxity

We saw similar anterior-posterior (AP) kinematics during both neutral flexion and posterior laxity for all three models, as shown in Figure 5-5. Laxity during all motions was calculated as the absolute difference between kinematics during neutral flexion, and kinematics during the laxity test. Average laxities during the posterior laxity test for the externally rotated model (external), the baseline model (baseline), and the internally rotated model (internal) were 4.2±0.8 mm, 4.2±0.3 mm, and 4.6±0.5 mm, respectively. From Figure 6-6 the total ligament forces acting in the AP direction are shown, and they are also similar between all models. The difference in average ligament tensions in the AP direction between neutral flexion and the posterior laxity test for the external, baseline, and internal models during early flexion (0°-15°) were 11.6±13.4 N, 14.0±10.1 N, and 7.5±5.9 N respectively. During flexion (30° to 90°) the average difference in laxities for the same were 59.0±18.4 N, 64.2±19.4 N, and 60.4±22.4 N.

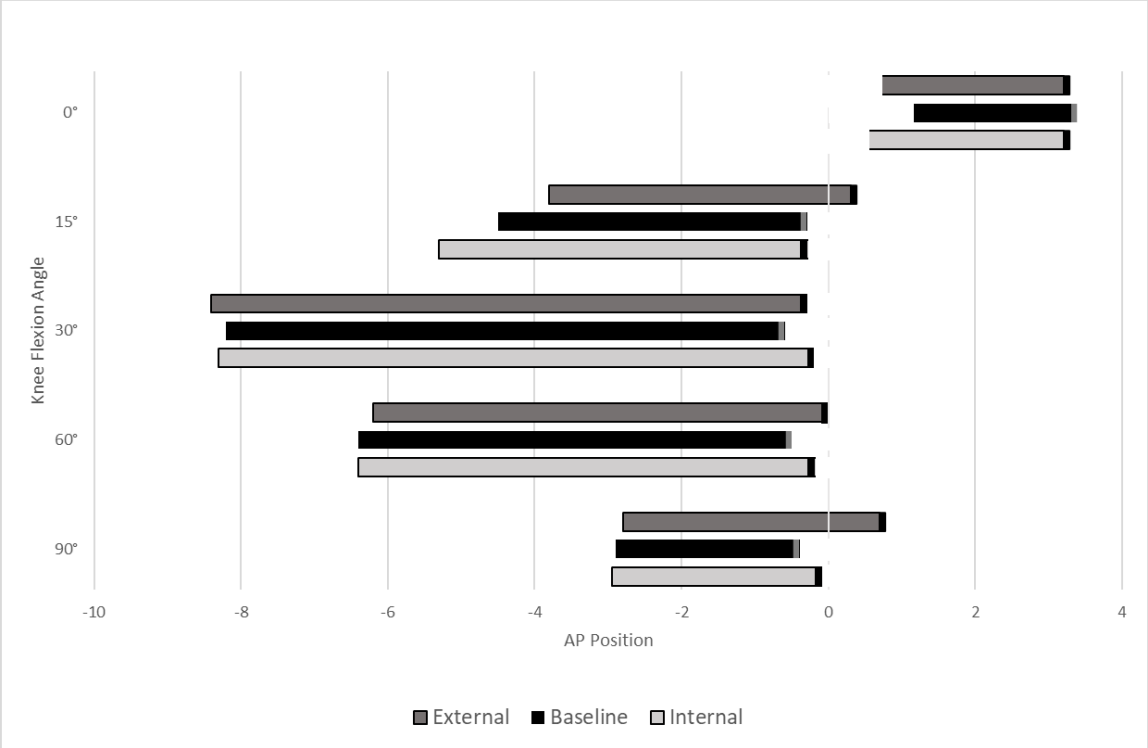

Figure 5-5: AP kinematics for three computational knee models with varied femoral implant rotation during posterior laxity. Baseline has a femoral component internal rotation of 3°, internal is over-rotated to 4.5° and external was under-rotated to 1.5°. AP position during neutral flexion is denoted with a solid vertical bar. Negative values denote a tibial position that is posterior with respect to its reference pose.

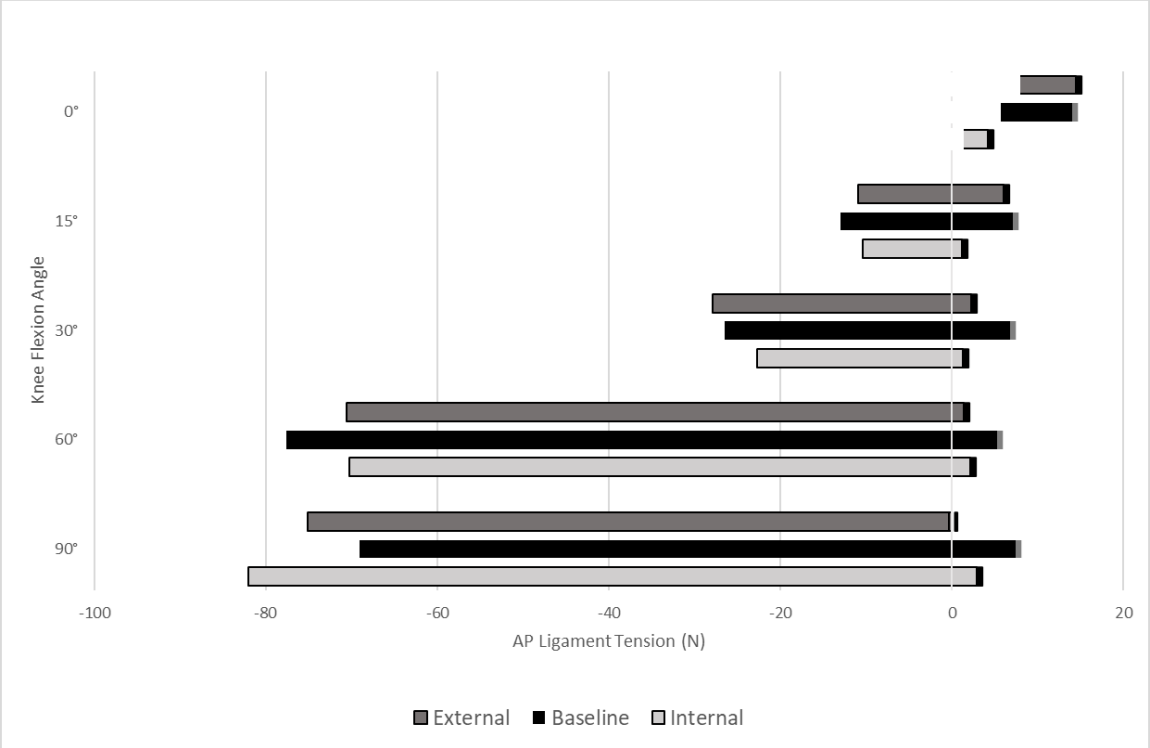

Figure 5-6: Net ligament forces in the AP direction for three computational knee models with varied femoral implant rotation during posterior laxity. Baseline has a femoral component internal rotation of 3°, internal is over-rotated to 4.5° and external was under-rotated to 1.5°. AP ligament forces during neutral flexion are denoted with a solid vertical bar. Negative values denote a ligament tension that pulls the tibia anteriorly.

Varus-Valgus Laxity

From Figure 5-7 we can see that varus-valgus (VV) kinematics are similar between 0° and 30° of flexion, but during late flexion we see that the more externally rotated femoral implants lead to a more varus knee. This pattern is even more apparent during neutral flexion. Average varus laxities were 3.8±0.8°, 4.0±0.6°, and 3.6±0.6° for the external, baseline, and internal models, respectively. The average valgus laxities for the same were 4.1±0.9°, 3.5±0.6°, 4.2±0.6°. Figure 5-8 shows that ligament tensions in the VV direction don't follow as clear of a pattern. Particularly, ligament tensions during valgus laxity (positive tensions), which are relatively even between all three models. Average absolute

differences in ligament tensions acting in the VV direction between neutral motion and varus laxity test were 4.5±0.8 Nm, 4.8±0.4 Nm, and 3.6±0.3 Nm. The average differences in ligament tensions between neutral motion and valgus laxity were 4.0±0.9 Nm, 3.1±0.5 Nm, and 4.3±0.4 Nm for the same. The baseline differences are varied due to forces during neutral motion, which pull more varus than either the internally or externally rotated models.

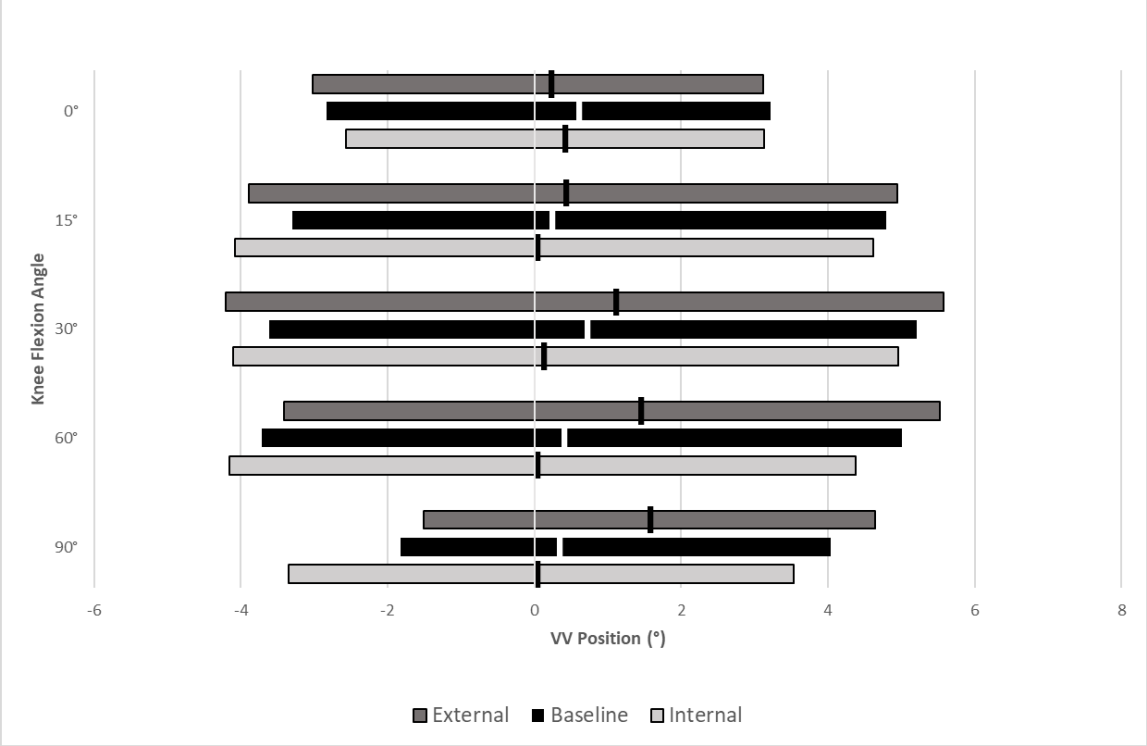

Figure 5-7: VV kinematics for three computational knee models with varied femoral implant rotation during posterior laxity. Baseline has a femoral component internal rotation of 3°, internal is over-rotated to 4.5° and external was under-rotated to 1.5°. VV position during neutral flexion is denoted with a solid vertical bar. Negative values denote a valgus VV position.

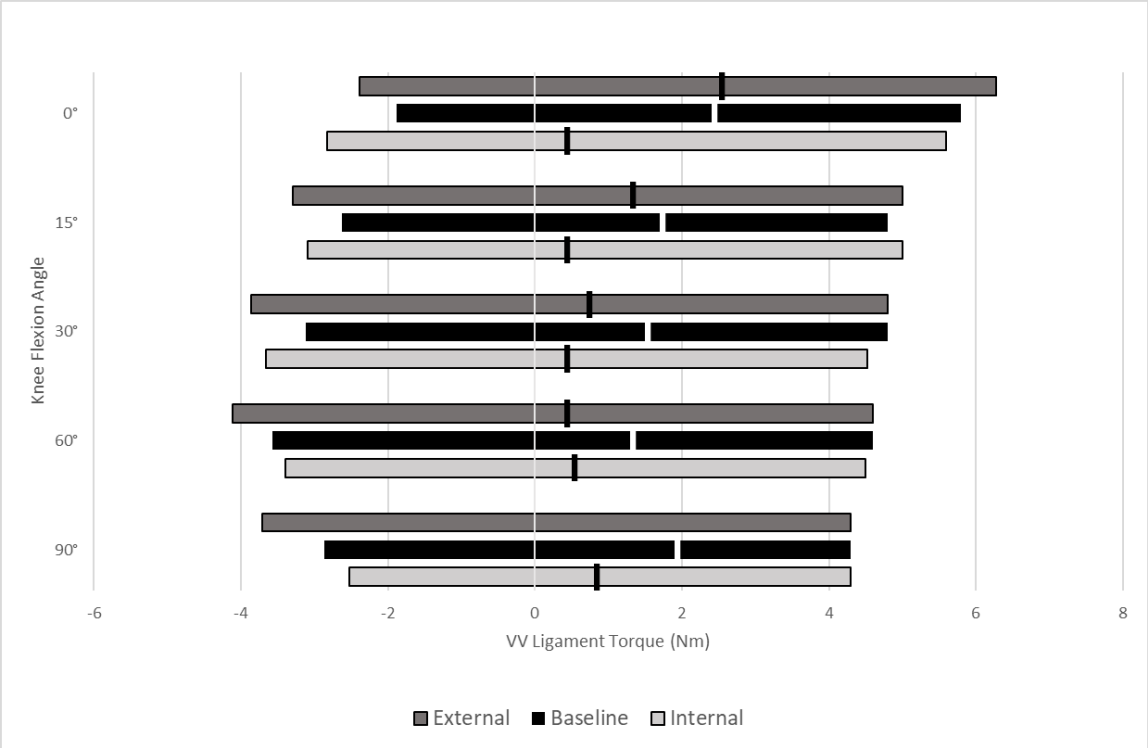

Figure 5-8: Net torque due to ligaments in the VV direction for three computational knee models with varied femoral implant rotation during posterior laxity. Baseline has a femoral component internal rotation of 3°, internal is over-rotated to 4.5° and external was under-rotated to 1.5°. VV ligament forces during neutral flexion are denoted with a solid vertical bar. Negative values denote a ligament tension that pulls the femur valgus.

Internal-External Laxity

Internal-external (IE) kinematics during neutral flexion and IE laxity tests are described in Figure 5-9 for all three conditions of model rotation. We see similar kinematics between all conditions during neutral flexion, and external laxity. During late flexion with an internal torque applied to the knee, the internally rotated component results in a tighter knee. Average internal laxity was 33.6±3.4°, 32.6±4.6°, and 31.4±5.1° for the external, baseline, and internal models, respectively. The corresponding external laxities were 13.1±1.4°, 12.7±1.9°, 12.6±1.9°. IE ligament tensions were not affected by either over- or under-rotated femoral components. Average difference in IE ligament tensions

between neutral flexion and internal laxity were 1.1±0.2 Nm, 1.3±0.3 Nm, 0.9±0.1 Nm for the external, baseline, and internal models, respectively. During external laxity these differences were 2.2±0.1Nm, 2.6±0.1 Nm, 2.9±0.2 Nm for the same.

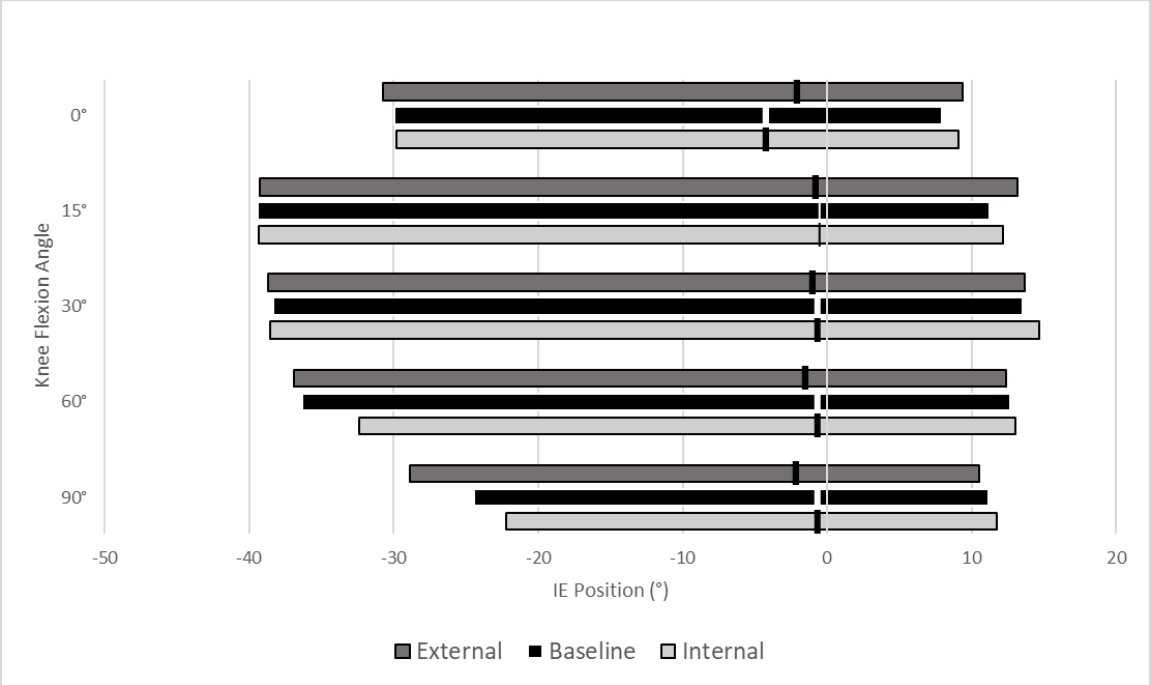

Figure 5-9: IE kinematics for three computational knee models with varied femoral implant rotation during posterior laxity. Baseline has a femoral component internal rotation of 3°, internal is over-rotated to 4.5° and external was under-rotated to 1.5°. IE position during neutral flexion is denoted with a solid vertical bar. Negative values denote an internally rotated tibia with respect to the reference pose.

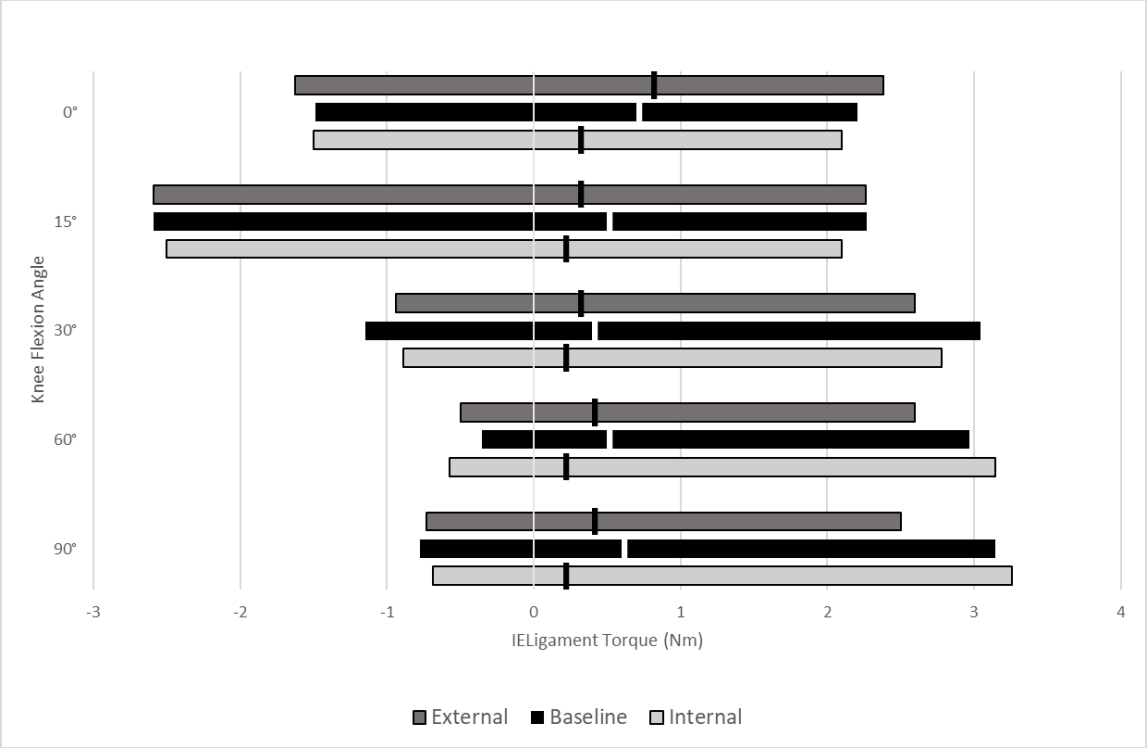

Figure 5-10: Net torques due to ligaments in the IE direction for three computational knee models with varied femoral implant rotation during posterior laxity. Baseline has a femoral component internal rotation of 3°, internal is over-rotated to 4.5° and external was under-rotated to 1.5°. IE ligament forces during neutral flexion are denoted with a solid vertical bar. Negative values denote a ligament tension that pulls the tibia internally.

5.4 Discussion

This study examined the biomechanical effects of varied femoral implant rotation following TKA surgery. This biomechanical testing was done using a novel application of joint simulation software that previously only accompanied a physical joint motion simulator. We predicted that the effect of malrotation would be most noticeable during late flexion, as an IE rotation in extension will manifest as a varus or valgus rotation once the knee is flexed to the point of the condyles being in contact with the UHMWPE insert. This was reflected in the kinematic results obtained during varus and valgus laxity, as well as during internal laxity.

During varus and valgus laxities, as well as during neutral flexion, under-internally rotated implants lead to a more varus knee. Figure 5-11 demonstrates how an external rotation in extension will manifest as a valgus rotation in flexion. In flexion, this effectively increases the joint gap on the lateral side while reducing the joint gap on the medial side. This results in an overall varus knee. If the medial joint gap is reduced, the sMCL insertions will be closer together leading to a reduced strain and thus lower tension in extension. The sMCL will exert tension in the inferior-superior (IS) direction – which serves to reduce the joint – but it will also exert a small varus torque. Similarly, the LCL exerts a valgus torque in the VV degree of freedom. If an externally rotated implant reduces the separation of insertions on the medial side thereby reducing the strain exerted by the sMCL and increasing the strain exerted by the LCL, then it is logical that the external model's ligaments exerted a higher torque during varus laxity.

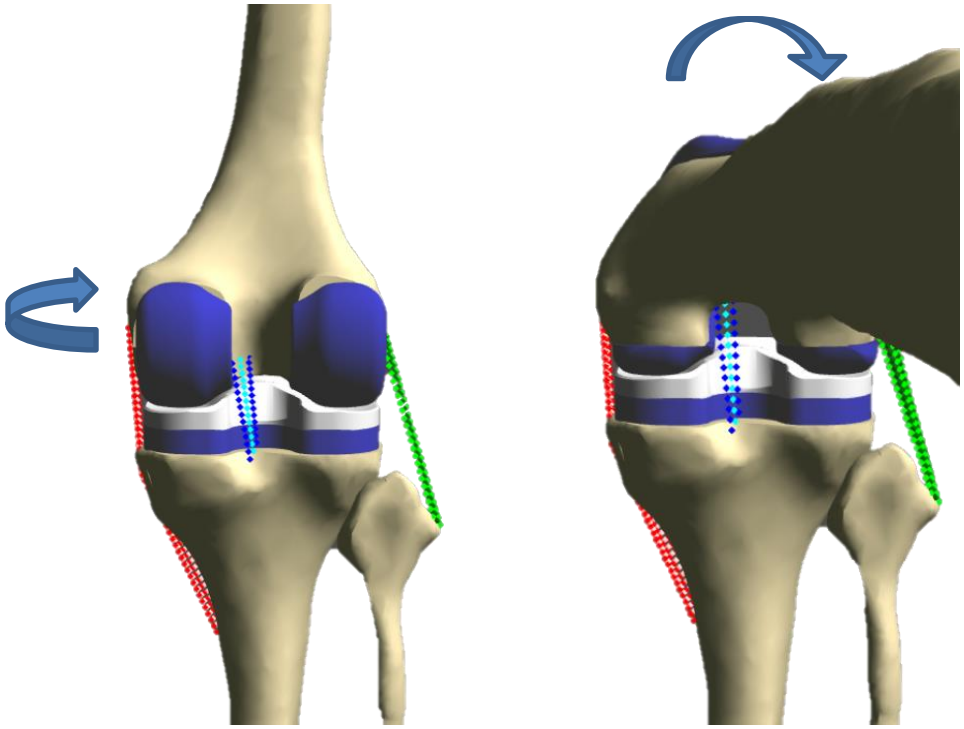

Figure 5-11: Externally rotating the femoral component with respect to the femur in extension results in a valgus component once the knee is flexed. This results in a more varus knee.

Inversely, a more internally rotated femoral component will become varus in deep flexion. This increases the medial joint gap and reduces the lateral joint gap resulting in a

more valgus knee. This leads to increased force contribution from the sMCL, and a reduced contribution from the LCL which manifests as a lesser overall ligament torque during varus laxity as seen in Figure 5-4 in the results section. Interestingly, component malrotation seemed to have little influence on knee kinematics during both neutral flexion and valgus laxity tests. This is likely due to the dominance of the force exerted by the sMCL during these motions. With no other forces acting on the knee, the medial side will tighter in both the healthy and the TKA knee due to medial side ligaments exerting higher forces than their lateral counterparts [87], [93]. This describes neutral flexion, which is simple flexion sans applied forces, and during valgus laxity, the medial side of the joint is opened up increasing the strain on the medial ligaments and reducing the strain on the lateral side ligaments. Jeffcote et al. demonstrated that the MCL strain will be greater than that of the LCL during neutral flexion in a balanced TKA knee [94]. This fact combined with the greater stiffness of sMCL bundles compared to the stiffnesses of the LCL bundles proves that the sMCL will be exerting a much higher force except for motions where the LCL is forced to be engaged such as varus laxity. Our results show that during motions where the sMCL is clearly more engaged than the LCL, the effect of rotational malalignment is difficult to discern. This suggests that for femoral component rotations between 1.5°-4.5°, ligament balancing can reduce the effect of malrotation during some motions.

We also showed that femoral component malrotation had an effect during internal laxity testing at points of late flexion including 60° and 90°. The greater the femoral component rotation, the greater the internal laxity of the knee as shown in Figure 6-5. There is an opposite but much smaller effect during external rotation. Component malrotation seems to have no effect on the knee's IE position during neutral flexion. The kinematic effect of malrotation is easily explained by the fact that the externally rotated model's ligaments exert a weaker external torque to resist the applied internal torque. This is exhibited clearly at 60° and 90° in Figure 6-6. One of the functions of both collateral ligaments is to resist unusual internal and external motion. We've already addressed how the sMCL will contribute a higher force than the LCL, so anytime the sMCL force increases the entire ligament force contribution will increase. As discussed, an internally rotated component increases the gap between femoral and tibial sMCL insertions, effectively

increasing the force exerted by that ligament. An overall increase in force means there is more resistance to the internal torque applied. This led to a tighter internal model, and a more lax external model during the internal laxity test at late flexion.

Overall, component malrotation did not have a noticeable effect on either AP kinematics or mechanics during either neutral flexion or posterior laxity. The key soft tissue force contributor in AP direction following a cruciate-retaining TKA is the PCL [95]. Due to the PCL insertions' proximity to the femur's center of rotation, PCL strain patterns will not be as deeply affected by implant rotations in either IE or VV degrees of freedom. Furthermore, during posterior laxity contact between implants occurs at the anterior lip of the UHMWPE insert and the anterior-facing surface of the femoral component – which is the inferior surface of the femoral component as the knee is flexed. A small IE rotation of the femoral component will not be enough to drastically change these contact surfaces, thus the AP position during posterior laxity will not be influenced by femoral component malrotation. However, a poorly aligned femoral component in the sagittal could lead to a change in kinematics within the AP degree of freedom [64].

A limitation of this study was that results were only obtained from one model. Testing more models with different knee geometries or kinematically aligned implants would allow for quantitative statistical analysis to be performed and thus allow for stronger conclusions to be made. Wrapping in VIVO Sim is also limited to a single surface which didn't pose an issue except during internal laxity testing. During internal laxity, the tibia would rotate so much that the ligament was in a position where it could pass through the UHMWPE insert and the tibial tray. Furthermore, VIVO Sim also only records data at the five points of flexion shown above meaning it cannot be used to study continuous motions or flexion up to 120° which can be an important clinical marker and is often reported in the literature [16]. VIVO Sim also only records ligament force data as total tension of all ligaments (sMCL, LCL, and PCL) within a specific degree of freedom. Having tensions exerted by each individual bundle would have provided additional data to better analyze results. Obtaining individual bundle tension values is possible within VIVO Sim, but not during automated motions and thus incurs a huge time cost. Another limitation would be the subject used to create the model. Though TKA surgeries are not

unheard of in younger populations, the majority of TKAs are performed on patients over the age of fifty so using a 29-year-old's bone geometry may limit the generalizability of the study [24].

In summary, we compared the biomechanical effects of femoral component malrotation during TKA surgery using the visualization software VIVO Sim. We demonstrated that either under- or over-rotating the femoral component has a clear effect on VV kinematics during neutral flexion, varus laxity tests, and valgus laxity tests. It also affects total ligament tensions during varus laxity, though the impact of the sMCL reduces the malrotation effect on ligament forces during valgus laxity and neutral flexion. Malrotation also influences internal motion limits and IE forces during internal laxity tests. We successfully simulated motion for a TKA knee to examine the effects of femoral component malrotation. However, malrotation seemed to have little influence over most motions so future testing could examine more extreme malrotation beyond what is defined in the literature.

Chapter 6

6 General Summary and Future Works

This chapter summarizes the objectives and hypotheses of this thesis and the experiments conducted to realize those objectives. Limitations and strengths are also addressed in this study. Additionally, the future directions that this study can take and its significance for biomechanical analysis of TKA knees is considered.

6.1 Summary

Total knee arthroplasty is a common surgical procedure performed as an end-stage treatment option for patients suffering from knee osteoarthritis. However, patient satisfaction rates remain low relative to other joint arthroplasties and unicondylar knee arthroplasty demonstrating a need to better understand the loads crossing the post-TKA knee joint. A cost-effective and time-efficient way to study knee biomechanics is computational modelling. Though computational modelling lacks the biological accuracy of *in vivo* and cadaver studies that use joint motion simulators, it benefits from being easily repeatable, cheaper, and it has the capacity to perform parametric analysis. Furthermore, computational models are able to examine all loads acting on the knee in detail, something that is unable to be done on either cadaver or *in vivo* knees. Despite being a popular study design for knee biomechanics, computational knee models vary heavily in how they represent ligaments. Everything from ligament parameters like stiffness and reference strain, to the number of bundles used to represent each ligament can change from study to study. Thus, there is a need to examine the different biomechanical effects different ligament modelling strategies can have on a TKA knee model. This study established a computational knee model in simulation software that is typically used in tandem with a physical joint motion simulator (the AMTI VIVO). This was a novel use for the simulation software (VIVO Sim) and therefore the computational model had to be validated against a similar study using the physical joint motion simulator. After validation this computational knee model was used to examine the effects of ligament model complexity as a function of the number of bundles used to

represent each ligament, as well as the biomechanical effects of simulated ligament wrapping. This computational model was then used to examine the kinematic effects of TKA component malrotation and how it influences ligament force contributions.

In Chapter 3, the capacity VIVO Sim to be used as a virtual joint motion simulator for a rigid-body computational TKA knee model was assessed by comparing kinematics to an identical knee used in a live experiment using the physical joint motion simulator. The hypothesis was that kinematics would be nearly identical as the two models were based on the same knee and TKA implant geometries, and they also used identical virtual ligament models. Results showed nearly identical kinematics during posterior laxity, varus laxity, and valgus laxity. Similarly, ligament tensions of the virtual model reflected those of the experimental model. Correlations for kinematics and ligament tensions between the two models were greater than $R = 0.85$ except for ligament tension during valgus laxity. Thus, we concluded that VIVO Sim was able to be operated as an independent virtual joint motion simulator in TKA knee studies.

Chapter 4 examined the kinematic effects of various ligament modelling strategies. The primary objective was to assess the kinematic effect of ligament model complexity. Ligament model complexity was determined by the number of bundles used to model collateral ligaments (1, 3, or 5 bundles) and the posterior cruciate ligament (1, 2, or 3 bundles). Overall model complexity did not influence TKA knee kinematics, however in specific instances during posterior laxity with the knee in extension it prevented unnatural motions. When simulating ligament wrapping, these rare unnatural motions were corrected. However, simulating ligament wrapping without correctly compensating for the increased length with a reduced reference strain resulted in a much tighter joint than either the unwrapped, or the wrapped & compensated models. Overall, the wrapped & compensated model had similar behaviour to the unwrapped model. This again suggests that wrapping is not necessary except during posterior laxity with the knee in extension.

With increased confidence, our computational model was then used to investigate femoral component malalignment in Chapter 5. We used our Multi ligament model while simulating wrapping with compensation for this study. The model was tested with the

femoral component in the correct position (externally rotated by 3° with respect to the femur), as well as with the femoral component under- and over-rotated by 1.5° – an external rotation of 1.5° and 4.5°, respectively. We found that a malrotation had a more noticeable effect on kinematics when the knee was flexed beyond 30°. Malrotation specifically affects varus-valgus and internal-external positions of the knee. These changes in kinematics are likely due to changes in forces exerted by ligaments due to changes in the distance between femoral and tibial insertions.

This work has demonstrated that varied levels of virtual ligament model complexity are valid for modelling the TKA knee except during particular motions when a more complex ligament model performs better. If ligament wrapping is simulated, reference strain must be lowered to compensate. However, the compensated model will provide similar kinematics to an unwrapped ligament model. The work also provided a connection between varied kinematics due to femoral TKA component malrotation and changes in exerted ligament forces.

6.2 Limitations and Strengths

This work had some limitations associated with the virtual joint simulator used. VIVO Sim is limited in the type of data it collects. For instance, it only outputs net ligament forces within a given degree of freedom, not the individual ligament bundle tensions. These data would have aided with a more precise analysis of the soft tissue forces acting on the knee during all loading scenarios which would have been particularly useful during Chapter 5's study. The force contribution of individual bundles could be determined using the initial tibial and femoral insertions and the kinematic data in all six degrees of freedom at any given point of flexion. Furthermore, automated testing could only be done for discrete motions with data recorded at flexion angles of 0°, 15°, 30°, 60°, and 90°. This also limits us to studying motion within ninety degrees of flexion, while many range of motion studies examine flexion up to 120° [16], [17]. Flexion beyond 90° can be of particular interest when examining PCL force contributions since it is most engaged during late flexion under loading [96]. Note that the virtual simulator can provide these data but it must be extracted manually (as opposed to through automated testing) which is extremely inefficient. Finally, while VIVO Sim can quantify contact

force, it is unable to identify contact location upon the contact surfaces which would be limiting for studies investigating implant wear.

These studies only examined the tibiofemoral joint and thus neglected the patellofemoral joint. This has more significant implications for the study of component malrotation as many of the negative outcomes associated with component malrotation are related to patellar tracking, e.g. the subluxation of the patella [70]. VIVO Sim has the capability to model the patella and patellar ligaments and thus this should be included in future malrotation studies.

All motions tested in this thesis were quasi-static, meaning motions were discrete with data being recoded at each interval rather than being continuous without interruption to collect data, e.g., *in vivo* recording of gait kinematics. While quasi-static loading is a viable means of investigating knee motion, its constant strain rate will ignore any viscoelastic ligament behaviour which is affected by strain rate [51].

Another limitation of this study is the fact that only one model was tested. This makes it difficult to generalize our results. Thus, our work would benefit from testing varied models with either different bone geometry, implant geometry, or surgical alignment used. However, one model is common in parametric analysis studies such as this one.

Despite the limitations, our study contained many strengths. Most of which are associated with the novelty with the type of work we did. Other studies have done work to assess the effect of ligament model complexity, but none have looked at ligament complexity as a function of the number of bundles used in the virtual ligament model. For example, work has been done to assess the best way to represent ligaments when using finite element modelling and has found that more complex is better [57]. However, our work is specific to simple rigid-body computational models that do not have the capacity to model ligaments as a three-dimensional continuum of pre-defined material. Additionally, there has been little work done to investigate the kinematic effects of simulated ligament wrapping within computational models, despite many computational models applying this technique.

There have been many clinical studies on the resulting effects of poorly aligned femoral components during TKA [30], [65], [68], [90], [97]. However, none of these studies provide a biomechanical analysis to quantify the effects of malrotation, rather, they focus on important qualitative markers like patient satisfaction and surgery revision rates. Thus, one of this work's strengths is being able to quantify the kinematic effect of these malrotations.

Though there were some limitations associated with the virtual joint motion simulator, there were benefits to using it as well. There have been many studies investigating ligament modelling techniques for finite element models, however finite element modelling can be computationally costly and thus inefficient on most devices [54]–[56]. Ligament models were extremely easy to edit within the virtual which made testing the ligament wrapping conditions extremely efficient. Furthermore, testing was automated and multiple models could be tested on a single device which maximized efficiency.

6.3 Future Work

As mentioned above, the current studies would benefit from repeated motion testing with additional varied models. These models could use different bone geometry, or even more simply they could use a different TKA alignment (e.g., kinematic versus mechanical alignment). With more models tested, the conclusions made in these studies would be strengthened. Furthermore, we could perform quantitative statistical analysis on the data as opposed to the descriptive statistics used in this work.

As this was the first work done using this virtual joint motion simulator, there are a number of areas that could be focused on in the future. Since our work demonstrated that levels of ligament model complexity and simulated ligament wrapping techniques provided similar kinematics for discrete laxity tests, studies could be done to assess the effect of ligament modelling techniques during continuous motions or activities of daily living. This includes testing using more physiologically relevant loads. Also related to ligament modelling is the goal of extracting individual bundle contributions as opposed to only using net ligament forces. With the original insertions and kinematic data at each

point of flexion, ligament force contributions can be determined for each individual ligament bundle.

We defined the kinematic effects of component malrotation, but alignment within the coronal plane is also a topic of interest within the literature. Thus quantifying the kinematics and ligament forces exerted following coronal malrotation could also be of interest.

VIVO Sim could also be used to investigate other questions related to the TKA knee. This can include questions investigating alignment types (mechanical versus kinematic), and how ligament modelling techniques vary between them. We also used CR TKA components, but a number of other implant geometries exist. Thus we could compare CR kinematics to posterior-stabilized TKA as well as newer medial pivot implants.

6.4 Significance

This study is the first to use the simulation package VIVO Sim as an independent joint motion simulator. The only other mention of it in the literature are an abstract by its creator describing its functionality [75]. It has also been used as a visualization tool in tandem with its physical counterpart [85]. However this work demonstrates the virtual simulator's capacity to operate on its own to conduct meaningful biomechanical analysis. Furthermore, this work is the first to assess the kinematic effect of ligament model complexity as a function of number of bundles used, specifically for rigid-body models. We also quantified the effect of different simulated ligament wrapping techniques which does not exist in the literature as far as this author knows. This study concluded that outside of unique scenarios, ligament modelling techniques resulted in very similar kinematics. This work also provided kinematic and mechanical reasoning behind previously studied component malrotation following TKA.

References

[1] C. G. Helmick *et al.*, "Estimates of the prevalence of arthritis and other rheumatic conditions in the United States. Part I," *Arthritis and Rheumatism*, vol. 58, no. 1, pp. 15–25, Jan. 2008, doi: 10.1002/art.23177.

[2] "Canadian Joint Replacement Registry Annual Report," 2018. Accessed: Jan. 16, 2020. [Online]. Available: www.cihi.ca

[3] Y.-J. Choi and H. J. Ra, "Patient Satisfaction after Total Knee Arthroplasty," *Knee Surgery & Related Research*, vol. 28, no. 1, pp. 1–15, Mar. 2016, doi: 10.5792/ksrr.2016.28.1.1.

[4] R. L. Lau, R. Gandhi, S. Mahomed, and N. Mahomed, "Patient Satisfaction after Total Knee and Hip Arthroplasty," *Clinics in Geriatric Medicine*, vol. 28, no. 3. pp. 349–365, Aug. 2012. doi: 10.1016/j.cger.2012.05.001.

[5] C. M. Khella, R. Asgarian, J. M. Horvath, B. Rolauffs, and M. L. Hart, "An evidence-based systematic review of human knee post-traumatic osteoarthritis (Ptoa): Timeline of clinical presentation and disease markers, comparison of knee joint ptoa models and early disease implications," *International Journal of Molecular Sciences*, vol. 22, no. 4. MDPI AG, pp. 1–48, Feb. 02, 2021. doi: 10.3390/ijms22041996.

[6] A. Apostolopoulos *et al.*, "Kinematic and Kinetic Analysis of the Knee Joint before and after a PCL Retaining Total Knee Replacement during Gait and Single Step Ascent," *Journal of Long-Term Effects of Medical Implants*, vol. 21, no. 4, pp. 339–348, 2011, doi: 10.1615/JLongTermEffMedImplants.v21.i4.70.

[7] S. Sasaki *et al.*, "Effect of medial collateral ligament release and osteophyte resection on medial laxity in total knee arthroplasty," *Knee Surgery, Sports Traumatology, Arthroscopy*, 2020, doi: 10.1007/s00167-020-06257-1.

[8] A. Chhabra, J. S. Starman, M. Ferretti, A. F. Vidal, and F. H. Fu, “Kinematic Evaluation of the Anterior Cruciate Ligament and Its Two Functional Bundles,” 2006. [Online]. Available: http://journals.lww.com/jbjsjournal

[9] C. M. Laprade, D. M. Civitarese, M. T. Rasmussen, and R. F. Laprade, “Emerging Updates on the Posterior Cruciate Ligament A Review of the Current Literature,” vol. XX, no. X, pp. 1–16, 2015, doi: 10.1177/0363546515572770.

[10] A. Bedi, R. F. LaPrade, and M. T. Burrus, “Radiographic and Anatomic Landmarks of the Major Knee Ligaments,” *The Journal of Bone and Joint Surgery*, vol. 100, no. 14, pp. 1241–1250, Jul. 2018, doi: 10.2106/JBJS.17.01135.

[11] J. F. Abulhasan and M. J. Grey, “Anatomy and physiology of knee stability,” *Journal of Functional Morphology and Kinesiology*, vol. 2, no. 4. MDPI Multidisciplinary Digital Publishing Institute, Dec. 01, 2017. doi: 10.3390/jfmk2040034.

[12] S. Scheffler, “The cruciate ligaments: Anatomy, biology, and biomechanics,” in *The Knee Joint*, Paris: Springer Paris, 2012, pp. 11–21. doi: 10.1007/978-2-287-99353-4_2.

[13] R. Serra Cruz, J. Olivetto, C. S. Dean, J. Chahla, and R. F. LaPrade, “Superficial Medial Collateral Ligament of the Knee: Anatomic Augmentation With Semitendinosus and Gracilis Tendon Autografts,” *Arthroscopy Techniques*, vol. 5, no. 2, pp. e347–e352, Apr. 2016, doi: 10.1016/j.eats.2016.01.011.

[14] X. He, H. Cai, and K. Zhang, “Pie-crusting technique is effective and safe to release superficial medial collateral ligament for total knee arthroplasty,” *Journal of Orthopaedic Translation*, vol. 13, pp. 33–40, Apr. 2018, doi: 10.1016/j.jot.2018.01.001.

[15] T. Saigo *et al.*, “Morphology of the Insertions of the Superficial Medial Collateral Ligament and Posterior Oblique Ligament Using 3-Dimensional Computed Tomography: A Cadaveric Study,” *Arthroscopy - Journal of Arthroscopic and*

Related Surgery, vol. 33, no. 2, pp. 400–407, Feb. 2017, doi: 10.1016/j.arthro.2016.07.030.

[16] A. Hosseini, W. Qi, T. Y. Tsai, Y. Liu, H. Rubash, and G. Li, "In vivo length change patterns of the medial and lateral collateral ligaments along the flexion path of the knee," *Knee Surgery, Sports Traumatology, Arthroscopy*, vol. 23, no. 10, pp. 3055–3061, Oct. 2015, doi: 10.1007/s00167-014-3306-9.

[17] S. H. Hosseini Nasab, C. R. Smith, P. Schütz, B. Postolka, R. List, and W. R. Taylor, "Elongation Patterns of the Collateral Ligaments After Total Knee Arthroplasty Are Dominated by the Knee Flexion Angle," *Frontiers in Bioengineering and Biotechnology*, vol. 7, p. 323, Nov. 2019, doi: 10.3389/fbioe.2019.00323.

[18] J. Victor, "Optimising position and stability in total knee arthroplasty," *EFORT Open Reviews*, vol. 2, no. 5, pp. 215–220, May 2017, doi: 10.1302/2058-5241.2.170001.

[19] M. Schiraldi, G. Bonzanini, D. Chirillo, and V. de Tullio, "Mechanical and kinematic alignment in total knee arthroplasty," *Annals of Translational Medicine*, vol. 4, no. 7. AME Publishing Company, Apr. 01, 2016. doi: 10.21037/atm.2016.03.31.

[20] C. Rivière *et al.*, "Alignment options for total knee arthroplasty: A systematic review," *Orthopaedics and Traumatology: Surgery and Research*, vol. 103, no. 7. Elsevier Masson SAS, pp. 1047–1056, Nov. 01, 2017. doi: 10.1016/j.otsr.2017.07.010.

[21] Y. S. Lee *et al.*, "Kinematic alignment is a possible alternative to mechanical alignment in total knee arthroplasty," *Knee Surgery, Sports Traumatology, Arthroscopy*, vol. 25, no. 11, pp. 3467–3479, Nov. 2017, doi: 10.1007/s00167-017-4558-y.

[22] L. Fahlman, E. Sangeorzan, N. Chheda, and D. Lambright, “Older Adults without Radiographic Knee Osteoarthritis: Knee Alignment and Knee Range of Motion.,” *Clinical medicine insights. Arthritis and musculoskeletal disorders*, vol. 7, pp. 1–11, Jan. 2014, doi: 10.4137/CMAMD.S13009.

[23] T. Vos *et al.*, “Years lived with disability (YLDs) for 1160 sequelae of 289 diseases and injuries 1990-2010: A systematic analysis for the Global Burden of Disease Study 2010,” *The Lancet*, vol. 380, no. 9859, pp. 2163–2196, 2012, doi: 10.1016/S0140-6736(12)61729-2.

[24] “Hip and Knee Replacements in Canada: CJRR Annual Statistics Summary, 2018–2019.”

[25] “Triathlon ® Knee System Surgical Protocol.” Stryker.

[26] K. A. Gustke, G. J. Golladay, M. W. Roche, L. C. Elson, and C. R. Anderson, “Primary TKA patients with quantifiably balanced soft-tissue achieve significant clinical gains sooner than unbalanced patients,” *Advances in Orthopedics*, vol. 2014, 2014, doi: 10.1155/2014/628695.

[27] B. K. Daines and D. A. Dennis, “Gap balancing vs. measured resection technique in total knee arthroplasty,” *Clinics in Orthopedic Surgery*, vol. 6, no. 1. Korean Orthopaedic Association, pp. 1–8, 2014. doi: 10.4055/cios.2014.6.1.1.

[28] C. R. Smith, M. F. Vignos, R. L. Lenhart, J. Kaiser, and D. G. Thelen, “The influence of component alignment and ligament properties on tibiofemoral contact forces in total knee replacement,” *Journal of Biomechanical Engineering*, vol. 138, no. 2, Feb. 2016, doi: 10.1115/1.4032464.

[29] Y. H. Kim, J. W. Park, J. S. Kim, and S. D. Park, “The relationship between the survival of total knee arthroplasty and postoperative coronal, sagittal and rotational alignment of knee prosthesis,” *International Orthopaedics*, vol. 38, no. 2, pp. 379–385, Feb. 2014, doi: 10.1007/s00264-013-2097-9.

[30] D. M. Fang, M. A. Ritter, and K. E. Davis, “Coronal Alignment in Total Knee Arthroplasty,” *The Journal of Arthroplasty*, vol. 24, no. 6, Sep. 2009, doi: 10.1016/j.arth.2009.04.034.

[31] J. N. Torrão, M. P. S. dos Santos, and J. A. Ferreira, “Instrumented knee joint implants: innovations and promising concepts,” *Expert Review of Medical Devices*, vol. 12, no. 5, pp. 571–584, Sep. 2015, doi: 10.1586/17434440.2015.1068114.

[32] B. J. Fregly *et al.*, “Grand challenge competition to predict in vivo knee loads,” *Journal of Orthopaedic Research*, vol. 30, no. 4. pp. 503–513, Apr. 2012. doi: 10.1002/jor.22023.

[33] R. Willing and P. S. Walker, “Measuring the sensitivity of total knee replacement kinematics and laxity to soft tissue imbalances,” *Journal of Biomechanics*, vol. 77, pp. 62–68, Aug. 2018, doi: 10.1016/j.jbiomech.2018.06.019.

[34] R. Willing, A. Moslemian, G. Yamomo, T. Wood, J. Howard, and B. Lanting, “Condylar-Stabilized TKR May Not Fully Compensate for PCL-Deficiency: An In Vitro Cadaver Study,” *Journal of Orthopaedic Research*, vol. 37, no. 10, pp. 2172–2181, Oct. 2019, doi: 10.1002/jor.24392.

[35] E. S. Grood and W. J. Suntay, “A joint coordinate system for the clinical description of three-dimensional motions: Application to the knee,” *Journal of Biomechanical Engineering*, vol. 105, no. 2, pp. 136–144, 1983, doi: 10.1115/1.3138397.

[36] L. Blankevoort and R. Huiskes, “Ligament-bone interaction in a three-dimensional model of the knee,” *Journal of Biomechanical Engineering*, vol. 113, no. 3, pp. 263–269, 1991, doi: 10.1115/1.2894883.

[37] K. H. Bloemker, T. M. Guess, L. Maletsky, and K. Dodd, “Computational Knee Ligament Modeling Using Experimentally Determined Zero-Load Lengths,” 2012. [Online]. Available: www.slicer.org

[38] A. E. Peters, R. Akhtar, E. J. Comerford, and K. T. Bates, “Tissue material properties and computational modelling of the human tibiofemoral joint: A critical review,” *PeerJ*, vol. 2018, no. 1, pp. 1–48, 2018, doi: 10.7717/peerj.4298.

[39] T. M. Guess, S. Razu, and H. Jahandar, “Evaluation of Knee Ligament Mechanics Using Computational Models,” *The journal of knee surgery*, vol. 29, no. 2, pp. 126–137, Feb. 2016, doi: 10.1055/s-0036-1571954.

[40] K. Subburaj, B. Ravi, and M. Agarwal, “Automated identification of anatomical landmarks on 3D bone models reconstructed from CT scan images,” *Computerized Medical Imaging and Graphics*, vol. 33, no. 5, pp. 359–368, Jul. 2009, doi: 10.1016/j.compmedimag.2009.03.001.

[41] W. S. Jeong *et al.*, “An analysis of the posterior cruciate ligament isometric position using an in vivo 3-dimensional computed tomography-based knee joint model,” *Arthroscopy - Journal of Arthroscopic and Related Surgery*, vol. 26, no. 10, pp. 1333–1339, Oct. 2010, doi: 10.1016/j.arthro.2010.02.016.

[42] T. M. Guess and S. Razu, “Loading of the medial meniscus in the ACL deficient knee: A multibody computational study,” *Medical Engineering and Physics*, vol. 41, pp. 26–34, Mar. 2017, doi: 10.1016/j.medengphy.2016.12.006.

[43] M. H. Pope, C. J. Stankewich, B. D. Beynnon, and B. C. Fleming, “Effect of Knee Musculature on Anterior Cruciate Ligament Strain In Vivo.”

[44] J. C. Gardiner, “COMPUTATIONAL MODELING OF LIGAMENT MECHANICS,” 2002.

[45] M. Frisfn, M. Magi, A. Vlldlk, and G. Sweden, “RHEOLOGICAL ANALYSIS OF SOFT COLLAGENOUS TISSUE PART 1: THEORETICAL CONSIDERATIONS"’,” 1969.

[46] A. Viidik, “Biomechanics and Functional Adaption of Tendons and Joint Ligaments,” 1968.

[47] M. K. Kwan, T. H.-C. Lin, and S. L.-Y. Woo, “On the viscoelastic properties of the anteromedial bundle of the anterior cruciate ligament,” *Journal of Biomechanics*, vol. 26, no. 4–5, Apr. 1993, doi: 10.1016/0021-9290(93)90008-3.

[48] R. E. Cohen, C. J. Hooley, and N. G. McCrum, “Viscoelastic creep of collagenous tissue,” *Journal of Biomechanics*, vol. 9, no. 4, Jan. 1976, doi: 10.1016/0021-9290(76)90002-6.

[49] Y. C. Fung, “Bio-viscoelastic Solids,” in *Biomechanics*, New York, NY: Springer New York, 1981. doi: 10.1007/978-1-4757-1752-5_7.

[50] R. de Pascalis, I. D. Abrahams, and W. J. Parnell, “On nonlinear viscoelastic deformations: A reappraisal of Fung’s quasi-linear viscoelastic model,” *Proceedings of the Royal Society A: Mathematical, Physical and Engineering Sciences*, vol. 470, no. 2166, Jun. 2014, doi: 10.1098/rspa.2014.0058.

[51] D. P. Pioletti, L. R. Rakotomanana, J.-F. Benvenuti, and P.-F. Leyvraz, “Viscoelastic constitutive law in large deformations: application to human knee ligaments and tendons,” 1998.

[52] G. Li, J. Gil, A. Kanamori, and S. L.-Y. Woo, “A validated three-dimensional computational model of a human knee joint,” *Journal of Biomechanical Engineering*, vol. 121, pp. 657–662, Dec. 1999.

[53] J. P. Halloran, A. J. Petrella, and P. J. Rullkoetter, “Explicit finite element modeling of total knee replacement mechanics,” *Journal of Biomechanics*, vol. 38, no. 2, pp. 323–331, Feb. 2005, doi: 10.1016/j.jbiomech.2004.02.046.

[54] A. M. Kiapour *et al.*, “The Effect of Ligament Modeling Technique on Knee Joint Kinematics: A Finite Element Study,” *Applied Mathematics*, vol. 04, no. 05, pp. 91–97, 2013, doi: 10.4236/am.2013.45a011.

[55] J. P. Halloran, S. K. Easley, A. J. Petrella, and P. J. Rullkoetter, “Comparison of deformable and elastic foundation finite element simulations for predicting knee

replacement mechanics," *Journal of Biomechanical Engineering*, vol. 127, no. 5, pp. 813–818, Oct. 2005, doi: 10.1115/1.1992522.

[56] H. Naghibi Beidokhti, D. Janssen, S. van de Groes, J. Hazrati, T. van den Boogaard, and N. Verdonschot, "The influence of ligament modelling strategies on the predictive capability of finite element models of the human knee joint," *Journal of Biomechanics*, vol. 65, pp. 1–11, Dec. 2017, doi: 10.1016/j.jbiomech.2017.08.030.

[57] O. S. Kwon, T. Purevsuren, K. Kim, W. M. Park, T. K. Kwon, and Y. H. Kim, "Influence of bundle diameter and attachment point on kinematic behavior in double bundle anterior cruciate ligament reconstruction using computational model," *Computational and Mathematical Methods in Medicine*, vol. 2014, 2014, doi: 10.1155/2014/948292.

[58] J. J. Cherian, B. H. Kapadia, S. Banerjee, J. J. Jauregui, K. Issa, and M. A. Mont, "Mechanical, anatomical, and kinematic axis in TKA: Concepts and practical applications," in *Current Reviews in Musculoskeletal Medicine*, 2014, vol. 7, no. 2, pp. 89–95. doi: 10.1007/s12178-014-9218-y.

[59] J. Bellemans, W. Colyn, H. Vandenneucker, and J. Victor, "Is Neutral Mechanical Alignment Normal for All Patients? The Concept of Constitutional Varus," in *Clinical Orthopaedics and Related Research*, Jan. 2012, vol. 470, no. 1, pp. 45–53. doi: 10.1007/s11999-011-1936-5.

[60] P. Moewis, S. Checa, I. Kutzner, H. Hommel, and G. N. Duda, "Physiological joint line total knee arthroplasty designs are especially sensitive to rotational placement – A finite element analysis," *PLoS ONE*, vol. 13, no. 2, Feb. 2018, doi: 10.1371/journal.pone.0192225.

[61] Z. Chen *et al.*, "Prediction of in vivo joint mechanics of an artificial knee implant using rigid multi-body dynamics with elastic contacts," *Proceedings of the Institution of Mechanical Engineers, Part H: Journal of Engineering in Medicine*, vol. 228, no. 6, pp. 564–575, 2014, doi: 10.1177/0954411914537476.

[62] Y. Feng *et al.*, “Motion of the femoral condyles in flexion and extension during a continuous lunge,” *Journal of Orthopaedic Research*, vol. 33, no. 4, pp. 591–597, Apr. 2015, doi: 10.1002/jor.22826.

[63] K. Gromov, M. Korchi, M. G. Thomsen, H. Husted, and A. Troelsen, “What is the optimal alignment of the tibial and femoral components in knee arthroplasty?,” *Acta Orthopaedica*, vol. 85, no. 5, pp. 480–487, Sep. 2014, doi: 10.3109/17453674.2014.940573.

[64] M. A. Ritter, K. E. Davis, J. B. Meding, J. L. Pierson, M. E. Berend, and R. A. Malinzak, “The Effect of Alignment and BMI on Failure of Total Knee Replacement,” *Journal of Bone and Joint Surgery*, vol. 93, no. 17, Sep. 2011, doi: 10.2106/JBJS.J.00772.

[65] R. D. Scott, “Femoral and tibial component rotation in total knee arthroplasty,” *The Bone & Joint Journal*, vol. 95-B, no. 11_Supple_A, Nov. 2013, doi: 10.1302/0301-620X.95B11.32765.

[66] Y. Cho and M. C. Lee, “Rotational alignment in total knee arthroplasty,” *Asia-Pacific Journal of Sports Medicine, Arthroscopy, Rehabilitation and Technology*, vol. 1, no. 4. Elsevier (Singapore) Pte Ltd, pp. 113–118, Oct. 01, 2014. doi: 10.1016/j.asmart.2014.08.001.

[67] M. Akagi *et al.*, “Effect of Rotational Alignment On Patellar Tracking in Total Knee Arthroplasty,” *Clinical Orthopaedics and Related Research*, vol. 366, Sep. 1999, doi: 10.1097/00003086-199909000-00019.

[68] H. Boya, Ö. Özcan, and Gö. Maralcan, “An investigation of consistency between posterior condylar axis +3 degree external rotation line and clinical transepicondylar axis line techniques in primary total knee arthroplasty,” *Eklem Hastaliklari ve Cerrahisi*, vol. 25, no. 2, pp. 70–74, 2014, doi: 10.5606/ehc.2014.16.

[69] M. K. Abdelnasser, M. E. Elsherif, H. Bakr, M. Mahran, M. H. M. Othman, and Y. Khalifa, “All types of component malrotation affect the early patient-reported outcome measures after total knee arthroplasty,” *Knee Surgery and Related Research*, vol. 31, no. 1, Dec. 2019, doi: 10.1186/s43019-019-0006-2.

[70] L. E. Rubin and K. T. Murgo, “Brief report: total knee arthroplasty performed with patient-specific, pre-operative CT-guided navigation,” *Rhode Island Medical Journal*, vol. 96, no. 3, pp. 34–37, Mar. 2013.

[71] C. Maag, A. Metcalfe, I. Cracaoanu, C. Wise, and D. D. Auger, “The development of simulator testing for total knee replacements,” *Biosurface and Biotribology*, vol. 7, no. 2, pp. 70–82, Jun. 2021, doi: 10.1049/bsb2.12001.

[72] J.-G. Seo, Y.-W. Moon, B.-C. Jo, Y.-T. Kim, and S.-H. Park, “Soft Tissue Balancing of Varus Arthritic Knee in Minimally Invasive Surgery Total Knee Arthroplasty: Comparison between Posterior Oblique Ligament Release and Superficial MCL Release,” *Knee Surgery & Related Research*, vol. 25, no. 2, pp. 60–64, Jun. 2013, doi: 10.5792/ksrr.2013.25.2.60.

[73] D. M. Tetreault and F. E. Kennedy, “FRICTION AND WEAR BEHAVIOR OF ULTRAHIGH MOLECULAR WEIGHT POLYETHYLENE ON Co-C2 AND TITANIUM ALLOYS IN DRY AND LUBRICATED ENVIRONMENTS,” 1989.

[74] J. Deck and B. White, “JOINT-RELATIVE FORCES USING THE GROOD-SUNTAY UNIT VECTOR DIRECTIONS,” *Orthopaedic Proceedings*, vol. 98-B, Feb. 2018.

[75] K. WANG, A. STREET, A. DOWRICK, and S. LIEW, “Clinical outcomes and patient satisfaction following total joint replacement in haemophilia - 23-year experience in knees, hips and elbows,” *Haemophilia*, vol. 18, no. 1, pp. 86–93, Jan. 2012, doi: 10.1111/j.1365-2516.2011.02579.x.

[76] E. N. Hansen, K. L. Ong, E. Lau, S. M. Kurtz, and J. H. Lonner, “Unicondylar Knee Arthroplasty Has Fewer Complications but Higher Revision Rates Than

Total Knee Arthroplasty in a Study of Large United States Databases," *Journal of Arthroplasty*, vol. 34, no. 8, pp. 1617–1625, Aug. 2019, doi: 10.1016/j.arth.2019.04.004.

[77] X. Gasparutto, N. Sancisi, E. Jacquelin, V. Parenti-Castelli, and R. Dumas, "Validation of a multi-body optimization with knee kinematic models including ligament constraints," *Journal of Biomechanics*, vol. 48, no. 6, pp. 1141–1146, Apr. 2015, doi: 10.1016/j.jbiomech.2015.01.010.

[78] K. C and A. L, "Various Knee Model Measurement Techniques to Find the Knee Geometries," *International Journal of Pharmacy and Biomedical Engineering*, vol. 3, no. 3, pp. 4–6, Dec. 2016, doi: 10.14445/23942576/ijpbe-v3i3p102.

[79] Liu *et al.*, "Insertion Geometry of Medial Collateral Ligament in Normal Human Knees."

[80] D. Crottet *et al.*, "Ligament balancing in TKA: Evaluation of a force-sensing device and the influence of patellar eversion and ligament release," *Journal of Biomechanics*, vol. 40, no. 8, pp. 1709–1715, 2007, doi: 10.1016/j.jbiomech.2006.08.004.

[81] S. L. Logterman, F. B. Wydra, and R. M. Frank, "Posterior Cruciate Ligament: Anatomy and Biomechanics," *Current Reviews in Musculoskeletal Medicine*, vol. 11, no. 3. Humana Press Inc., pp. 510–514, Sep. 01, 2018. doi: 10.1007/s12178-018-9492-1.

[82] F. Galbusera *et al.*, "Material models and properties in the finite element analysis of knee ligaments: A literature review," *Frontiers in Bioengineering and Biotechnology*, vol. 2, no. NOV. Frontiers Media S.A., 2014. doi: 10.3389/fbioe.2014.00054.

[83] S. G. Clarke, A. T. M. Phillips, and A. M. J. Bull, "Evaluating a suitable level of model complexity for finite element analysis of the intact acetabulum," *Computer*

Methods in Biomechanics and Biomedical Engineering, vol. 16, no. 7, pp. 717–724, Jul. 2013, doi: 10.1080/10255842.2011.633906.

[84] N. O. Sarpong *et al.*, "Virtual reconstruction of the posterior cruciate ligament for mechanical testing of total knee arthroplasty implants," *Knee*, vol. 27, no. 1, pp. 151–156, Jan. 2020, doi: 10.1016/j.knee.2019.10.023.

[85] P. S. Trent, P. S. Walker, and B. Wolf, "Ligament length patterns, strength, and rotational axes of the knee joint.," *Clinical Orthopaedics and Related Research*, no. 117, pp. 263–270, Jun. 1976, doi: 10.1097/00003086-197606000-00034.

[86] D. T. Harfe, C. R. Chuinard, L. M. Espinoza, K. A. Thomas, and M. Solomonow, "Elongation patterns of the collateral ligaments of the human knee," *Clinical Biomechanics*, vol. 13, no. 3, pp. 163–175, Apr. 1998, doi: 10.1016/S0268-0033(97)00043-0.

[87] L. G. Hallén and O. Lindahl, "the screw-home movement in the knee-joint," *Acta Orthopaedica*, vol. 37, no. 1, pp. 97–106, 1966, doi: 10.3109/17453676608989407.

[88] P. Weber *et al.*, "Increase in the Tibial Slope in Unicondylar Knee Replacement: Analysis of the Effect on the Kinematics and Ligaments in a Weight-Bearing Finite Element Model," *BioMed Research International*, vol. 2018, 2018, doi: 10.1155/2018/8743604.

[89] J. K. Lee, S. Lee, S. H. Chun, K. T. Kim, and M. C. Lee, "Rotational alignment of femoral component with different methods in total knee arthroplasty: A randomized, controlled trial," *BMC Musculoskeletal Disorders*, vol. 18, no. 1, May 2017, doi: 10.1186/s12891-017-1574-5.

[90] H. Wang, K. J. Simpson, S. Chamnongkich, T. Kinsey, and O. M. Mahoney, "Biomechanical influence of TKA designs with varying radii on bilateral TKA patients during sit-to-stand," *Dynamic Medicine*, vol. 7, no. 1, 2008, doi: 10.1186/1476-5918-7-12.

[91] C.-J. Wang, J.-W. Wang, and H.-S. Chen, “Comparing Cruciate-Retaining Total Knee Arthroplasty and Cruciate-Substituting Total Knee Arthroplasty: A Prospective Clinical Study,” 2004.

[92] S. H. Hosseini Nasab *et al.*, “Length-Change Patterns of the Collateral Ligaments During Functional Activities After Total Knee Arthroplasty,” *Annals of Biomedical Engineering*, pp. 1–11, Jan. 2020, doi: 10.1007/s10439-020-02459-3.

[93] B. Jeffcote, R. Nicholls, A. Schirm, and M. S. Kuster, “The variation in medial and lateral collateral ligament strain and tibiofemoral forces following changes in the flexion and extension gaps in total knee replacement A LABORATORY EXPERIMENT USING CADAVER KNEES,” *THE JOURNAL OF BONE AND JOINT SURGERY*, doi: 10.1302/0301-620X.89B11.

[94] P. Stirling, N. D. Clement, D. MacDonald, J. T. Patton, R. Burnett, and G. J. Macpherson, “Early functional outcomes after condylar-stabilizing (deep-dish) versus standard bearing surface for cruciate-retaining total knee arthroplasty,” *Knee Surgery & Related Research*, vol. 31, no. 1, p. 3, Dec. 2019, doi: 10.1186/s43019-019-0001-7.

[95] S. H. H. Nasab, R. List, K. Oberhofer, S. F. Fucentese, J. G. Snedeker, and W. R. Taylor, “Loading patterns of the posterior cruciate ligament in the healthy knee: A systematic review,” *PLoS ONE*, vol. 11, no. 11, Nov. 2016, doi: 10.1371/journal.pone.0167106.

[96] “View of Coronal Alignment in TKA: Traditional Principles Versus New Concepts | Reconstructive Review.” https://reconstructivereview.org/ojs/index.php/rr/article/view/213/276 (accessed Jan. 15, 2020).

Appendices

Appendix A

The following appendix contains the MATLAB script used to convert cartesian kinematic rotations outputted from VIVO Sim into clinical rotations as described by Grood and Suntay [35].

```
function [alpha, beta, gamma] =
VIVOSim_to_GS_V3(ML,AP,IS,FE,VV,IE)
% the purpose of this script is to convert inputted
coordinates from
% machine actuator coordinates from a cartesian
coordinate system to

%% Define femoral (I,J,K) and tibial (i,j,k) coordinate
systems at ref pose

I_ref = [1 0 0]; i_ref = I_ref;
J_ref = [0 1 0]; j_ref = J_ref;
K_ref = [0 0 1]; k_ref = K_ref;

%% Build transformation matrix for each bone
% tibia: ML, AP, IS, IE,
% femur: FE, VV
Rx1 = [1 0 0;
    0 cosd(18) -sind(18);
    0 sind(18) cosd(18)];

Rx2 = [1 0 0;
    0 cosd(FE-18) -sind(FE-18);
    0 sind(FE-18) cosd(FE-18)];

Ry = [cosd(VV) 0 sind(VV);
    0 1 0;
    -sind(VV) 0 cosd(VV)];


Rz = [cosd(IE) -sind(IE) 0;
    sind(IE) cosd(IE) 0;
    0 0 1];
```

```
R_fem = Rx1*Ry*Rx2; % apply rotations in XY sequence
R_tib = Rz.';
clear Rx Ry Rz

T_tib = zeros(4,4);
T_tib(1:4,1:3) = [R_tib; 0 0 0];
T_tib(1:4,4) = [ML;AP;IS;1];
% femur only undergoes rotations, no translation



%% Transform reference coordinate system

% femur
I = I_ref*R_fem;
J = J_ref*R_fem;
K = K_ref*R_fem;

%tibia
i = [i_ref 1]*T_tib;
i = i(1:3);

j = [j_ref 1]*T_tib;
j = j(1:3);

k = [k_ref 1]*T_tib;
k = k(1:3);

%% Build GS matrix and extract clinical rotations (from
GS paper)

RT = [dot(I,i) dot(J,i) dot(K,i);
    dot(I,j) dot(J,j) dot(K,j);
    dot(I,k) dot(J,k) dot(K,k)];

% alpha --> FE rotation
% beta --> VV rotation
% gamma --> IE rotation

% I*k = cos(beta)
beta1 = acosd(RT(3,1));
beta = 90-beta1;

% I*j = sin(gamma)sin(beta)
gamma = -1*asind(RT(2,1)/sind(beta1));
```

```
% K*k = cos(alpha)sin(beta)
alpha = acosd(RT(3,3)/sind(beta1));
```

Appendix B

The following appendix contains detailed kinematic results for individual computational knee models: either varied in ligament complexity or level of simulated ligament wrapping.

Ligament Model Complexity

Posterior Laxity

For all results, laxity is calculated as the absolute difference between the joint's position during the laxity testing and the joint's position during all points of neutral flexion. That is to say, these are comparisons of laxity values averaged over 0°, 15°, 30°, 60°, and 90°. The average posterior laxity through flexion for the Multi, Guess, and Single models were 4.9±2.5 mm, 4.6±2.6 mm, and 4.7±1.9 mm, respectively. Therefore, there is no clear indication that ligament model complexity affects posterior laxity in the knee joint. Figure 0-1 shows anterior-posterior (AP) kinematics for all three ligament models during posterior laxity.

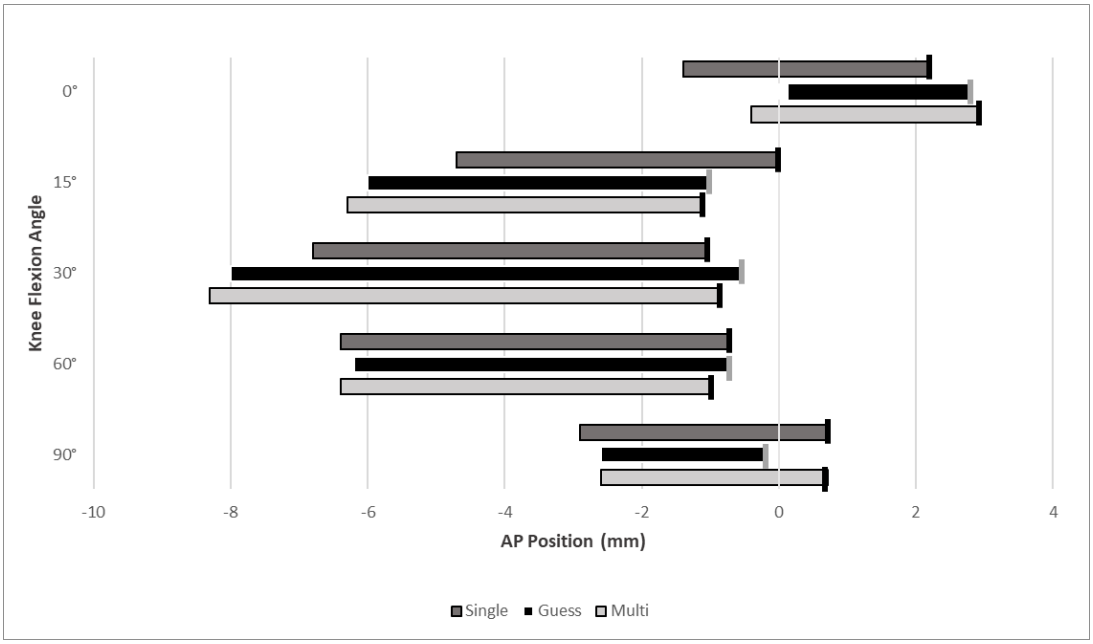

Figure 0-1: AP kinematics during neutral flexion and with a 100 N force directed posteriorly against the tibia for three ligament models of increasing complexity from Single, to Guess, to Multi. Kinematics during neutral flexion are represented by solid vertical bars. Negative values denote positions where the tibia is shifted posteriorly relative to the reference pose, positive values denote a relative anterior position.

Varus-Valgus Laxity

Average varus laxities of 3.2±0.9°, 3.9±0.3°, and 4.7±0. 7° for Single, Guess, and Multi, respectively, show an increase in laxity with an increase in model complexity. However, average valgus laxities of 2.8±1.0°, 4.3±1.3°, 3.6±1.0° for the same indicate that ligament model complexity is not the only factor responsible for VV laxity. Figure 0-2 shows a similar VV position during neutral flexion for all ligament models. It is also shown that varus laxity increases with increased model complexity. Note the outlying valgus motion limits during mid-flexion of the Guess model.

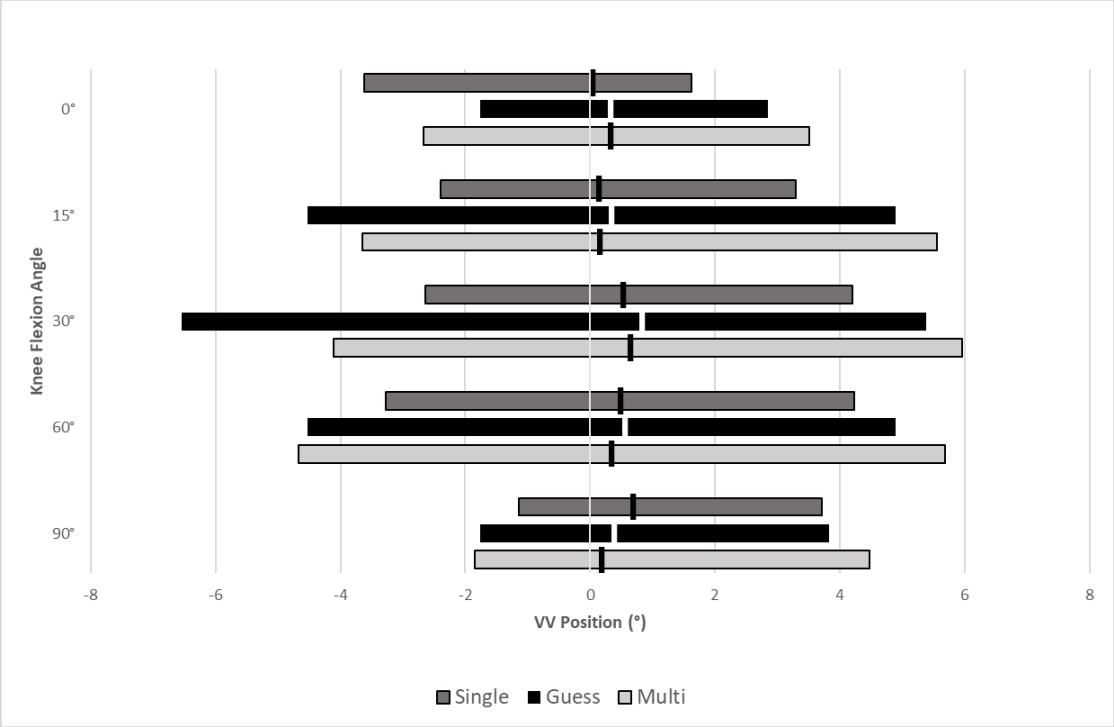

Figure 0-2: VV kinematics during neutral flexion and with a positive or negative 8 Nm torque applied to the femur for varus and valgus laxity tests, respectively. Results for three ligament models of increasing complexity from Single, to Guess, to Multi are shown. Kinematics during neutral flexion are represented by solid vertical bars, valgus laxity resulted in negative VV position, and varus laxity results in a positive VV position.

Internal-External Laxity

Average joint laxity during internal laxity testing was 23.2±7.1°, 29.6±5.4°, and 31.4±7.0° for the Single, Guess, and Multi models, respectively. Again, we see similar kinematics no matter the complexity of the ligament model. However, in Figure 0-3 below it can be seen that IE position during neutral flexion varies heavily between models with simpler ligament models leading to a joint that is more internally rotated as the knee is flexed. Average external laxities were 22.3±6.3°, 18.7±5.4°, and 16.3±6.9° for the Single, Guess, and Multi models, respectively. For most points of flexion, external laxity was highest for the simpler Single model with the Multi model leading to lower laxity.

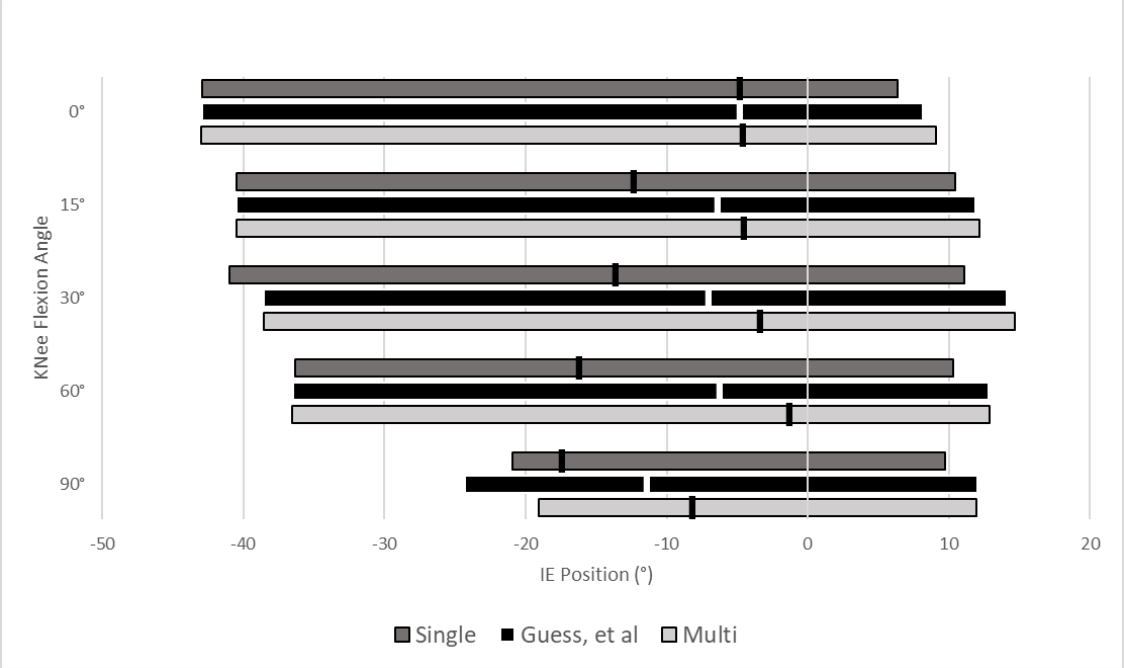

Figure 0-3: IE kinematics during neutral flexion and with a positive or negative 4 Nm torque applied to the femur for internal and external laxity tests, respectively. Results for three ligament models of increasing complexity from Single, to Guess, to Multi are shown. IE position during neutral flexion is denoted by vertical bars for all three models. Positive values indicate external rotation of the tibia, negative values indicate internal rotation.

Simulated Ligament Wrapping

Multi Model Results

Where laxity is calculated as the absolute difference between kinematics during neutral flexion and kinematics during a laxity test, the average AP laxities for the unwrapped, wrapped, and wrapped & compensated conditions were 4.9±2.6 mm, 4.2±3.0 mm, and 4.9±2.5 mm, respectively. Figure 0-4 demonstrates that simulating wrapping without compensating the reference strain evidently restricts laxity, except at 90° of flexion when it has higher laxity. The wrapped & compensated model had lower average laxity than

the unwrapped model. However, with large standard deviations for each condition this study cannot show conclusively that one condition restricts AP laxity more than another.

Figure 0-5 shows VV kinematics during varus and valgus laxity for all three ligament model conditions. Average varus laxity was 4.8±0.74°, 3.6±0.70°, and 4.1±0.6° for the unwrapped, wrapped, and wrapped & compensated models, respectively. It is evident from both the figure and the averages that the unwrapped joint is the most lax, and the simple wrapped model has the tightest joint. Valgus laxities for the same were 3.7±1.1°, 2.5±0.9°, and 3.8±0.9°. Again, we see that the wrapped model without compensation provides the tightest joint. However, this time it's the wrapped and compensated model that has the highest laxity. When considering standard deviations and the fact that this is only one specimen, it is difficult to state conclusively that one model provides a joint that is more lax than another.

In Figure 0-6 we see the IE kinematics during internal and external laxity tests. The average laxities during the internal laxity test were 31.3±6.9°. 26.2±5.4°, and 32.5±0.7°, for the unwrapped, wrapped, and wrapped & compensated models, respectively. The average values during external laxity were 16.3±6.9°, 15.3±4.4°, and 13.1±4.5°. Once again, the wrapped and uncompensated model restricts movement due to applied forces the most. The most internally rotated position during neutral flexion occurs for the wrapped model without compensation.

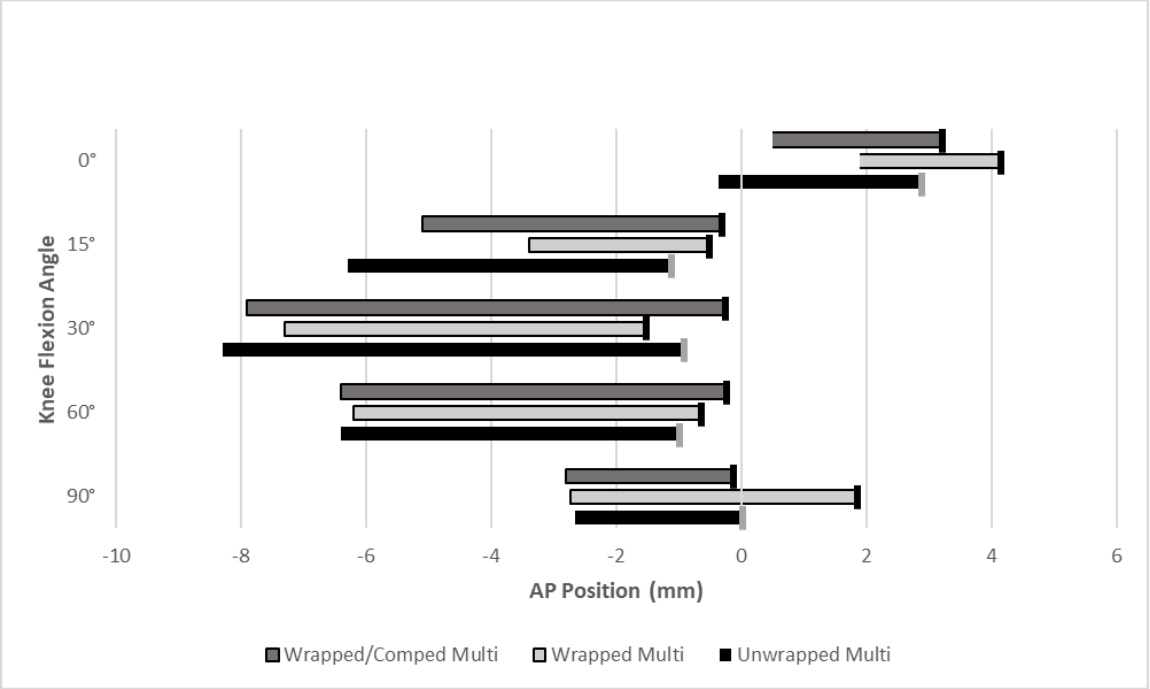

Figure 0-4: AP kinematics during neutral flexion and with a 100 N force directed posteriorly against the tibia with the Multi ligament model using three different wrapping conditions: unwrapped, wrapped, and wrapped & compensated. Kinematics during neutral flexion are represented by solid vertical bars. Negative values denote positions where the tibia is shifted posteriorly relative to the reference pose, positive values denote a relative anterior position.

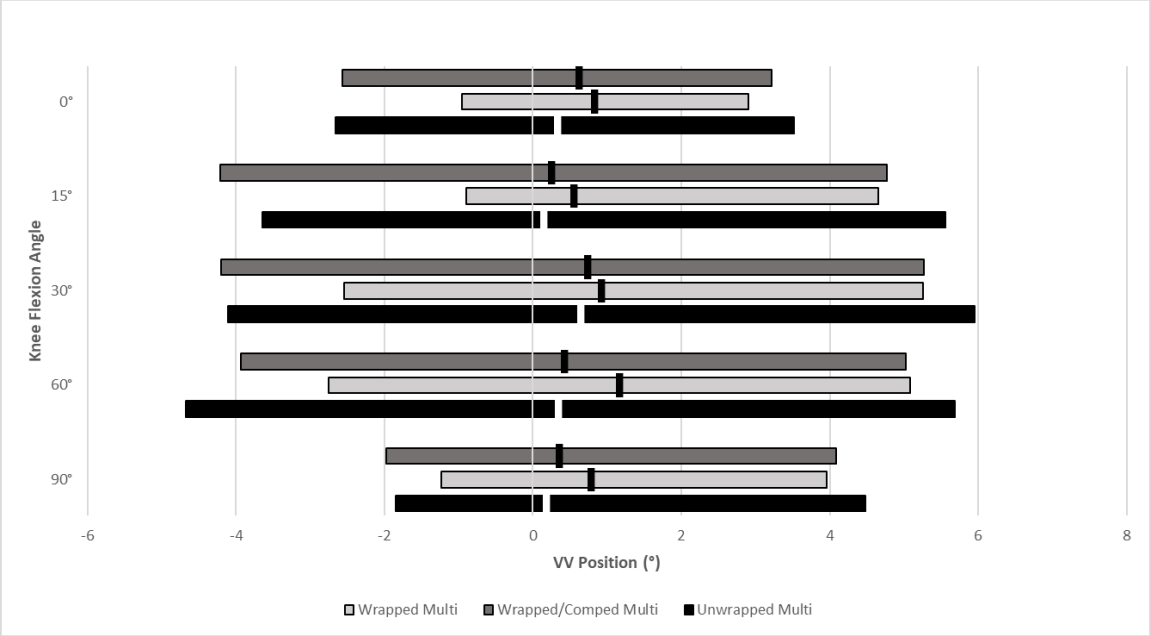

Figure 0-5: VV kinematics during neutral flexion and with a 8 Nm torque applied to simulate varus and valgus laxity to the Multi ligament model using three different wrapping conditions: unwrapped, wrapped, and wrapped & compensated. Kinematics during neutral flexion are represented by solid vertical bars. Negative values denote a valgus femoral position and positive values show that the femur was varus with respect to the tibia.

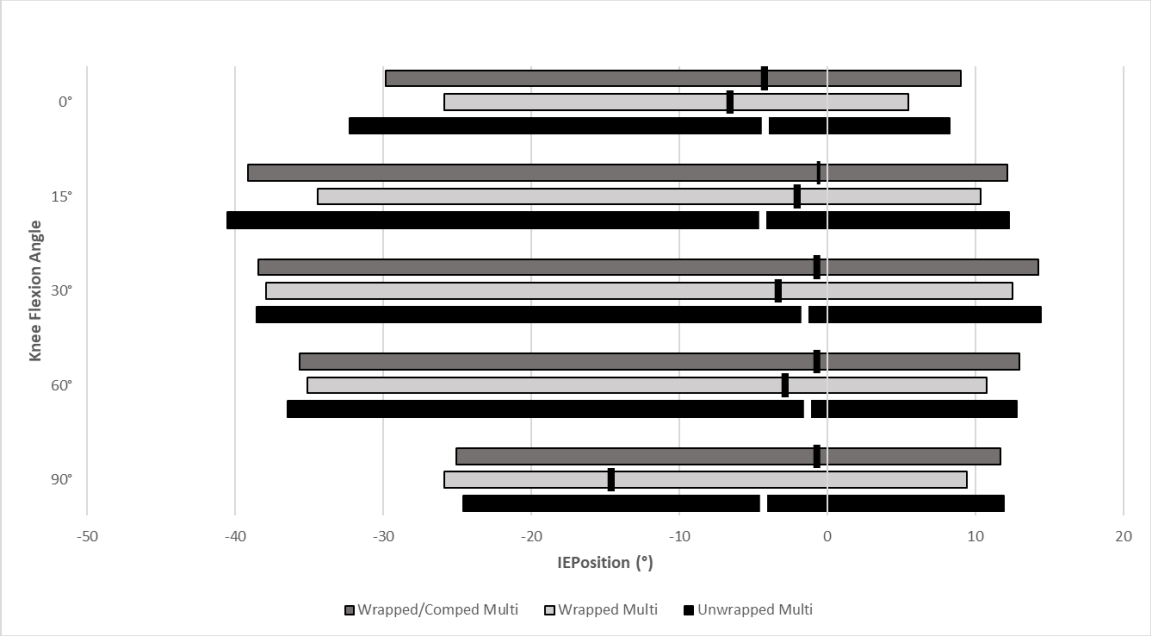

Figure 0-6: IE kinematics during neutral flexion and with a 4 Nm torque applied to simulate internal and external laxity to the Multi ligament model using three different wrapping conditions: unwrapped, wrapped, and wrapped & compensated. Kinematics during neutral flexion are represented by solid vertical bars. Negative values denote an internally rotated tibial position and positive values show that the tibia was externally rotated with respect to the tibia.

Guess Model Results

The average posterior laxities for the unwrapped, wrapped, and wrapped & compensated models were 5.31±2.04°, 4.51±2.94°, and 7.22±2.64°, respectively. Figure 0-7 below shows that the unwrapped model results in a more negative motion limit during early flexion, however, in deep flexion the posterior motion limits are similar between all models. The wrapped & compensated model has the highest joint laxity for all points of flexion due to an excessively anterior position during neutral flexion. The wrapped ligament model without compensation resulted in the tightest joint during posterior laxity testing.

Average varus laxities during VV laxity testing were 4.09±0.82°, 3.38±0.77°, and 3.09±0.79° for the unwrapped, wrapped, and wrapped & compensated models,

respectively. The average valgus laxities for the same were 3.90±1.53°, 2.56±0.99°, and 4.09±0.89°. In both cases the wrapped ligament model without compensation results in the most restrained joint during both varus and valgus laxity tests. Similar varus motion limits exist between the three models, but the unwrapped model ultimately has the highest laxity. That is to say, the unwrapped model restricts VV motion during neutral flexion. The wrapped model without compensation severely limits valgus movement as shown in Figure 0-8. The unwrapped model has a much greater valgus motion limit than the other two models during mid- to late-flexion, however the wrapped & compensated model still has a higher overall valgus laxity.

Average internal laxities for the unwrapped, wrapped, and wrapped & compensated models were 29.60±5.43°, 25.00±4.97°, and 21.42±4.93°, respectively. Average external laxities for the same were 18.74±5.37°, 16.03±4.14°, and 22.85±4.58°. The wrapped & compensated has the most internally rotated position during neutral flexion as well as similar internal and external laxities. For the other two models, internal laxity is far greater than external laxity. The internal and external motion limits are very similar between the three models as seen in Figure 0-9, the variance exists during neutral motion.

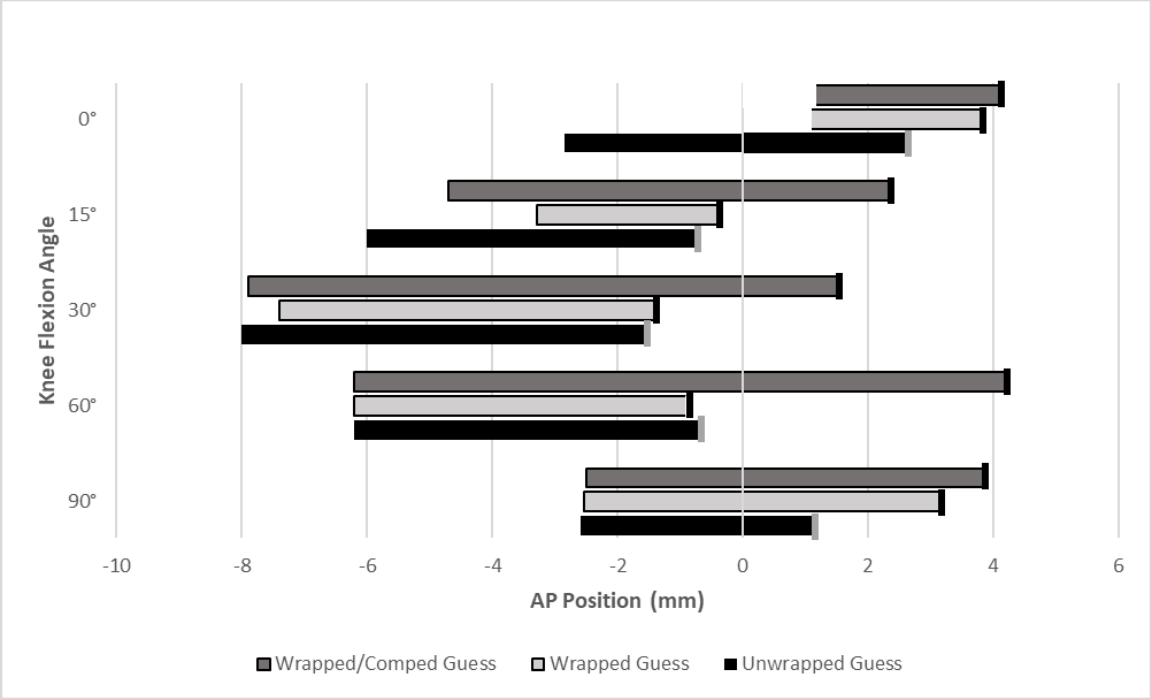

Figure 0-7: AP kinematics during neutral flexion and with a 100 N force directed posteriorly against the tibia with the Guess ligament model using three different wrapping conditions: unwrapped, wrapped, and wrapped & compensated. Kinematics during neutral flexion are represented by solid vertical bars. Negative values denote positions where the tibia is shifted posteriorly relative to the reference pose, positive values denote a relative anterior position.

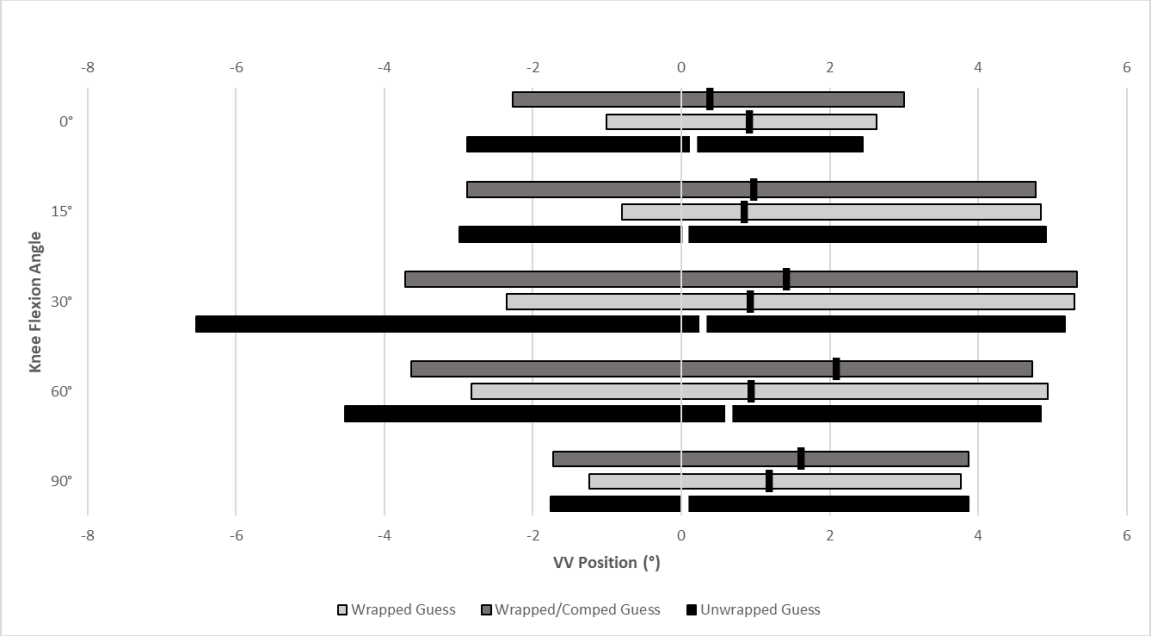

Figure 0-8: VV kinematics during neutral flexion and with a 8 Nm torque applied to simulate varus and valgus laxity to the Guess ligament model using three different wrapping conditions: unwrapped, wrapped, and wrapped & compensated. Kinematics during neutral flexion are represented by solid vertical bars. Negative values denote a valgus femoral position and positive values show that the femur was varus with respect to the tibia.

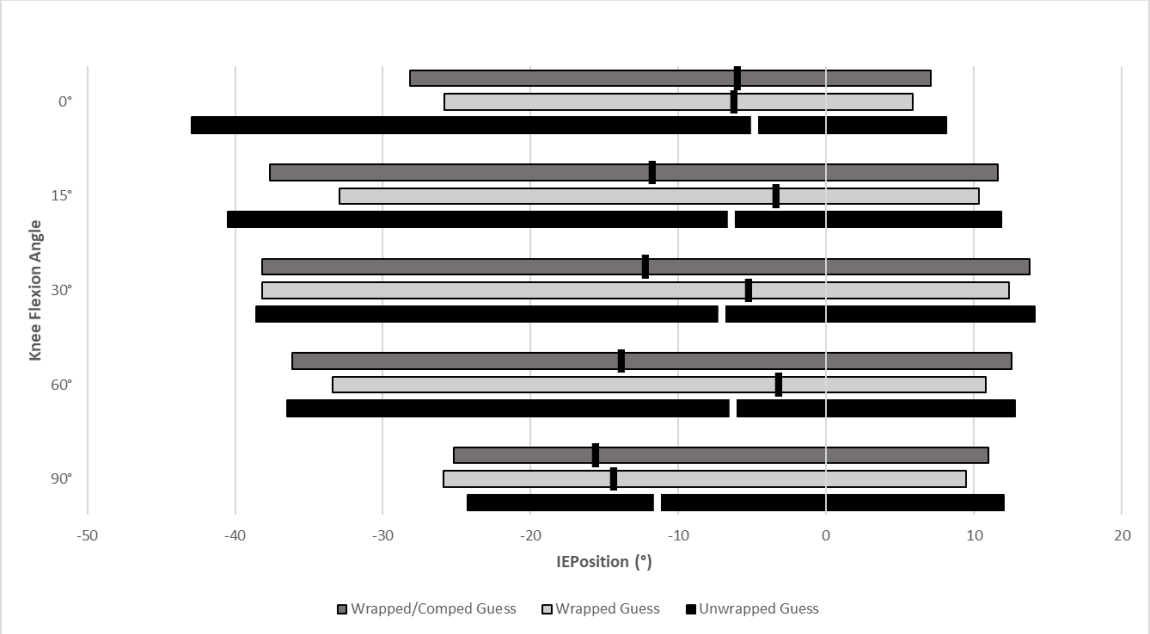

Figure 0-9: IE kinematics during neutral flexion and with a 4 Nm torque applied to simulate internal and external laxity to the Guess ligament model using three different wrapping conditions: unwrapped, wrapped, and wrapped & compensated. Kinematics during neutral flexion are represented by solid vertical bars. Negative values denote an internally rotated tibial position and positive values show that the tibia was externally rotated with respect to the tibia.

Single Model Results

Average posterior laxities were 6.15±1.90°, 6.44±2.50°, and 4.37±2.76° for the unwrapped, wrapped, and wrapped & compensated models, respectively. The wrapped & compensated model displays a much lower average laxity than the other two models. This is an effect of having a far more posterior position during neutral flexion, which can be seen in Figure 0-10. The wrapped model without compensation had a more anterior position during neutral flexion, leading it to have the greatest overall laxity despite having the lowest posterior motion limit at most points of flexion. Posterior motion limits during late flexion were very similar between all ligament models.

After testing VV laxities, the average varus laxities for the unwrapped, wrapped, and wrapped & compensated models were 3.20±0.78°, 2.38±0.85°, and 3.46±0.67°,

respectively. The average valgus laxities were 3.06±0.95°, 2.24±0.79°, and 2.58±0.75° for the same. The wrapped model without compensation is more varus during neutral flexion and has a far lower valgus motion limit which is shown in Figure 0-11. It also has the lowest average varus and valgus laxities. The unwrapped and wrapped & compensated models have similar kinematics during both the laxity tests and neutral flexion.

Following IE laxity tests, the average recorded internal laxities for the unwrapped, wrapped, and wrapped & compensated models were 23.18±7.07°, 19.44±3.94°, and 28.40±3.99°, respectively. Average external laxities for the same were 22.26±6.29°, 19.04±3.27°, and 12.99±3.93°. From Figure 0-12 the wrapped & compensated model has a more neutral position during neutral flexion, whereas the other two models are far more internally rotated. The unwrapped model has greater internal motions limits during early flexion, but motion limits are similar at other flexion angles. The external motion limits are similar between all three models.

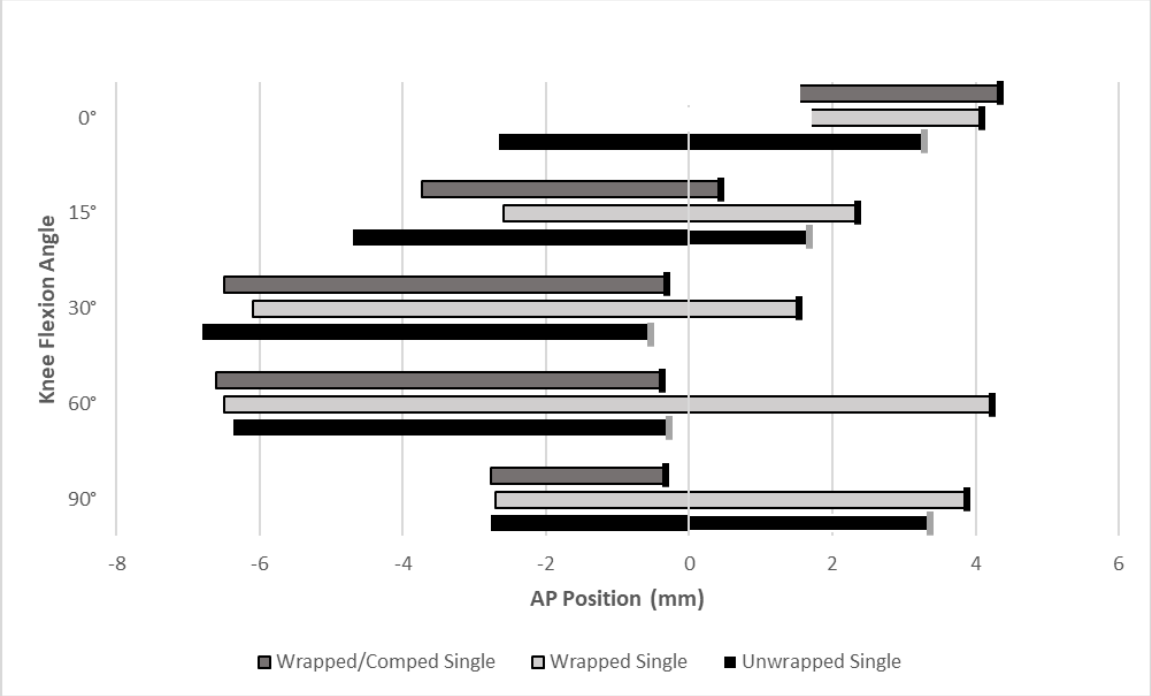

Figure 0-10: AP kinematics during neutral flexion and with a 100 N force directed posteriorly against the tibia with the Single ligament model using three different

wrapping conditions: unwrapped, wrapped, and wrapped & compensated. Kinematics during neutral flexion are represented by solid vertical bars. Negative values denote positions where the tibia is shifted posteriorly relative to the reference pose, positive values denote a relative anterior position.

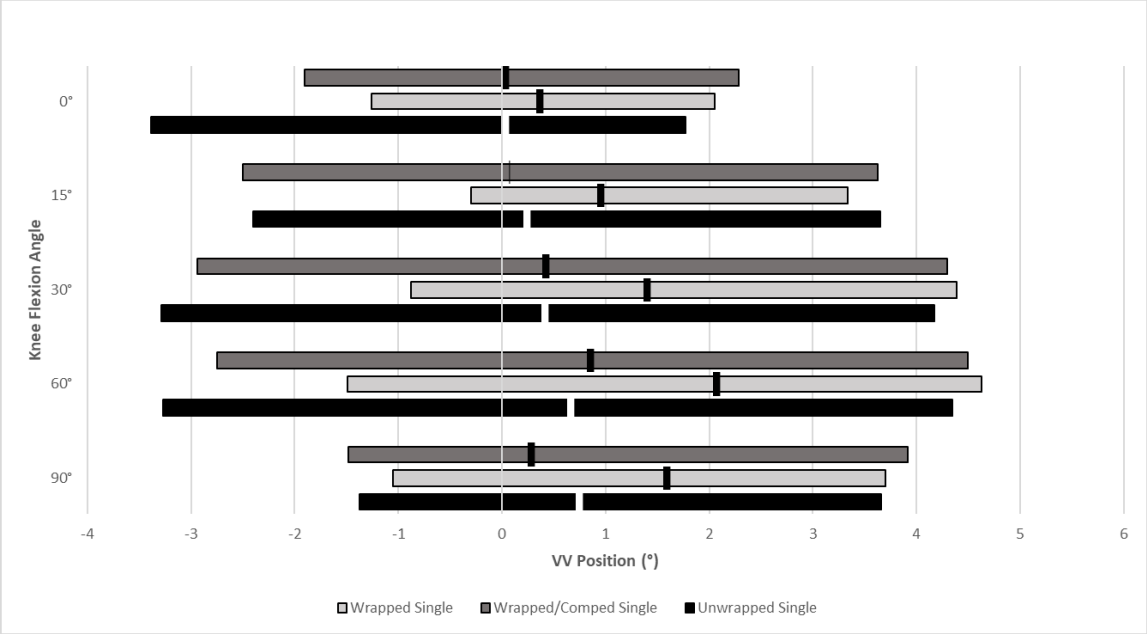

Figure 0-11: VV kinematics during neutral flexion and with a 8 Nm torque applied to simulate varus and valgus laxity to the Guess ligament model using three different wrapping conditions: unwrapped, wrapped, and wrapped & compensated. Kinematics during neutral flexion are represented by solid vertical bars. Negative values denote a valgus femoral position and positive values show that the femur was varus with respect to the tibia.

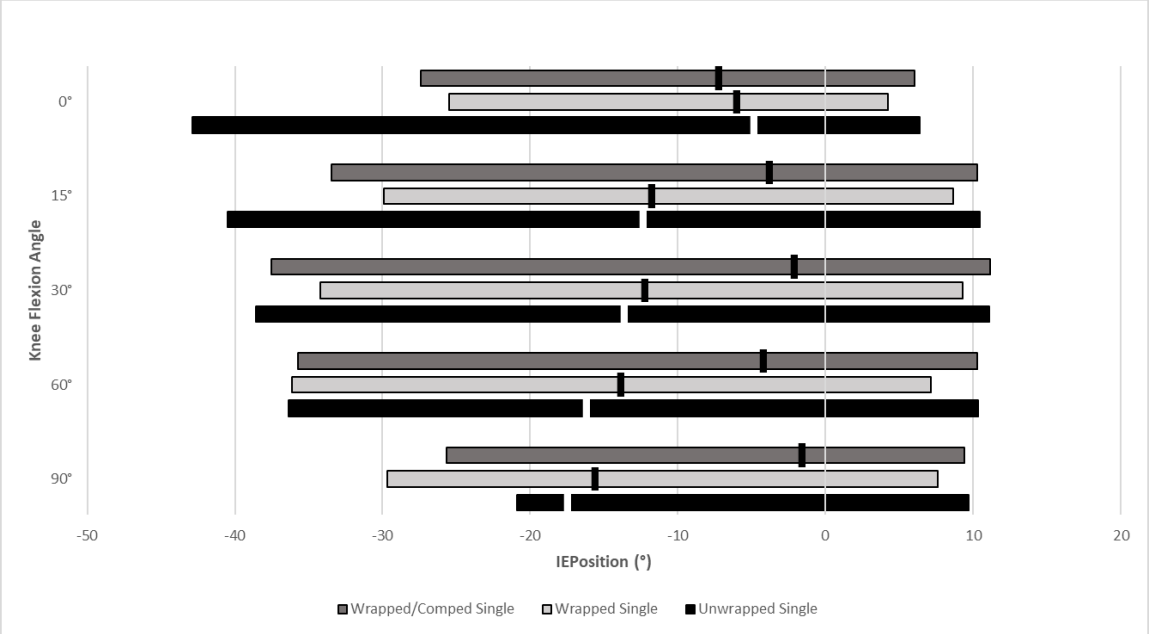

Figure 0-12: IE kinematics during neutral flexion and with a 4 Nm torque applied to simulate internal and external laxity to the Guess ligament model using three different wrapping conditions: unwrapped, wrapped, and wrapped & compensated. Kinematics during neutral flexion are represented by solid vertical bars. Negative values denote an internally rotated tibial position and positive values show that the tibia was externally rotated with respect to the tibia.

Ligament Model Complexity Comparison

Overall, we saw similar behaviour between the three levels of ligament model complexity: Multi, Guess, and Single. However, the AP kinematics during neutral flexion did vary. For the Multi model, none of the ligament models had anterior (+) AP positions during mid-flexion. The wrapped and unwrapped conditions for the Single model, and the wrapped & compensated conditions for the Guess model all had anterior AP positions during neutral flexion. Furthermore, the unwrapped condition for all complexity models during posterior laxity in extension led to a tibia being 4.09 mm, 15.55 mm, and 22.95 mm lateral with respect to the femur for the Multi, Guess, and Single models respectively. This was reduced to less than 2 mm for all three complexity models with either the wrapped or wrapped & compensated conditions. VV laxity tests were similar between all three levels of complexity: similar varus motion limits, and the wrapped

condition producing a noticeably reduced valgus motion limit. For the Guess model, the ligament condition which gave the most varus position was the wrapped & compensated, whereas for the Multi and Single models it was the wrapped ligament condition. The motion limits during internal and external rotation were similar between complexity models: similar for all ligament conditions except the wrapped condition produced a tighter joint in the early flexion stages of internal laxity. For the Multi model, all ligament wrapping condition models had similarly neutral IE positions throughout flexion. With the Guess model, the wrapped & compensated condition resulted in a joint that was more internally rotated during neutral flexion. For the Single model, it was the wrapped and unwrapped conditions that had an internally rotated position throughout neutral flexion. Thus, the ligament complexity didn't seem to have an effect on the kinematics of the motion limits, but neutral flexion kinematics were affected.

Curriculum Vitae

Name: Liam Montgomery

Post-secondary Education and Degrees: University of Western Ontario
London, Ontario, Canada
2016-2020 B.Sc.

Honours and Awards:

Related Work Experience

Publications: